National Library of Canada
Bibliothèque nationale du Canada

Canadian Theses Service
Service des thèses canadiennes

Ottawa, Canada
K1A 0N4

NOTICE

The quality of this microform is heavily dependent upon the quality of the original thesis submitted for microfilming. Every effort has been made to ensure the highest quality of reproduction possible.

If pages are missing, contact the university which granted the degree.

Some pages may have indistinct print especially if the original pages were typed with a poor typewriter ribbon or if the university sent us an inferior photocopy.

Reproduction in full or in part of this microform is governed by the Canadian Copyright Act, R.S.C. 1970, c. C-30, and subsequent amendments.

AVIS

La qualité de cette microforme dépend grandement de la qualité de la thèse soumise au microfilmage. Nous avons tout fait pour assurer une qualité supérieure de reproduction.

S'il manque des pages, veuillez communiquer avec l'université qui a conféré le grade.

La qualité d'impression de certaines pages peut laisser à désirer, surtout si les pages originales ont été dactylographiées à l'aide d'un ruban usé ou si l'université nous a fait parvenir une photocopie de qualité inférieure.

La reproduction, même partielle, de cette microforme est soumise à la Loi canadienne sur le droit d'auteur, SRC 1970, c. C-30, et ses amendements subséquents.

NL-339 (r. 88/04) c

Canada

UNIVERSITY OF ALBERTA

RADIOIODINATED SUGAR-COUPLED 2-NITROIMIDAZOLES: NOVEL NON-INVASIVE MARKERS OF HYPOXIC TUMOR TISSUE

BY

REZAUL HASAN MANNAN

A THESIS

SUBMITTED TO THE FACULTY OF GRADUATE STUDIES AND RESEARCH IN PARTIAL FULFILMENT OF THE REQUIREMENTS FOR THE DEGREE OF

DOCTOR OF PHILOSOPHY

IN

PHARMACEUTICAL SCIENCES (BIONUCLEONICS)

FACULTY OF PHARMACY AND PHARMACEUTICAL SCIENCES

EDMONTON, ALBERTA

FALL, 1991

National Library of Canada
Bibliothèque nationale du Canada

Canadian Theses Service
Service des thèses canadiennes

Ottawa, Canada
K1A 0N4

The author has granted an irrevocable non-exclusive licence allowing the National Library of Canada to reproduce, loan, distribute or sell copies of his/her thesis by any means and in any form or format, making this thesis available to interested persons.

The author retains ownership of the copyright in his/her thesis. Neither the thesis nor substantial extracts from it may be printed or otherwise reproduced without his/her permission.

L'auteur a accordé une licence irrévocable et non exclusive permettant à la Bibliothèque nationale du Canada de reproduire, prêter, distribuer ou vendre des copies de sa thèse de quelque manière et sous quelque forme que ce soit pour mettre des exemplaires de cette thèse à la disposition des personnes intéressées.

L'auteur conserve la propriété du droit d'auteur qui protège sa thèse. Ni la thèse ni des extraits substantiels de celle-ci ne doivent être imprimés ou autrement reproduits sans son autorisation.

ISBN 0-315-70118-8

Canada

UNIVERSITY OF ALBERTA

RELEASE FORM

NAME OF AUTHOR	REZAUL HASAN MANNAN
TITLE OF THESIS	RADIOIODINATED SUGAR-COUPLED 2-NITROIMIDAZOLES: NOVEL NON-INVASIVE MARKERS OF HYPOXIC TUMOR TISSUE.
DEGREE	DOCTOR OF PHILOSOPHY
YEAR THIS DEGREE GRANTED	FALL, 1991

PERMISSION IS HEREBY GRANTED TO THE UNIVERSITY OF ALBERTA LIBRARY TO REPRODUCE SINGLE COPIES OF THIS THESIS AND TO LEND OR SELL SUCH COPIES FOR PRIVATE, SCHOLARLY OR SCIENTIFIC RESEARCH PURPOSES ONLY.

THE AUTHOR RESERVES OTHER PUBLICATION RIGHTS, AND NEITHER THE THESIS NOR EXTENSIVE EXTRACTS FROM IT MAY BE PRINTED OR OTHERWISE REPRODUCED WITHOUT THE AUTHOR'S WRITTEN PERMISSION.

521-R, MICHENER PARK

EDMONTON, ALBERTA

T6H 4M5, CANADA

Date: Aug. 07, 1991

"God has sent down both the
disease and the cure,
and He has appointed a cure
for every disease,
so treat yourselves medically,
but use nothing unlawful"

- Al-Hadith

UNIVERSITY OF ALBERTA

FACULTY OF GRADUATE STUDIES AND RESEARCH

THE UNDERSIGNED CERTIFY THAT THEY HAVE READ, AND RECOMMEND TO THE FACULTY OF GRADUATE STUDIES AND RESEARCH FOR ACCEPTANCE, A THESIS ENTITLED **RADIOIODINATED SUGAR-COUPLED 2-NITROIMIDAZOLES: NOVEL NON-INVASIVE MARKERS OF HYPOXIC TUMOR TISSUE** SUBMITTED BY **REZAUL HASAN MANNAN** IN PARTIAL FULFILLMENT OF THE REQUIREMENTS FOR THE DEGREE OF **DOCTOR OF PHILOSOPHY IN PHARMACEUTICAL SCIENCES (BIONUCLEONICS).**

Dr. Leonard I. Wiebe (Supervisor)

Dr. John R. Mercer (Co-supervisor)

Dr. Alexander J. McEwan

Dr. Alec Shysh

Mr. John Scott

Dr. J. Allalunis-Turner

Dr. Donald Lyster (External Examiner)

Date:

DEDICATION

The loving memory of my grandmother, the late Mrs. Saleha Khatun (whom I lost during my sojourn) for her endless love and affection for me. Her encouragement was one of the driving forces on my intellectual pursuits.

My mother Mrs. Monowara Begum, for her unparallel determination, courage and excellent teaching to lead her children into intellectual endeavour through many hardships and sacrifices. Her affection, love, patience along with faith, encouragement and strict discipline made it all possible for me to acquire the light of knowledge.

My father Dr. Abdul Mannan, Professor and former Vice-chancellor, University of Dhaka, for his uncompromising principles as a dedicated teacher, researcher and administrator. It is him, who exemplified in his struggling life "perseverance" is the key for success. He is the one, who taught his children to walk on the road of science. He is the architect in all my academic endeavours, it is him, who dreamt my Ph.D. He always made my path easier through his unique examples along with guidance, affection, love and encouragement.

My wonderful wife and sincere friend Nipa, for her devotion, dutifulness and patience. Her unparallel courage, sacrifice and hardship through thick and thin made it all possible for me to complete this work. Her inspiration and

understanding contributed much in facing many adverse situations.

Saqib, our beloved son, who was born during my sojourn, for his sacrifice and understanding to let his father work, when he needed him most. His presence always motivated me in my studies. He brought with him hope and certainty in my life.

My dearest younger brothers and sisters: Akash, Rosie, Shaheen, Bulu and Ratan, for their amazing understanding and deepest love for me. Their sincere effort and endless sacrifice to take care of our parents through many ups and downs helped me to overcome my home-sickness and to concentrate on my studies.

ABSTRACT

A series of four, novel, (radio)iodinated, sugar-coupled 2-nitroimidazoles were evaluated as non-invasive markers of tumor hypoxia. The compounds investigated were IAZA (1-[5-iodo-5-deoxy-ß-D-arabinofuranosyl]-2-nitroimidazole), IAZG (1-[6-iodo-6-deoxy-ß-D-galactopyranosyl]2-nitroimidazole), IAZP (1-[4-iodo-4-deoxy-ß-L-xylopyranosyl]-2-nitroimidazole and FIAZP (1-[2-fluoro-2-deoxy-4-iodo-4-deoxy-ß-L-xylopyranosyl]-2-nitroimidazole).

The compounds were selectively cytotoxic to hypoxic EMT-6 cells in vitro. The cytotoxic effect of IAZA was higher than the others in the series; and was at least 10 times higher than misonidazole.

The radiosensitizing effectiveness of these compounds was determined by gamma irradiation of EMT-6 cell cultures under hypoxic conditions with various concentrations of test substrate. IAZG was the best radiosensitizer in the series with an SER value of 1.8 at 0.5 mM. The other compounds showed similar though reduced SER values and all compounds were superior to misonidazole.

The radioiodinated compounds were shown to undergo selective binding with hypoxic EMT-6 cells in culture, at a rate 7-30 times higher than with aerobic cells. IAZG had the highest binding rate (1100 pmol/10^6 cells/h) at 100 µM, followed by IAZA and IAZP. All compounds had higher binding rates than the reference compound misonidazole. Binding

studies were performed at several oxygen concentrations and indicated a strong oxygen dependency below a concentration of 0.3%.

In vivo biodistribution of the four compounds as their ^{125}I analogs was performed in Balb/c mice bearing subcutaneous EMT-6 tumors. The maximum tumor to blood ratios for the test compounds were; IAZA, 8.7 at 8 h; IAZG, 1.6 at 4 h; IAZP, 13.9 at 24 h; FIAZP, 5.9 at 24 h. All four compounds showed a rapid excretion (>97% in 24 h) with moderate tissue levels, which in general declined as a function of blood clearance.

Whole-body scintigraphic studies in the Balb/c: EMT-6 mouse tumor model, delineated tumor tissue with ^{123}I labelled IAZA and IAZG at 8 h and 4 h post injection, respectively. These favourable results make these radioiodinated sugar-coupled analogs of 2-nitroimidazole potential markers of hypoxic tumor tissue.

ACKNOWLEDGEMENTS

With extreme pleasure and pride I have the honour to express my sincere gratitude and indebtedness to my supervisor Dr. Leonard I. Wiebe, Professor and Associate Dean of the Faculty of Pharmacy, for his constant and thoughtful guidance, keen interest and conceptual development of this research project. His patience, inspiration, affection, dynamic supervision and painstaking effort to read the thesis manuscript as well as valuable criticism and discussion made it all possible in successful completion of this work. I am especially obliged to him for his moral support through thick and thin and excellent teaching in every sphere of my studies. His enormous contributions in advancement of my academic career will always be remembered.

I am also indebted to my co-supervisor Dr. John R. Mercer, Adjunct Associate Professor of Faculty of Pharmacy, for his continuous, patient and thoughtful guidance along with encouragement and warm friendship throughout my studies. I am particularly thankful to him for his generous help in constructing Figures and Structures given in the thesis. His patience in reading the thesis manuscript and constructive criticism all through contributed much in successful completion of this work.

My heartfelt thanks and appreciation are due to Dr. J.D. Chapman, former Professor of Radiology, Cross cancer

Institute, for his help and advice in various aspects of this work and also for his facilities to perform radiobiological studies. Thanks are also extended to Mrs. Jane Lee for her help in doing *in vitro* studies as well as for supplying routinely EMT-6 tumor cells.

I am specially thankful to Dr. V.V. Somayaji, for her contribution in initial synthesis of the compounds studied in this project.

My sincere thanks and appreciations are extended to Daria Stypinski, Leock Ngo, Megan Wiebe and Madhu Jawanda, for their help in *in vivo* biodistribution studies, as part of their undergraduate summer studentship funded by Alberta Heritage Foundation for Medical Research.

My heartfelt thanks are also due to all of my committee members for their good will, suggestion and criticism on various aspects of the thesis. I am specially thankful to Mr. John Scott for his generous help in calculation of dosimetry and to Dr. Alec Shysh for his affection and ever willingness to help.

I am grateful to Dr. J. Bachynsky, former Dean and Dr. R. Moskalyk, Dean of Faculty of Pharmacy, for their help in various occasions. My Thanks are also due to all the teachers and staff of Faculty of Pharmacy, for their good will and friendship.

I wish to say "Thank you very much" to all my colleagues and friends, especially Fassil, Prassad, Saleh, Delwar,

Manju and Shradha, for their help, company, heartful co-operation, criticism and encouragement.

I am very much indebted to my Canadian grandmother Mrs. Kathelene Bell and grandfather Mr. Martin Bell for their love, affection and encouragement.

I am grateful to the Chairman of Department of Pharmacy, Vice-chancellor, University of Dhaka, Bangladesh, for granting me leave of absence to continue my Ph.D. program. I am also thankful to my teachers and colleagues at the University of Dhaka, especially to Drs. Azad chowdhury and Abdul Jabber for their excellent teaching during my study years at the Department of Pharmacy.

The financial supports in part by the University of Alberta/Canadian International Development Agency in the form of scholarship and the Faculty of Pharmacy in the form of part-time teaching assistantship is gratefully acknowledged. This work was funded by a grant from the Alberta Cancer Board, Grant # RI 15.

TABLE OF CONTENTS

Chapter		Page
1.	INTRODUCTION	1
2.	SURVEY OF RELATED LITERATURE	5
2.1.	HYPOXIA AND RADIOSENSITIVITY IN TUMORS	5
2.1.1.	Hypoxia in Tumors : Cause-effect relationships	5
2.1.2.	Radiosensitization of Hypoxic cells	7
2.1.3.	Development of Radiosensitizers	8
2.1.4.	Nitroimidazoles as Radiosensitizers	12
2.2.	BIOLOGICAL PROPERTIES OF NITROIMIDAZOLE RADIOSENSITIZERS	23
2.2.1.	General Metabolic Reactions of Nitroimidazoles	23
2.2.2.	Biochemistry of Nitro-Reduction	31
2.3.	TECHNIQUES FOR THE DETECTION OF TISSUE HYPOXIA	36
2.3.1.	Introduction	36
2.3.2.	Radiolabelled Radiosensitizers for the Detection of Tissue Hypoxia	38
3.	EXPERIMENTAL	48
3.1.	MATERIALS	48
3.1.1.	Chemicals, Solvents, Gases and Equipment	48
3.1.2.	Instruments	48
3.1.3.	Radioisotopes	50
3.1.4.	Animals	50
3.1.5.	Tumor Cell Line	50
3.2.	METHODS	51
3.2.1.	Synthesis of 1(5-Iodo-5-deoxy-ß-D-arabinofuranosyl)-2-nitroimidazole <Iodoazomycin Arabinoside:IAZA> (45)	51
3.2.2.	Synthesis of 1-(6-Iodo-6-deoxy-ß-D-galactopyranosyl)-2-nitro-imidazole <Iodoazomycin Galacto-side:IAZG> (49)	52
3.2.3.	Synthesis of 1(4-Iodo-4-deoxy-ß-L-xylopyranosyl)-2-nitroimidazole <Iodoazomycin Pyranoside:IAZP> (54)	52

3.2.4. Synthesis of 1-(2-Fluoro-2-deoxy-4-iodo-4-deoxy-β-L-xylopyranosyl)-2-nitroimidazole <2'-Fluoro-iodoazomycin Pyranoside:FIAZP> (60).....53

3.2.5. Exchange Radioiodination of 1-(5-Iodo-5-deoxy-β-D-arabinofuranosyl)-2-nitroimidazole <IAZA> (^{125}I-45),(^{123}I-45.....53
3.2.5.1. Solvent Exchange Method.....53
3.2.5.2. Pivalic Acid Melt Method.....55
3.2.6. Exchange Radioiodination of 1-(6-Iodo-6-deoxy-β-D-galactopyranosyl)-2-nitroimidazole <IAZG> (^{125}I-49), (^{123}I-49).....56
3.2.7. Preparation of <^{125}I> 1-(4-Iodo-4-deoxy-β-L-xylopyranosyl)-2-nitroimidazole (<^{125}I>-IAZP).....57
3.2.8. Preparation of <^{125}I> 1-(2-Fluoro-2-deoxy-4-iodo-4-deoxy-β-L-xylopyranosyl)-2-nitroimidazole (<^{125}I>-FIAZP).....58
3.2.9. Purification of Radiolabelled Compounds.....58
3.2.10. Measurement of Partition Coefficient....59
3.2.11. Study of Phosphorolysis of Test Compounds.....62
3.2.12. Animal Studies.....64
3.2.12.1. Preparation of the Animal Model.....64
3.2.12.2. Administration of Radiopharmaceuticals.....65
3.2.12.3. Collection of Tissue Samples..65
3.2.12.4. Biodistribution Study.....66
3.2.12.5. Whole-Body Scintigraphy.....67
3.2.12.6. *In vivo* Toxicity Study.....68

3.2.13. *In vitro* Study with EMT-6 Tumor cells...68
3.2.13.1. Cytotoxicity.....69
3.2.13.2. Initial Binding Rate.....70
3.2.13.3. Radiosensitization.....71

4. RESULTS AND DISCUSSION.....72

4.1. 1-(5-Iodo-5-Deoxy-β-D-Arabinofuranosyl)-2-Nitroimidazole (Iodoazomycin Arabinoside:IAZA)(45)...72
4.1.1. Chemistry.....72
4.1.2. *In vivo* Toxicity.....76
4.1.3. Cytotoxicity.....77
4.1.4. Radiosensitization.....81
4.1.5. Initial Binding Rate.....85
4.1.6. Biodistribution and Elimination.....89
4.1.7. Whole-Body Scintigraphy.....97

4.2. 1-(6-Iodo-6-Deoxy-ß-D-Galactopyranosyl)-2-Nitroimidazole (Iodoazomycin Galactoside:IAZG) (49).....107
4.2.1. Chemistry.....107
4.2.2. Cytotoxicity.....111
4.2.3. Radiosensitization.....114
4.2.4. Initial Binding Rate.....117
4.2.5. Biodistribution and Elimination.....120
4.2.6. Whole-Body Scintigraphy.....127

4.3. 1-(4-Iodo-4-Deoxy-ß-L-Xylopyranosyl)-2-Nitroimidazole (Iodoazomycin Pyranoside:IAZP) (54)...132
4.3.1. Chemistry.....132
4.3.2. *In vivo* Toxicity.....135
4.3.3. Cytotoxicity.....135
4.3.4. Radiosensitization.....138
4.3.5. Initial Binding Rate.....141
4.3.6. Biodistribution and Elimination.....145

4.4. 1-(2-Fluoro-2-Deoxy-4-Iodo-4-Deoxy-ß-L-Xylopyranosyl)-2-Nitroimidazole (2'-Fluoro-iodoazomycin Pyranoside: FIAZP) (60).....152
4.4.1. Chemistry.....152
4.4.2. Cytotoxicity.....154
4.4.3. Radiosensitization.....157
4.4.4. Biodistribution and Elimination.....159

5. COMPARATIVE SUMMARY OF PHYSICO-CHEMICAL AND BIOLOGICAL PROPERTIES OF VARIOUS SUGAR-COUPLED 2-NITROIMIDAZOLES.....167
5.1. Partition Coefficient.....167
5.2. Phosphorolysis.....171
5.3. Cytotoxicity.....172
5.4. Radiosensitization.....175
5.5. Initial Binding Rate.....179
5.6. Biodistribution.....182

6. CONCLUSIONS.....185

BIBLIOGRAPHY.....190

APPENDICES.....213
Appendix 1. Characteristics of the survival curve for cytotoxicity study.....213
Appendix 2. Calculation of initial binding rate.....215
Appendix 3. Characteristics of radiation-survival curve.....216
Appendix 4. Radiation dose estimates for the adult for ^{123}I-IAZA.....218

LIST OF TABLES

Table 1. Dependence of hypoxic cell radiosensitivity and cytotoxicity on reduction potential of various nitroimidazoles in chinese hamster V79 cells.....17

Table 2. Biodistribution of ^{125}I-IAZA following i.v. administration in Balb/c mice bearing EMT-6 tumors at various time intervals.....90

Table 3. Thyroid radioactivity as percent injected dose of ^{125}I-IAZA/organ, in Balb/c mice bearing EMT-6 tumors.....91

Table 4. Percent radiochemical yield of ^{125}I-IAZG and percent decomposition at various reaction times using Method A.....110

Table 5. Biodistribution of ^{125}I-IAZG following i.v. administration in Balb/c mice bearing EMT-6 tumors at various time intervals.....121

Table 6. Thyroid radioactivity as percent injected dose of ^{125}I-IAZG/organ, in Balb/c mice bearing EMT-6 tumors.....123

Table 7. Biodistribution of ^{125}I-IAZP following i.v. administration in Balb/c mice bearing EMT-6 tumors at various time intervals.....146

Table 8. Thyroid radioactivity as percent injected dose of ^{125}I-IAZP/organ, in Balb/c mice bearing EMT-6 tumors.....149

Table 9. Biodistribution of ^{125}I-FIAZP following i.v. administration in Balb/c mice bearing EMT-6 tumors at various time intervals.....160

Table 10. Thyroid radioactivity as percent injected dose of ^{125}I-FIAZP/organ, in Balb/c mice bearing EMT-6 tumors.....164

Table 11. Partition coefficient (P) for the sugar-coupled 2-nitroimidazoles and reference compounds.....168

Table 12. Calculated values of the substituent constants (π_x) for various sugar-coupled 2-nitroimidazoles.....170

Table 13. Partition coefficient and cytotoxicity (hr^{-1}) of sugar-coupled 2-nitroimidazoles.....175

Table 14. Partition coefficient and SER of sugar-coupled 2-nitroimidazoles.....177

Table 15. Cytotoxicity and SER of sugar-coupled 2-nitroimidazoles.....178

Table 16. Initial binding rate, partition coefficient and cytotoxicity of iodinated sugar-coupled 2-nitroimidazoles.....182

LIST OF FIGURES

Figure 1. Surviving fractions of hypoxic EMT-6 cells incubated with various concentrations of IAZA at various time intervals.....78

Figure 2. Surviving fractions of hypoxic EMT-6 cells incubated with various concentrations of AZA at various time intervals.....78

Figure 3. Comparison of hypoxic cell cytotoxicity as a function of reciprocal of time (hr^{-1}) for 90% cell kill with various concentrations of IAZA and AZA.....80

Figure 4. Surviving fractions of EMT-6 cells at various radiation doses in air, nitrogen and nitrogen plus various concentrations of IAZA.....82

Figure 5. Surviving fractions of EMT-6 cells at various radiation doses in air, nitrogen and nitrogen plus various concentrations of AZA.....82

Figure 6. Comparison of sensitizer enhancement ratios (SER) of IAZA and AZA as a function of substrate concentration in vitro with hypoxic EMT-6 cells.....84

Figure 7. ^{125}I Activity bound to acid-insoluble fraction of EMT-6 cells after incubation with various concentrations of ^{125}I-IAZA at various time periods under hypoxic and aerobic conditions.....86

Figure 8. The initial binding rates, expressed as pmol/10^6 cells/h, of ^{125}I-IAZA to the acid-insoluble fraction of hypoxic EMT-6 cells at various concentrations of the test substrate.....86

Figure 9. ^{125}I Activity bound to the acid-insoluble fraction of EMT-6 cells under hypoxia and various levels of oxygen incubated with 10 μM ^{125}I-IAZA, at several time periods.....88

Figure 10. The initial binding rate of 10 μM ^{125}I-IAZA to the acid-insoluble fraction of EMT-6 cells under hypoxia and various levels of oxygenation.....88

Figure 11. Tissue to blood ratios of radioactivity at various time intervals following i.v. administration of ^{125}I-IAZA in Balb/c mice bearing EMT-6 tumors.....92

Figure 12. Tissue to blood ratios of radioactivity at various time intervals following i.v. administration of ^{125}I-IAZA in Balb/c mice bearing EMT-6 tumors.....92

Figure 13. Whole-body elimination and blood clearance of radioactivity following i.v. administration of ^{125}I-IAZA in Balb/c mice bearing EMT-6 tumors.....95

Figure 14. Static whole-body gamma scintigram of ^{125}I-IAZA at 2 hour post injection, in a Balb/c mouse bearing an EMT-6 tumor.....98

Figure 15. Static whole-body gamma scintigram of ^{125}I-IAZA at 8 hour post injection in a Balb/c mouse bearing an EMT-6 tumor.....99

Figure 16. Static whole-body gamma scintigram of ^{123}I-IAZA in a Balb/c mouse bearing an EMT-6 tumor, without thyroid block.....101

Figure 17. Static whole-body gamma scintigram of ^{123}I-IAZA in a Balb/c mouse bearing an EMT-6 tumor, without thyroid block.....102

Figure 18. Static whole-body gamma scintigram of ^{123}I-IAZA in a Balb/c mouse bearing an EMT-6 tumor, with blocked thyroid.....103

Figure 19. Static whole-body gamma scintigram of ^{123}I-IAZA in a Balb/c mouse bearing an EMT-6 tumor, with blocked thyroid.....104

Figure 20. Surviving fractions of hypoxic EMT-6 cells incubated with various concentrations of IAZG at various time intervals.....112

Figure 21. Surviving fractions of hypoxic EMT-6 cells incubated with various concentrations of AZG at various time intervals.....112

Figure 22. Comparison of hypoxic cell cytotoxicity as a function of reciprocal of time (hr^{-1}) for 90% cell kill with various concentrations of IAZG and AZG.....113

Figure 23. Surviving fractions of EMT-6 cells at various radiation doses in air, nitrogen and nitrogen plus various concentrations of IAZG.....115

Figure 24. Surviving fractions of EMT-6 cells at various radiation doses in air, nitrogen and nitrogen plus various concentrations of AZG.....115

Figure 25. Comparison of sensitizer enhancement ratios (SER) of IAZG and AZG as a function of substrate concentration in vitro with hypoxic EMT-6 cells.....116

Figure 26. ^{125}I Activity bound to the acid-insoluble fraction of EMT-6 cells after incubation with various concentrations of ^{125}I-IAZG at various time periods, under hypoxic and aerobic conditions.....118

Figure 27. The initial binding rates expressed as pmol/10^6 cells/h of ^{125}I-IAZG to the acid-insoluble fraction of hypoxic EMT-6 cells at various concentrations of test substrate.....118

Figure 28. ^{125}I Activity bound to the acid-insoluble fraction of EMT-6 cells under hypoxia and various levels of oxygen incubated with 10 μM ^{125}I-IAZG, at several time periods.....119

Figure 29. The initial binding rate of 10 μM ^{125}I-IAZG to the acid-insoluble fraction of EMT-6 cells under hypoxia and various levels of oxygenation.....119

Figure 30. Tissue to blood ratios of radioactivity at various time intervals following i.v. administration of ^{125}I-IAZG in Balb/c mice bearing EMT-6 tumors.....124

Figure 31. Tissue to blood ratios of radioactivity at various time intervals following i.v. administration of ^{125}I-IAZG in Balb/c mice bearing EMT-6 tumors.....124

Figure 32. Whole-body elimination and blood clearance of radioactivity following i.v. administration of ^{125}I-IAZG in Balb/c mice bearing EMT-6 tumors.....126

Figure 33. Static whole-body gamma scintigram of ^{123}I-IAZG in a Balb/c mouse bearing an EMT-6 tumor, without thyroid block.....128

Figure 34. Static whole-body gamma scintigram of ^{123}I-IAZG in a Balb/c mouse bearing an EMT-6 tumor, with a thyroid block.....129

Figure 35. Static whole-body gamma scintigram of ^{123}I-IAZG in a Balb/c mouse bearing an EMT-6 tumor, without thyroid block.....131

Figure 36. Surviving fractions of hypoxic EMT-6 cells incubated with various concentrations of IAZP at various time intervals.....136

Figure 37. Surviving fractions of hypoxic EMT-6 cells incubated with various concentrations of AZP at various time intervals...136

Figure 38. Comparison of hypoxic cell cytotoxicity as a function of the reciprocal of time (hr^{-1}) for 90% cell kill, with various concentrations of IAZP and AZP.....137

Figure 39. Surviving fractions of EMT-6 cells at various radiation doses in air, nitrogen and nitrogen plus various concentrations of IAZP.....139

Figure 40. Surviving fractions of EMT-6 cells at various radiation doses in air, nitrogen and nitrogen plus various concentrations of AZP.....139

Figure 41. Comparison of sensitizer enhancement ratios (SER) of IAZP and AZP as a function of substrate concentration *in vitro* with hypoxic EMT-6 cells.....140

Figure 42. ^{125}I Activity bound to the acid-insoluble fraction of EMT-6 cells after incubation with various concentrations of ^{125}I-IAZP at various time periods under hypoxic and aerobic conditions.....142

Figure 43. The initial binding rates expressed as pmol/10^6 cells/h of ^{125}I-IAZP bound to the acid-insoluble fraction of hypoxic EMT-6 cells at various concentrations of the test substrate.....142

Figure 44. ^{125}I Activity bound to the acid-insoluble fraction of EMT-6 cells under hypoxia and various levels of oxygen incubated with 10 μM ^{125}I-IAZP at several time periods.....144

Figure 45. The initial binding rate of 10 μM ^{125}I-IAZP bound to the acid-insoluble fraction of EMT-6 cells under hypoxia and various levels of oxygenation.....144

Figure 46. Tissue to blood ratios of radioactivity at various time intervals following i.v. administration of ^{125}I-IAZP in Balb/c mice bearing EMT-6 tumors.....147

Figure 47. Tissue to blood ratios of radioactivity at various time intervals following i.v. administration of ^{125}I-IAZP in Balb/c mice bearing EMT-6 tumors.....147

Figure 48. Whole-body elimination and blood clearance of radioactivity following i.v. administration of ^{125}I-IAZP in Balb/c mice bearing EMT-6 tumors.....150

Figure 49. Surviving fractions of hypoxic EMT-6 cells incubated with various concentrations of FIAZP at various time intervals.....155

Figure 50. Surviving fractions of hypoxic EMT-6 cells incubated with various concentrations of FAZP at various time intervals.....155

Figure 51. Comparison of hypoxic cell cytotoxicity as a function of the reciprocal of time (hr^{-1}) for 90% cell kill with various concentrations of FIAZP and FAZP.....156

Figure 52. Surviving fractions of EMT-6 cells at various radiation doses in air, nitrogen and nitrogen plus various concentrations of FIAZP.....158

Figure 53. Surviving fractions of EMT-6 cells at various radiation doses in air, nitrogen and nitrogen plus various concentrations of FAZP.....158

Figure 54. Comparison of sensitizer enhancement ratios (SER) of FIAZP and FAZP as a function of substrate concentration *in vitro* with hypoxic EMT-6 cells.....159

Figure 55. Tissue to blood ratios of radioactivity at various time intervals following i.v. administration of ^{125}I-FIAZP in Balb/c mice bearing EMT-6 tumors.....162

Figure 56. Tissue to blood ratios of radioactivity at various time intervals following i.v. administration of ^{125}I-FIAZP in Balb/c mice bearing EMT-6 tumors.....162

Figure 57. Whole-body elimination and blood clearance of radioactivity following i.v. administration of ^{125}I-FIAZP in Balb/c mice bearing EMT-6 tumors.....165

Figure 58. Comparison of cytotoxicity, defined as the reciprocal of time to kill 90% of the hypoxic EMT-6 cells, as a function of substrate concentration for sugar-coupled 2-nitroimidazoles and reference compounds.....173

Figure 59. Comparison of sensitizer enhancement ratio as a function of substrate concentration for sugar-coupled 2-nitroimidazoles and reference compounds.....176

Figure 60. Comparison of initial binding rates of sugar-coupled 2-nitroimidazoles and reference compounds to the acid-insoluble fraction of hypoxic EMT-6 cells plotted as a function of substrate concentration.....180

Figure 61. Comparison of tumor to blood ratios at various time periods following i.v. administration of ^{125}I labelled test substrates into Balb/c mice bearing EMT-6 tumors.....183

LIST OF SCHEMES

Scheme 1. Sequence of the reduction and electron transfer process in nitroimidazoles.....25

Scheme 2. Sequence of nitroimidazole ring fragmentation.....27

Scheme 3. Pathways of nitroimidazole conjugation reaction.....29

Scheme 4. A schematic of the biochemical process of electron transfer of nitroimidazoles.....32

Scheme 5. A proposed scheme for the reaction of reduced intermediate species of nitroimidazole with GSH.....35

Scheme 6. Synthesis of 1-(5-iodo-5-deoxy-ß-D-arabinofuranosyl)-2-nitroimidazole (IAZA, 45).....73

Scheme 7. Synthesis of radioiodinated 1-(5-iodo-5-deoxy-ß-D-arabinofuranosyl)-2-nitroimidazole 74

Scheme 8. Synthesis of 1-(6-iodo-6-deoxy-ß-D-galactopyranosyl)-2-nitroimidazole (IAZG, 49).....108

Scheme 9. Synthesis of radioiodinated 1-(6-iodo-6-deoxy-ß-D-galactopyranosyl)-2-nitroimidazole.....109

Scheme 10. Synthesis of 1-(4-iodo-4-deoxy-ß-L-xylopyranosyl)-2-nitroimidazole (IAZP, 54).....133

Scheme 11. Synthesis of radioiodinated 1-(4-iodo-4-deoxy-ß-L-xylopyranosyl)-2-nitroimidazole.....134

Scheme 12. Synthesis of 1-(2-fluoro-2-deoxy-4-iodo-4-deoxy-ß-L-xylopyranosyl)-2-nitroimidazole (FIAZP, 60).....152

Scheme 13. Synthesis of radioiodinated 1-(2-fluoro-2-deoxy-4-iodo-4-deoxy-ß-L-xylopyranosyl)-2-nitroimidazole.....153

LIST OF ABBREVIATIONS

AZA	azomycin arabinoside
AZG	azomycin galactoside
AZP	azomycin pyranoside
AZR	azomycin riboside
BBB	blood brain barrier
BUdR	bromo-deoxyuridine
°C	degree Celsius
CHO	Chinese hamster ovary
Ci	curie
cm	centimeter(s)
CO_2	carbon dioxide
cpm	count per minute
DMF	dimethyl formamide
DNA	deoxyribonucleic acid
dpm	disintegration per minute
dThd	deoxythymidine
dUrd	deoxyuridine
E_7^1	one electron reduction potential
FAZP	2'-fluoroazomycin pyranoside
FIAZP	2'-fluoro-4'-iodoazomycin pyranoside
g	gram(s)
GBq	gigabecquerel
GSH	glutathione

GSSG	oxidized glutathione
Gy	Gray
h	hour(s)
H_2O_2	hydrogen peroxide
HPLC	high pressure liquid chromatography
HBSS	Hanks' balance salt solution
IAZA	iodoazomycin arabinoside
IAZG	iodoazomycin galactoside
IAZP	iodoazomycin pyranoside
IAZR	iodoazomycin riboside
i.v.	intravenous
i.p.	intraperitoneal
kBq	kilobecquerel
kg	kilogram(s)
KI	potassium iodide
KOH	potassium hydroxide
L	litre(s)
LET	linear energy transfer
M	molar
MBq	megabecquerel
mCi	millicurie
µCi	microcurie
MEM	minimal essential medium
MeOH	methanol
mg	milligram(s)
µg	microgram(s)

min.	minute(s)
mL	millilitre(s)
mM	millimolar
mm	millimeter(s)
µm	micrometer(s)
mmol	millimole(s)
µmol	micromole(s)
mol	mole(s)
MRI	magnetic resonance imaging
mV	millivolt(s)
mol. wt.	molecular weight
N	normal
NADP	nicotinamide adenine dinucleotide phosphate
NADPH	nicotinamide adenine dinucleotide phosphate (reduced form)
NEM	N-ethylmaleimide
nm	nanometer(s)
nmol	nanomole(s)
NaOH	sodium hydroxide
NPPN	norpsuedopellitierine-N-oxyl
OER	oxygen enhancement ratio
P	partition coefficient
PET	positron emission tomography
pmol	picomole(s)
PNAP	paranitroacetophenone

r	correlation coefficient
S.D.	standard deviation
SER	sensitizer enhancement ratio
TAF	tumor angiogenesis factor
TAN	triethanolamine N-oxyl
TCA	trichloroacetic acid
TEF	tumor endothelial factor
TLC	thin layer chromatography
U	unit(s)
uv	ultraviolet

1. INTRODUCTION

Hypoxic cells are known to exist in both human and animal solid tumors. Tissues that contain hypoxic cells are 2.5 to 3 times more resistant to therapeutic ionizing radiation than normally oxygenated cells. The radiation sensitivity of normally oxygenated cells is directly attributed to the ability of oxygen to 'fix' radiation damage, a phenomenon referred to as the oxygen effect[1].

Over the past two decades a considerable effort has been given to the development and use of hypoxic cell radiosensitizers. These are compounds that mimic the effect of oxygen in sensitizing hypoxic cells to the damaging effects of ionizing radiation. Many compounds which were found to have *in vitro* radiosensitizing properties, however, showed little or no promise *in vivo* due to either toxicity limitations[2,3] or poor tumor penetration[4,5]. Nitroimidazoles emerged as a class of radiosensitizer with favourable properties of electron affinity and partition coefficient. Several members of this class have shown considerable radiation sensitization in experimental tumor models[6,7]. Nitroimidazoles, especially N^1-substituted 2-nitroimidazole derivatives, occupy a central role in the development of hypoxic cell radiosensitizers. Over the years, a number of these compounds showed promising results in sensitizing hypoxic cells to ionizing radiation both *in vivo* and *in vitro*. Misonidazole (1) is the

most widely studied compound of this class. Despite its dose-dependent neurotoxicity in humans, this compound is considered to be a reference standard against which the efficacy of other newly developed radiosensitizers is compared.

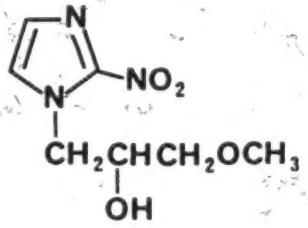

1

The selectivity of these 2-nitroimidazole radiosensitizers is related to their ability to form adducts to cellular molecules, via metabolic processes which are several times more active under hypoxia than under aerobic conditions[8,9]. It has been proposed that this selective adduct formation, between 2-nitroimidazoles and cellular molecules, might be exploited to assess tissue hypoxia[10]. The assessment of tissue hypoxia in tumors prior to and after treatment would be of invaluable assistance for designing treatment strategies and also for the evaluation of treatment response. A variety of methods to provide this information have been explored, all of which are either

invasive or impractical in the clinical milieu. A non-invasive, in vivo scintigraphic technique would therefore be a suitable alternative for the detection and assessment of hypoxic cells in tumor tissue in a clinical setting. It may be possible to accomplish this task by labelling 2-nitroimidazole derivatives with appropriate gamma emitting radionuclides. Theoretically, an hypoxic cell marker should possess all of the good qualities of an ideal radiosensitizer and at the same time must be suitable for labelling with a gamma emitting radionuclide without affecting its physico-chemical properties. Although misonidazole is a potential radiosensitizer, it is not suitable for non-invasive detection of tissue hypoxia. This is because the molecule contains C, N, H, O and there are no practical radioisotopes for use of these elements. Furthermore, analogs containing other more useful gamma emitters are subject to change in physico-chemical properties and biological activity.

A radioiodinated sugar-coupled 2-nitroimidazole (Iodoazomycin riboside: IAZR) (2) was synthesized to incorporate the properties required to maintain its usefulness as a non-invasive, scintigraphic marker of tumor hypoxia. The lipophilic nature of a previously investigated radioiodinated nitroimidazole[11] was moderated in IAZR (2) by introducing the sugar moiety. This structural feature presumably did not affect the electron affinity of the 2-nitroimidazole ring[12].

This compound, although very promising in terms of radiosensitization and selective binding to hypoxic cells *in vitro*[12], was radiochemically unstable *in vivo*[13]. This reduced stability severely limited its utility as an *in vivo* radiosensitizer or marker for the detection of hypoxic cells.

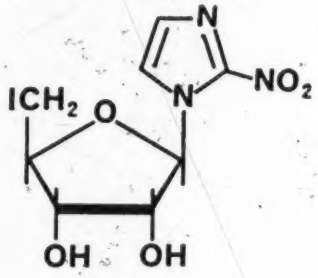

2

The results obtained with IAZR have now led to the investigation of a series of radioiodinated sugar-coupled 2-nitroimidazoles, in an effort to identify compounds with similar or better selective, hypoxia-dependent binding properties and with increased *in vivo* stability. The results of these *in vitro* and *in vivo* investigations are the subject of this thesis.

2. SURVEY OF RELATED LITERATURE

2.1. HYPOXIA AND RADIOSENSITIVITY IN TUMORS

2.1.1. Hypoxia in Tumors : Cause-effect relationships

Viable cells that lack oxygen are known as hypoxic cells. There are two distinct kinds of hypoxic cells reported to be present in tumors:-

a) Chronically hypoxic cells : Cells are chronically hypoxic because of inadequate diffusion of oxygen from blood vessels[14]. The reason for such inadequate diffusion is that oxygen supplied by the capillaries is depleted by metabolism in intervening cells closer to the capillaries[15].

b) Acutely hypoxic cells : These kinds of cells develop due to transiently reduced perfusion[16,17].

Studies with transplantable mouse tumors showed that the proliferating zones of tumor cells occur within a 100 ± 30 µm radius around blood vessels. This distance closely corressponds to computed maximum oxygen diffusion distances, when consumption of oxygen is accounted for by cellular respiration[18,19]. The necrotic zone in a tumor has been reported to occur beyond the distance of 200 ± 20 µm from the blood vessels[14]. Presumably hypoxia occurs between these two zones. This kind of heterogeneity in tumor growth is

related to a number of factors, of which the major is tumor vasculature and the resulting limited diffusion of oxygen and nutrients[18,20,21]. Tumor vasculature is regulated by a factor called tumor endothelial factor (TEF) or tumor angiogenesis factor (TAF)[21]. This factor, which is released by the tumor itself, induces proliferation of vascular endothelium and penetration of blood vessels into a tumor mass[21]. In a rapidly growing solid tumor the vasculature is often poor due to inadequate release of TAF or TEF. The resulting inadequate angiogenesis results in the formation of hypoxic, as well as necrotic, zones in the tumor[21,22,23].

The relationship between cellular oxygen tension and radiosensitivity has been demonstrated in many systems. The enhancement of radiation damage by oxygen was first demonstrated in 1921 by Holthusen[24].

The largest heterogeneity in tumor control by radiotherapy is due to the variation in radiosensitivity between normally oxygenated and hypoxic cells. Hypoxic cells show radioresistance about three times greater than well-oxygenated cells[25]. In addition to radioresistance, hypoxic cells have been clearly shown to lead to local recurrence of some human cancers[26].

2.1.2. Radiosensitization of Hypoxic Cells

A number of ways have been evaluated to increase the radioresponse of tumor cells that are hypoxic. These are as follows :

a) Fractionated radiotherapy : In this type of therapy the more sensitive oxygenated cells are killed by the initial fraction of radiation dose, thereby optimizing the reoxygenation process within the tumor. The hypoxic cells, after reoxygenation, are killed by the next fraction(s) of dose[27,28].

b) Oxygen delivery to tumor : Several methods of enhancing oxygen delivery to tumors have been investigated. Clinical trials for patients breathing hyperbaric oxygen during radiotherapy showed little improvement in tumor therapy[29,30]. Artificial oxygen carriers such as perfluorocarbon emulsions were investigated in preoperative and anaemic patients, as oxygen carriers or blood substitutes[31,32]. The most frequently used compound, fluosol-DA(20%), enhanced the radiation response of animal tumors when the animals breathed 100% oxygen during irradiation[33,34]. Characteristics of oxygen diffusion in tumor tissue were altered in another experiment by inhibiting oxygen consumption by normally oxygenated cells in tumor. This was proposed to facilitate further diffusion of oxygen from blood vessel to hypoxic tissue[35].

c) Heavy particle radiation : High LET radiations such as neutrons, negative pi-mesons and heavy charged particles exhibit smaller oxygen enhancement ratios[36] (OER)[a]. However, such radiation requires expensive and complex equipment, making it impractical at present for routine radiotherapy[37].

d) Radiosensitizers : Radiosensitizers are chemicals that behave like oxygen in sensitizing hypoxic tumor cells to radiation. Unlike oxygen, these compounds are often not consumed by cellular metabolism in oxygenated cells and therefore more readily diffuse to hypoxic cells[15,37].

2.1.3. Development of Radiosensitizers.

Most of the pioneering work in the development of radiosensitizers was carried out in the 1960's. N-Ethylmaleimide (NEM, 3) was one of the early radiosensitizers studied in hypoxic suspensions of E.coli bacteria[38]. Initially NEM (3) was thought to act as a radiosensitizer by depleting thiol groups[38]. Later, however, it was concluded that radiation-induced, fast, free-radical reaction processes were the main mechanism[39]. Investigations continued with a variety of other compounds including the stable free-radical type

---

[a]OER is the Oxygen Enhancement Ratio. This is calculated as the ratio of radiation dose in hypoxia to the radiation dose in air which generates the same level of damage.

sensitizers triacetoneamine-N-oxyl (TAN, 4)[40], norpseudopellitierine-N-oxyl (NPPN, 5)[41] and biradical Ro-03-6061 (6)[42]. All of these compounds were found to act as radiosensitizers in bacterial cell culture by undergoing either radiation-induced free-radical or oxidation/reduction reactions[40-42]. Further investigation of these compounds was limited due to their toxicity in mammalian cells[15].

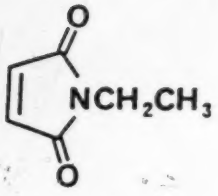

3

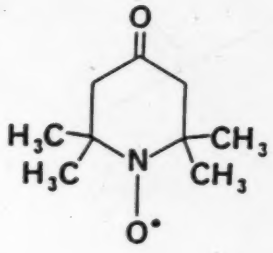

4

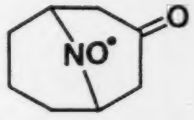

5

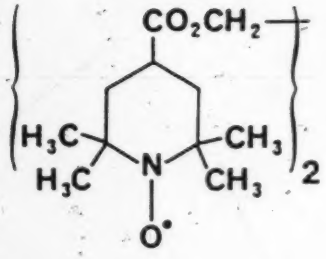

6

ICH_2CONH_2

7

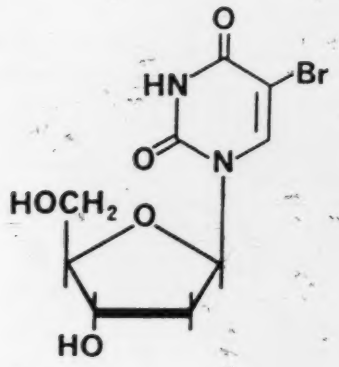

8

Narayan et al, in a review article[15], describe the in vitro study of two types of early radiosensitizers; iodoacetamide (7) and 5-bromodeoxyuridine (5-BUdR, 8). Iodoacetamide (7) was reported to act by forming a radiation-induced cytotoxic product, and 5-BUdR (8) by its incorporation into DNA thereby increasing the fragility of this structure to radiation.

The very important concept of electron affinity and its correlation with radiosensitizing effectiveness was introduced in early 1960's[43]. This represents a turning point with increased emphasis on the development of electron affinic radiosensitizers. Among the many electron affinic compounds synthesized were the conjugated diketones, quinones, aromatic and nitro ketones, unsaturated esters and derivatives of pyruvic acid[44]. Studies with various vegetative bacteria and bacterial spores showed that these compounds were effective as radiosensitizers under hypoxic conditions, but not in the presence of air[44].

Paranitroacetophenone (PNAP, 9) was one of the first nitro substituted aromatic compounds studied in mammalian cells in vitro[45-47]. At a concentration of 400 μM in hypoxic chinese hamster cells, a sensitizer enhancement ratio (SER)[a] of 1.7 was attained[46,47]. Moreover, sensitization

---

[a]SER is the Sensitizer Enhancement Ratio, calculated as the ratio of radiation dose without drug to the radiation dose with drug to achieve same level of damage.

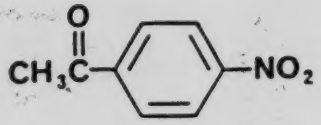

9

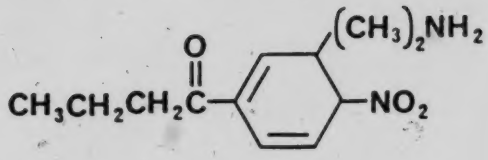

10

occurred at all phases of the cell cycle[46]. Only nitro substituted acetophenone appeared to be effective in sensitizing hypoxic mammalian cells[46,48]. Toxicity and low water solubility limited the use of PNAP (9) *in vivo*[45-47].

p-Nitro-3-dimethylamine propiophenone (NDPP, 10) was the first radiosensitizer used *in vivo* for sensitization of hypoxic cells[49]. NDPP (10) was given by intraperitoneal injection to mice hosting P-388 leukaemia cells as an ascitic suspension (ascitic tumor). An SER of 1.6 to 1.7 was reported, whereas the OER was 2.7[49]. An initial *in vitro* study of this compound with hypoxic chinese hamster cells showed an SER of 2.2 at very low drug concentration (18 μM)[50].

The favourable results obtained in these early experiments with nitroaromatic compounds led to the development of other hypoxic radiosensitizing compounds containing a nitro group. These included nitrofurans[51-53], nitropyrazoles[54] and

nitropyroles[55]. These radiosensitizers did not develop further, as other less toxic, electron affinic radiosensitizers were found; The nitroimidazole derivatives are the most important of these.

2.1.4. Nitroimidazoles as Radiosensitizers

The imidazole ring system was first described in 1858[56]. Much of the pioneering work on the chemistry of nitroimidazoles was carried out in the early part of this century[57]. Between the mid-twenties and early fifties, little further work appeared in the literature. The discovery of the naturally-occurring antibiotic azomycin (2-nitroimidazole, 11) in 1953[58] led to intense research during the late fifties. Until 1965, 2-nitroimidazole (11) and its homologs had not been prepared by total synthesis. In 1965 the synthesis of (11) was reported simultaneously by two different groups of researchers[59,60].

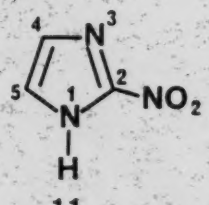

11

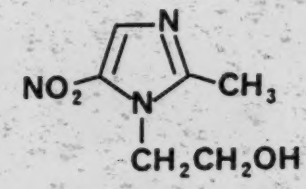

12

A well known trichomonacide, metronidazole (12), emerged as a nitroimidazole radiosensitizer, as a result of *in vitro* and *in vivo* studies. An SER of 2.0 was obtained *in vitro* with hypoxic chinese hamster V79 cells[61,62]. In various mouse tumor models, SER values ranged from 1.2 to 1.8[63-67]. These encouraging results enabled researchers to initiate a clinical trial. Metronidazole (12) was the first nitroimidazole given to patients[68,69]. In Phase 1 clinical studies, nausea and vomiting were observed as a result of dose-limiting toxicity[70].

At about the same time another nitroimidazole derivative, misonidazole (1), was reported to have a greater SER than metronidazole (12). SER values of 2.5 and 2.1 for misonidazole were obtained *in vitro* and *in vivo*, respectively[54,71]. As an hypoxic cell radiosensitizer, misonidazole was studied in detail both *in vitro*[71-73] and *in vivo*[74,75]. However, as well as being more effective *in vivo* and *in vitro*, misonidazole (1), with an LD_{50} of 1.8 mg/g body weight, was found to be 2 times more toxic to mice than metronidazole (12)[76]. Misonidazole (1) was the first 2-nitroimidazole derivative to undergo clinical trial as a radiosensitizer[77-79]. However, clinical evaluation of this drug (1) was a great disappointment due to its neurotoxicity at therapeutic dose levels[80-84]. At clinically safe doses it (1) appeared to have little or no radiosensitizing effect[84,85].

Investigations with nitroimidazoles continued further in an effort to identify compounds having similar or better radiosensitizing efficiency with less *in vivo* toxicity than misonidazole (1). In the development of novel radiosensitizers, major considerations were given to the electron affinity and partition coefficient.

The electron affinity of a compound is measured by its one electron reduction potential (E_7^1), using the pulse radiolysis method, which measures the one-electron transfer equilibrium between a given compound and reference solute of known potential. The values are expressed in units of -mV : the more electron affinic the compound the less negative the potential. As mentioned earlier, the electron affinity or reduction potential of a compound is related to its radiosensitizing efficiency. Three different mechanisms were found to be involved in this process :

a) An increase in reduction potential increases the cytotoxicity to hypoxic cells more than to aerobic cells. Greater cytotoxicity in hypoxic cells is due to the formation of toxic reduction intermediate products of nitroimidazoles[86].

b) Depletion of cellular glutathione (GSH) occurs when hypoxic cells are exposed to nitroimidazoles. This depletion is due to the formation of reactive reduction intermediates which form adducts with GSH[87]. The rate of adduct formation is faster when the reduction poten-

tial of the compound is higher[86]. Depletion of GSH levels increases cellular radiosensitivity by removing protective groups needed for repair of radiation damage[87].

c) Radiation-induced free radicals initiate another mechanism of sensitization[87]. In this process nitroimidazoles mimic the effect of oxygen by increasing the rates of radiation-induced DNA strand breakage in hypoxic cells as well as by oxidizing free radicals generated in DNA by the radiation.

The partition coefficient (P) is a measure of the relative solubility of a drug in water and lipid, and is used as a model for the drug's diffusion across a biological membrane. It is usually determined experimentally by measuring equilibrium partitioning of a drug between the aqueous phase and the 1-octanol phase in a water/octanol system. Lipophilic drugs possess a higher P value than hydrophillic ones. Most drugs cross cell membranes by passive diffusion. However, classic studies determined that the penetration rate is related to partition coefficient. Lipophilic drugs can diffuse through phospholipid bilayer membranes faster than hydrophillic ones[88,89].

The significance of reduction potential (E_7^1) on the <u>in vitro</u> radiosensitization of hypoxic cells was studied with a variety of nitroimidazole derivatives of various reduction

potentials[90-95]. Table 1 presents a number of nitroimidazoles along with their reduction potentials and partition coefficients as well as their radiosensitizing ability and cytotoxicity in chinese hamster V79 cells.

From the Table 1 it is clear that reduction potential influences the SER. The compound KA-161, a 2,4-dinitroimidazole derivative (15), which has the highest reduction potential (-229 mV) of those studied, showed a correspondingly high SER[91,92]. It is also evident from Table 1 that the position of the nitro group in the imidazole ring influences the reduction potential. The reduction potential is in the order of 2-nitro > 5-nitro > 4-nitro. The SER also is in the similar order, such that misonidazole (1) > nimorazole (16) > RWG 611 (19) for example. Some exceptions are also evident with the 5-substituted 4-nitroimidazoles (22-25). The *in vitro* SER for these compounds was found to be higher than would be predicted from their reduction potential[95]. The 5-substituents investigated are sulphamids, sulphonates and sulphone, with E_7^1 ranging from -523 mV to -342 mV[95].

It appears that the reduction potential not only influences the radiosensitizing property but also increases the cytotoxic property (Table 1). This is probably due to the increased rate of reduction of these compounds to toxic intermediates[96]. For the compounds (1,12-14,16,17) in Table 1, the cytotoxicity to hypoxic chinese hamster cells

Table 1. Dependence of hypoxic cell radiosensitivity and cytotoxicity on reduction potential of various nitroimidazoles in Chinese Hamster V79 cells.

Compound	E½ (mV)	P	SER	Conc. (mM)[a]	Conc. (mM)[b]	Ref.
Metronidazole (12)	-486	0.96	1.6	4.0	75.0	90, 96
Misonidazole (1)	-389	0.43	1.6	0.3	1.2	90, 96
Desmethylmiso (13)	-389	0.11	1.6	0.9	1.2	90, 96
Ro-11-3696 (14)	-476	1.10	1.6	1.0	35.0	90, 96
KA 161 (15)	-229	-	2.0	0.1	-	91, 92
Nimorazole (16)	-457	1.40	1.4	0.8	25.0	93, 94, 96
Benzonidazole (17)	-380	8.20	1.4	0.11	0.85	93, 94, 96
Ro-07-0269(18)	-384	1.50	1.4	0.29	-	93, 94
RGW 611 (19)	-554	0.42	1.4	3.0	-	93, 94
AM-1 (20)	-564	0.44	1.4	4.0	-	93, 94
RGW 607 (21)	-393	1.31	1.4	0.17	-	93, 94
NSC 38075 (22)	-395	0.23	1.6	37×10^{-3}	-	95
NSC 38083 (23)	-409	0.49	1.6	17×10^{-3}	-	95
NSC 38087 (24)	-342	12.30	1.6	2.6×10^{-3}	-	95
NSC 46509 (25)	-523	0.01	1.3	2.0	-	95
Tinidazole (26)	-464	0.44	1.4	0.9	-	94
Ornidazole (27)	-467	4.20	1.4	0.5	-	94

[a]Concentration required for quoted SER. [b]Concentration required for cytotoxicity at 10% survival in 5 hours.

increases with an increase in the reduction potential of the compounds[96]. A similar relationship was also observed for other nitroimidazoles in aerobic cells[94]. However, the mechanism of aerobic cell cytotoxicity seems to be different than hypoxic cell cytotoxicity[94]. The aerobic cytotoxicity of nitroimidazoles is reported to be due to the changing position of electron-transport equilibria in aerobic cells induced by higher electron affinic nitroimidazoles[94].

No general correlation between partition coefficient and *in vitro* radiosensitivity/cytotoxicity was obvious with the data presented in Table 1. Some selected correlations can be observed as for example with desmethylmisonidazole (13), which has an E_7^1 equal to misonidazole (1) but was found to be 3 times less effective as a radiosensitizer than misonidazole (1)[90,94]. This behaviour is related to the lower partition coefficient of this compound (13). It diffuses more slowly into the cell and thereby does not achieve the concentration needed to induce the maximum SER[90]. In general, P values higher than 0.04 do not influence the *in vitro* radiosensitization effectiveness of nitroimidazoles[90]. However, a loss of radiosensitizing efficiency was noted with compounds having P values lower than 0.04[97].

For *in vivo* radiosensitization an optimum balance of lipophilicity-hydrophilicity is very important. The therapeutic effects of radiosensitizers are ultimately related to the concentration of drug in the tumor at the time of

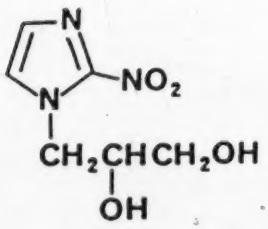

13

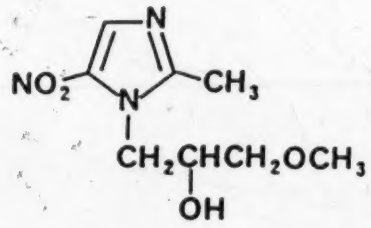

14

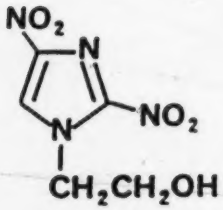

15

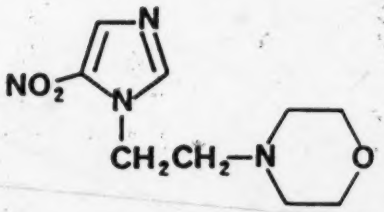

16

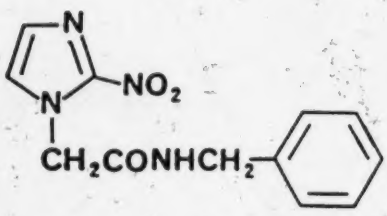

17

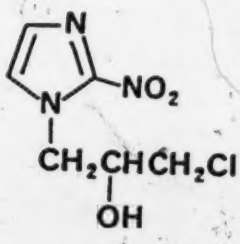

18

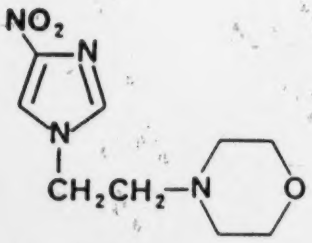

19

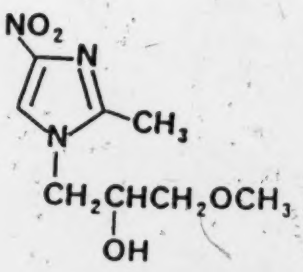

20

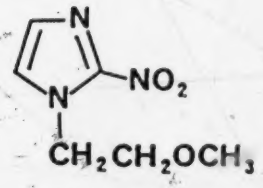

21

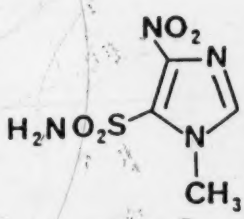

22

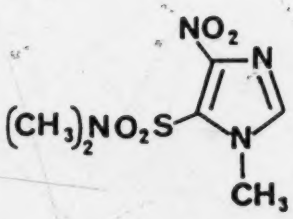

23

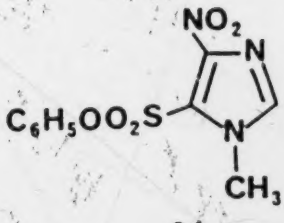

24

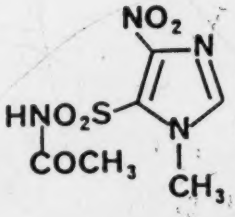

25

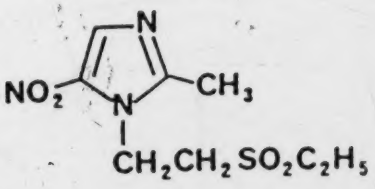

26

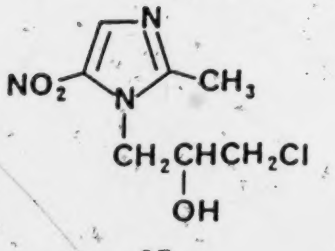

27

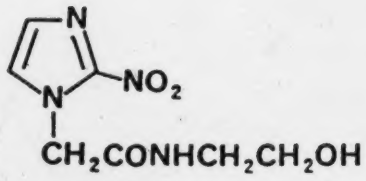

28

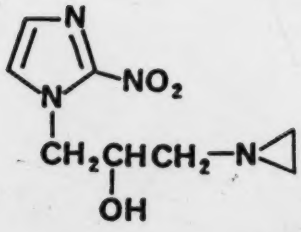

29

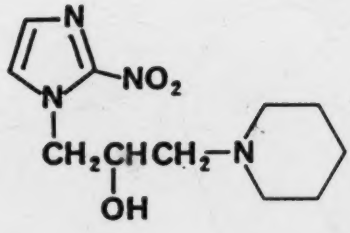

30

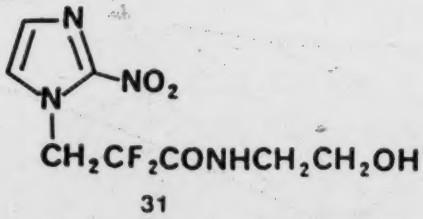

31

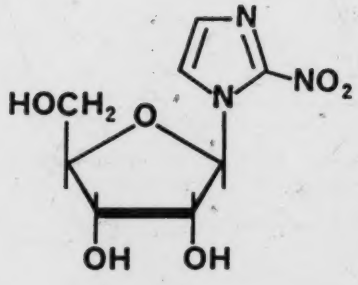

32

irradiation[98,99]. This balance of partition also minimizes the incidence of neurotoxicity, because the ability of a compound to cross the blood brain barrier (BBB) and concentrate in neural tissue is dependent on its partition coefficient[100-102]. Lipophilic compounds can more easily cross the BBB than the hydrophillic ones[101,102].

An N^1-substituted 2-nitroimidazole derivative, etanidazole (28), was found to have same radiosensitizing efficiency as misonidazole (1) but with less neurotoxicity. Etanidazole (28), because of its lower lipophilicity (P = 0.046) demonstrated less penetration into neural tissue[103-105]. It was predicted that 7.5 times more drug would be required for etanidazole (28) to achieve the same level of neurotoxicity as misonidazole (1)[103,105].

There are reports of several other nitroimidazole radiosensitizers tested both *in vivo*[106-111] and *in vitro*[106-108,110-114]. Among these the most promising compounds are RSU-1069 (29), pimonidazole (30)[106,107] and KU-2285 (31)[108]. Both *in vivo* and *in vitro* studies showed RSU-1069 (29) and pimonidazole (30) to be more effective radiosensitizers than misonidazole (1) when tested at equimolar concentrations[106,107]. KU-2285 (31) is a fluorinated 2-nitroimidazole reported to have improved radiosensitization properties relative to misonidazole (1) *in vitro* and *in vivo*, and comparable with etanidazole[108]. The higher *in vivo* sensitizing effect of this compound (31) is due to its high concentration in the tumor[109].

Azomycin riboside (AZR, 32) and iodoazomycin riboside (IAZR, 2) are sugar-coupled 2-nitroimidazole derivatives, which were shown in in vitro studies to be as good as, or better than, misonidazole (1)[12,110,112]. AZR (32) also showed cytotoxicity in vitro[110,112] and host toxicity in vivo[110] similar to that observed with misonidazole (1). IAZR (2), however, showed even higher in vitro cytotoxicity[12]. Although no report of in vivo toxicity was available, it was predicted that IAZR would be more neurotoxic than misonidazole (1)[12]. This prediction was made on the basis of its higher P value (2.1) relative to misonidazole (0.43)[12].

From the results described in this section it is apparent that reduction potential and partition coefficient are the governing factors for effective radiosensitizers. These factors can be manipulated to design radiosensitizers with improved therapeutic effect and reduced toxicity[115].

2.2. BIOLOGICAL PROPERTIES OF NITROIMIDAZOLE RADIOSENSITIZERS

2.2.1. General Metabolic Reactions of Nitroimidazoles

Metabolism is the only process for the biological degradation of xenobiotics. In this respect nitroimidazoles are no exception. The major pathways of nitroimidazole biotransformation include nitro-reduction, ring fragmentation, conjugation, and dealkylation and hydroxylation.

Nitro-reduction is an important step of nitroimidazole metabolism. The enzyme responsible for catalysing this reduction is nitroreductase, which is active in hypoxia[116]. Nitroreductase activity was also found in several other enzyme systems including cytosol xanthine oxidase and microsomal NADPH-cytochrome c reductase[117,118]. Non-protein thiol was found to facilitate the enzymatic reduction of nitroimidazoles to their reduced intermediate species[117].

The nitro-reduction process in nitroimidazoles is reported to be complex. Theoretically a nitroimidazole may accept up to six electrons in a complete reduction to the corresponding amine[119,120]. Scheme 1 shows the detailed process as proposed by Edwards[119], which includes sequential addition of electrons, protonation and disproportionation[119].

The process of nitro-reduction predominantly occurs in hypoxic cells of tumor[116] and liver[121] and by intestinal microflora[122,123]. The production of stable amine derivatives from the intermediate hydroxylamines may proceed in two ways as shown in Scheme 1. It is not clearly understood whether reduction of hydroxylamines is the predominant process[119].

The production of a nitro radical anion (Scheme 1) following single electron reduction can occur in either aerobic or hypoxic cells[119,124]. However, in aerobic cells, the radical anion reacts rapidly with oxygen. The higher electron affinity of oxygen (E_7^1 = -159 mV) allows it to scavenge electrons, resulting in the formation of a super-

Scheme 1. Sequence of the reduction and electron transfer process in nitroimidazoles (Adapted from Edwards[119])

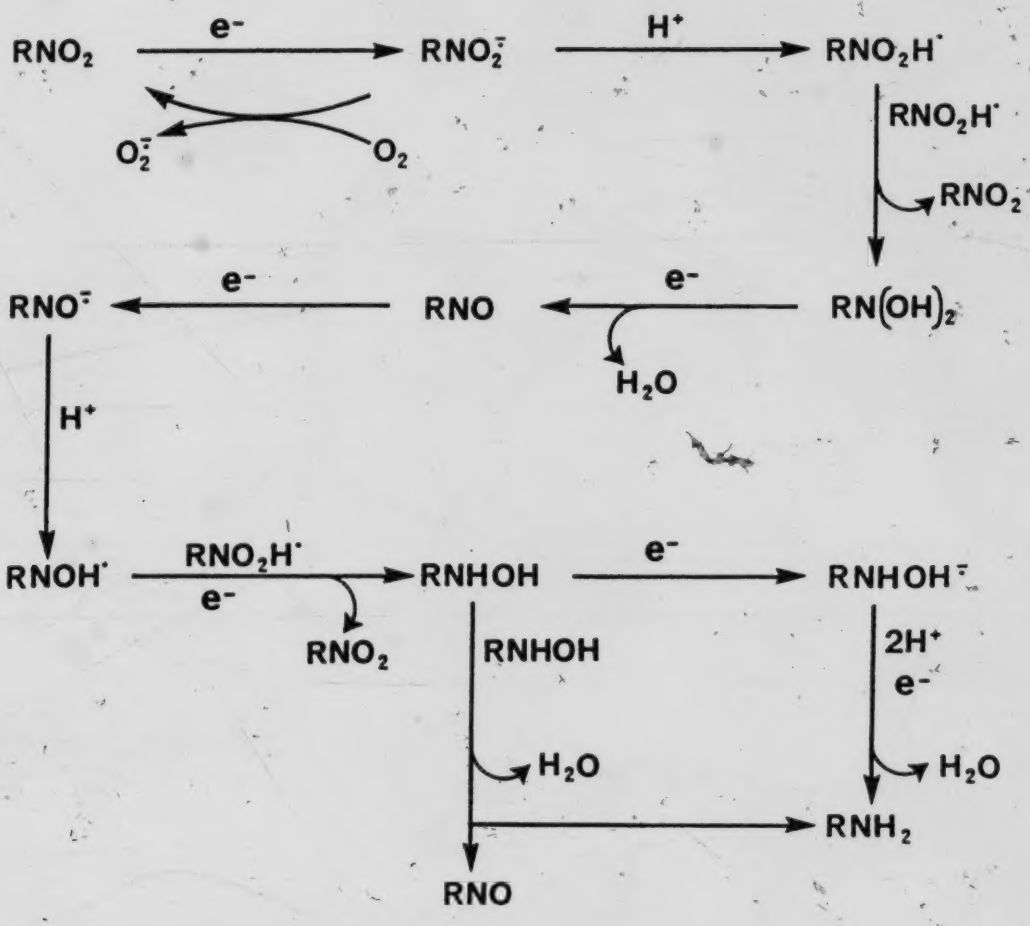

oxide anion with regeneration of intact nitroimidazole[124-127]. This reaction process inhibits further reduction of the one electron adduct (nitro radical anion) to more reduced products and is known as 'futile cycling'[124-127].

Futile cycling depends not only on the cellular oxygen level but also on the reduction potential of the nitroimidazole[128-130]. At lowered oxygen concentrations nitroimidazoles with higher reduction potentials are more resistant to futile cycling than those with lower reduction potentials[129,130]. This was supported by the fact that metronidazole (E_7^1 = -486 mV) underwent futile cycling at a lower oxygen concentration than that required for misonidazole (E_7^1 = -389 mV)[130]. In the absence of oxygen the net nitroreduction shown in Scheme 1 takes place[119,120,124,131].

Ring fragmentation of nitroimidazoles often originates with the hydroxylamine derivative. The mechanism of reductive fragmentation of nitroimidazoles was reported by a number of authors using different test systems[122,132-138].

The sequence of ring fragmentation shown in Scheme 2 is generally applicable to N^1-substituted 2-nitroimidazole derivatives. Product I involves the formation of glyoxal and guanidino compound. This process was identified in hypoxia by a number of authors[122,132-138]. Two alternate processes of glyoxal production were proposed by several authors[136-138]. One mechanism suggested the binding of rearranged hydroxylamine to guanosine[136,137], which upon release of guanidino leaves an equal amount of glyoxal-guanosine[136,137]. The other mechanism suggested the formation of an amino derivative of 2-amino-4,5-dihydro-4,5-dihydroxy imidazolium ion (DDI), which upon fragmentation gave glyoxal and guanidino[138].

Scheme 2. Sequence of nitroimidazole ring fragmentation.

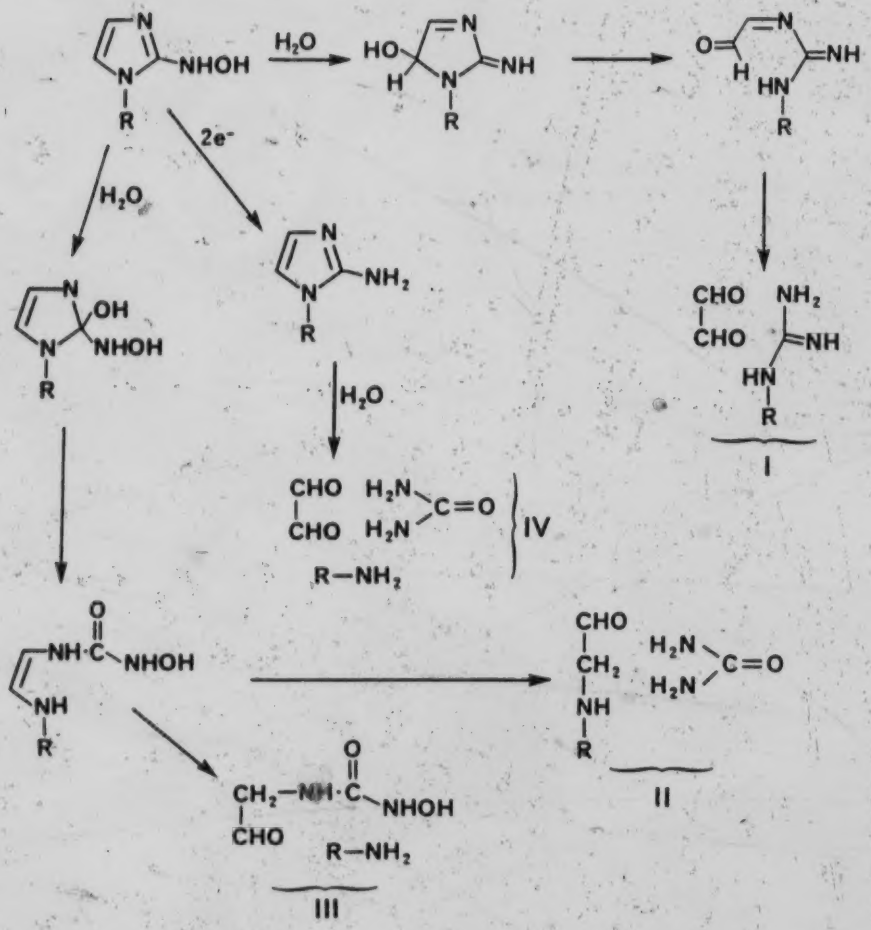

Products II and III result from the same intermediate species to form hydroxy urea, with hypothetical aldehyde (product II) and side chain amine with hypothetical aldehyde (product III). The different products are formed from cleavage of the ring at different positions[133,134]. Product IV is another way of getting glyoxal with urea and side chain amine[122,123,133-138]. This reaction, by alternate ring cleavage, also yields guanidino and urea[122]. However, all of these fragmentation reactions occur by attack of water on either the hydroxylamine or amine derivatives of the nitroimidazole.

The main fragmentation products of 5-nitroimidazoles were identified as an oxamic acid derivative and acetamide[139]. In addition to these, N-acetylalkylamide, glycine and acetic acid were identified as complementary products[139].

Nitroimidazoles have been found to conjugate with glucuronic acid[116,121,140-142], mercapturic acid[120] and glutathione[116,141-143]. The glucuronide conjugate of nitroimidazoles was identified in aerobic perfused liver[121,140], chinese hamster ovary (CHO) cells <u>in vitro</u>[116] and in urine and bile[144]. These results suggest that glucuronidation is a major metabolic pathway of nitroimidazoles under aerobic conditions[121,140,144,145]. However, under hypoxic conditions it is a minor pathway because of the deficiency (or low level) of the co-factor UDP-glucuronic acid[121]. As shown in Scheme 3, glucuronidation occurs when the nitro group is intact. This

Scheme 3. Pathways of nitroimidazole conjugation reaction[121,140-145]

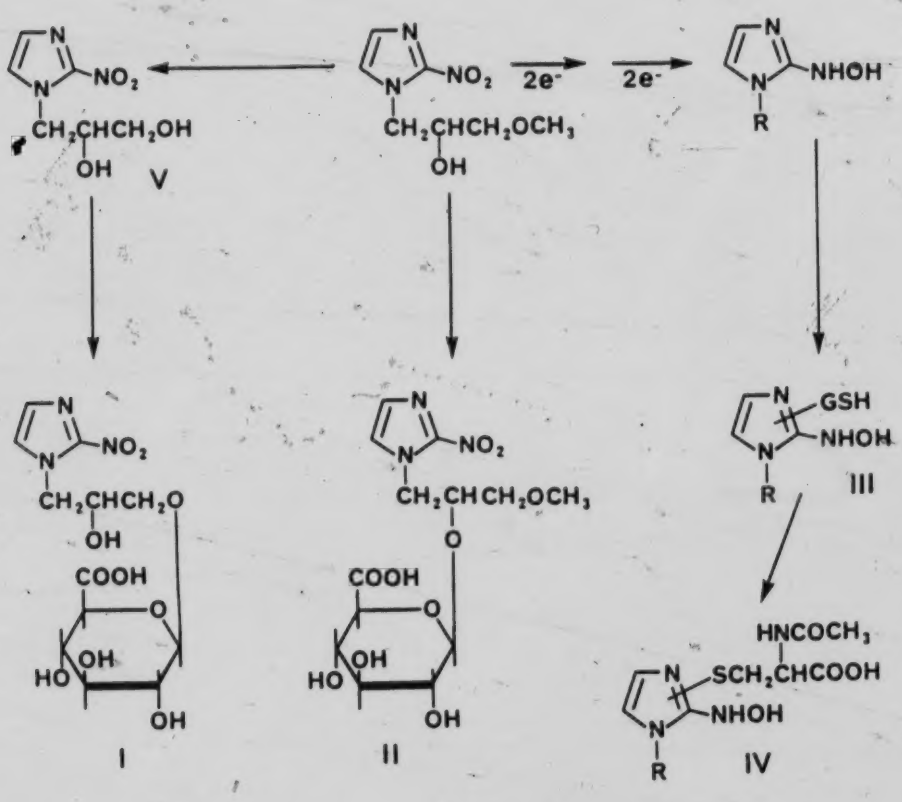

type of conjugation often occurs by the reaction of glucuronic acid either with the terminal hydroxyl group of the dealkylated compound (product V) or with the 2-hydroxy group of the side chain[116,121]. The resulting conjugated products are either I or II, respectively (Scheme 3).

Glutathione conjugation (product III) however, predominantly takes place under hypoxic conditions[121,142,143]. The mercapturate conjugate (product IV) is the result of glutathione conjugation followed by the conversion of the latter under hypoxic condition[121]. These metabolites were detected either in liver homogenate or CHO cells[121,143] or by incubation with glutathione (GSH) in vitro under hypoxic conditions[142].

Dealkylation of the terminal side chain of nitroimidazoles was observed with misonidazole (product V, Scheme 3) by a number of researchers and in a number of test systems[145-147]. The dealkylation process is reported to take place oxidatively, mediated by microsomal cytochrome P-450[145]. The dealkylated derivative of misonidazole is found to have radiosensitizing properties about equal to those of misonidazole[145,147].

Hydroxylation of the methyl group at the 2-position of the imidazole ring was observed with metronidazole (12)[148]. The product was identified as 1-(2-hydroxyethyl)-2-hydroxy methyl-5-nitroimidazole[148].

2.2.2 Biochemistry of Nitro-Reduction.

The reduction of nitroimidazoles is mediated by nitro-reductase enzymes known as flavoproteins[116]. Flavoproteins have been isolated in pure form and found to have the capacity to use nitroimidazoles or quinones as one-electron or two-electron acceptors[149].

The biochemical pathways for nitro-reduction shown in Scheme 4 are reproduced from reference 149. Glucose is the ultimate source of reducing equivalents for the reduction of nitro compounds. Oxygen-reactive intermediates are formed under aerobic conditions while under hypoxic conditions further reduction to hydroxylamines or amines takes place[149].

Under aerobic conditions, peroxide is formed by reaction with oxygen. Peroxide is known to cause serious damage to cells. The hydroxyl radical of peroxide is responsible for DNA-strand breaks, membranal lipid-protein peroxidation and enzyme inactivation[150]. Biochemical deactivation of peroxide in cells depends on the glutathione level (GSH)[149]. This process involves the reaction of peroxide with GSH in the presence of glutathione peroxidase to form oxidized glutathione (GSSG), followed by reduction to GSH in presence of glutathione reductase by NADPH[149].

Glutathione peroxidase is a selenium dependent enzyme, which is extremely specific for GSH and is capable of rapidly detoxifying hydrogen peroxide and certain hydroperoxides[151]. The maximal rates of GSH oxidation by glutathione

Scheme 4. A schematic of the biochemical process of electron transfer of nitroimidazoles (Biaglow[149]).

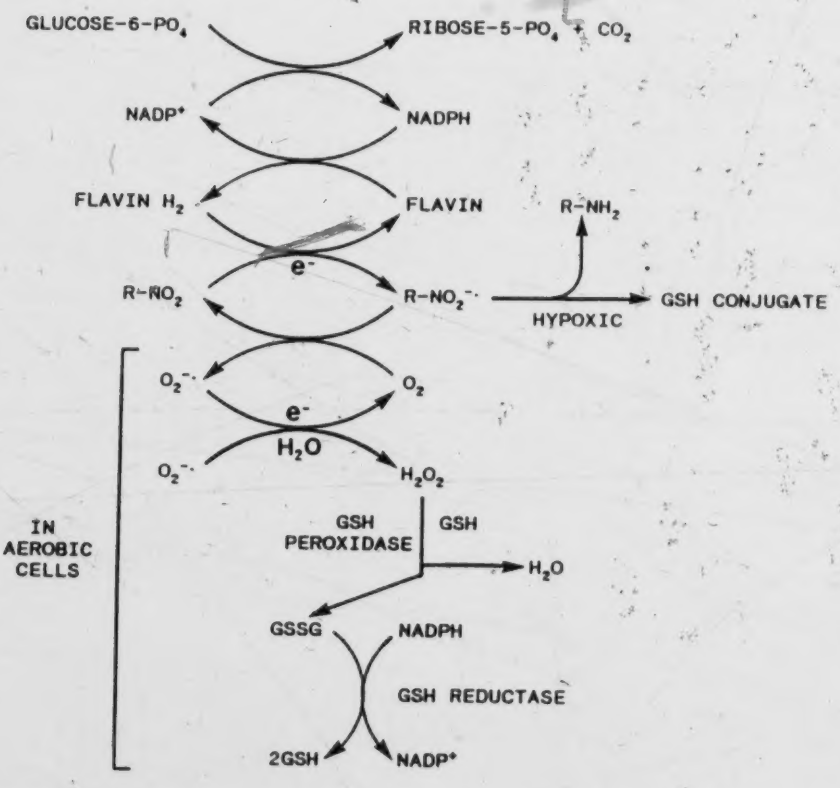

peroxidase and reduction of GSSG by glutathione reductase are 40 µmol and 10 µmol per min. per gram of liver respectively[152]. The glutathione redox cycle therefore plays an important role in minimizing cellular toxicity against the

reductive intermediates produced by the bio-reduction of nitro compounds under aerobic conditions[151]. This cycle utilizes NADPH and NADH reducing equivalents in the mitochondrial matrix[150,151] and in cytoplasm[151]. The mitochondrial redox cycle of glutathione regulates oxidation in the liver[151]. Hydrogen peroxide metabolism in mitochondria possesses a regulatory function in the oxidation of substrates by a coenzyme-A and lipoamide-dependent ketoacid oxidase[153]. It was proposed that steady-state formation of mitochondrial superoxide ($O_2^{\cdot}$) and peroxide (H_2O_2) may be related to the resulting oxidation of mitochondrial GSH and NADPH and the regulation of mitochondrial substrate oxidation[153].

In a study with Ehrlich ascites tumor cells under hypoxic conditions, misonidazole (1) was found to inhibit glycolysis[154]. This inhibition is concentration dependent and non-linear with incubation time[154]. Exogenous thiols such as cystamine appeared to prevent misonidazole-linked inhibition of glycolysis as well as restore the glucose uptake in misonidazole-treated cells[154]. Glutathione itself, however, had no effect on the prevention of misonidazole-induced inhibition of glycolysis, probably due to the fact it can not enter the cells[155]. The inhibition of glucose utilization and lactate production by hypoxic cells incubated with misonidazole is suggested to be a major factor responsible for cytotoxicity of this compound (1). This could be due to

the inhibition of energy yielding reactions as well as by alteration of the pentose cycle[154].

Under aerobic conditions glutathione must be depleted to very low levels for the toxicity of nitroimidazoles to occur via peroxidative cell damage[154]. However, peroxide production via electron transfer to oxygen causes metabolic alteration in aerobic cells, including alteration in the pentose cycle and in glycolysis[154]. The glutathione level in these cells is extremely important for the prevention of cell damage[151,154].

The glutathione level in hypoxic cells is also important for detoxifying the reduction intermediates of nitroimidazoles by the formation of stable adducts[156]. Details of the interaction between the hydroxylamine derivative of nitroimidazole and glutathione are shown in Scheme 5[156]. GSH initially reacts with the hydroxylamine to produce an unstable GS-conjugate. Further reaction of this product (II) occurs in presence of excess GSH to yield two stable aminoimidazoles with 4- or 5-position GS-adducts (product V and VI) and a saturated product (IV). Product IV may produce either V or VI by loosing one GSH.

In addition to alteration of both glycolysis and lactate production, various nitrocompounds including nitroimidazoles have been found to alter cellular oxygen utilization[157]. Glucose and endogenous reducing substrates such as GSH, NAD(P)H and glycolytic intermediates are known to influence this effect. Oxygen utilization is also dependent upon the

Scheme 5. A proposed scheme for the reaction of reduced intermediate species of nitroimidazole with GSH[156].

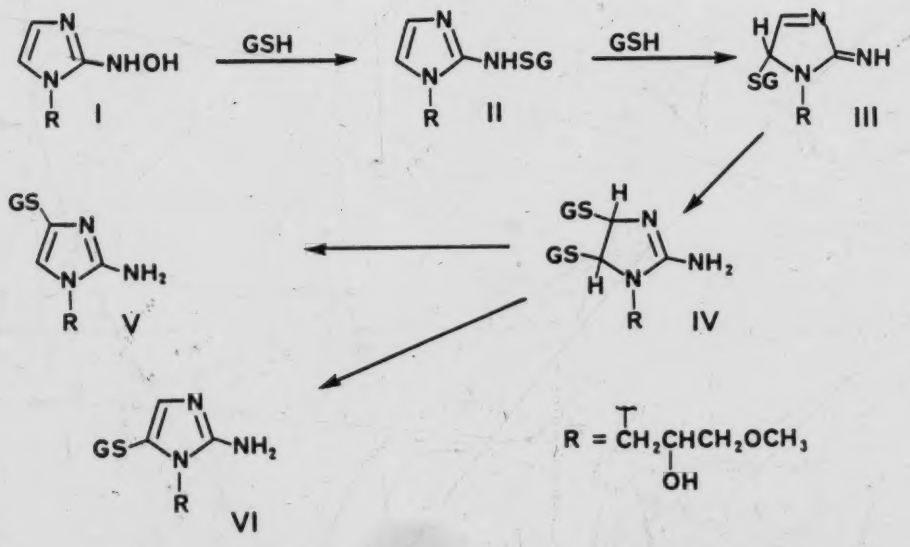

electron affinity and concentration of the compound. In the absence of glucose, none of the nitrocompounds (nitroimidazoles, nitropyroles, nitrofurans, nitrobenzenes) tested with Ehrlich ascites cells were found to stimulate oxygen utilization[157]. In the presence of glucose, nitrobenzene derivatives with reduction potentials more positive than -350 mV stimulate the rate of oxygen consumption[158]. Stimulation of

oxygen utilization results in the production of peroxide[149]. Misonidazole (1) was found to stimulate oxygen utilization by NADPH-cytochrome c reductase in a linear manner over the concentration range up to 10 mM[159]. Inhibition of cellular oxygen utilization results from direct reaction of either nitrocompounds, or their metabolically produced intermediates, with enzymes[157]. The reduced intermediates may also react with endogenous reducing substrates. The net effect is depletion of available reducing equivalents, leading to inhibition of cellular redox reactions such as respiration[157].

2.3. TECHNIQUES FOR THE DETECTION OF TISSUE HYPOXIA

2.3.1. Introduction

One of the earliest methods to measure low oxygen concentration in human tumors was the oxygen electrode method[160,161]. The technique involves direct implantation of an electrode into the tumor. This method is not only invasive, but is often unreliable as a measure of oxygenation status in the tumors[160,162]. Problems in obtaining accurate and reliable measurements by this method have been related to high oxygen consumption by the electrode itself, measurement of only the small volume of tissue immediately in the vicinity of electrode and disturbance of micro-

circulation patterns, as well as electrode-induced tissue damage[160,162].

A radiobiological method for detecting hypoxia in solid tumors was first reported in 1963[163]. The method is an indirect measurement, which relies upon the radiation response of cell populations in a tumor following whole-body irradiation. Several modifications of this technique were developed. These included the paired survival curve assay[164,165], the clamped tumor control dose (TD_{50}) assay[166] and the clamped tumor growth delay assay[167]. However, radiobiologic techniques for measuring hypoxia are not compatible with clinical practice. A large variability has been observed in hypoxic fractions of tumors from the same tumor cell line growing in different animals[168].

Tumor hypoxia was also detected by a cryophotometric technique[169] and by fluorescent labelled nitrofuran[170]. Both of these methods are invasive, since they require removal of representative samples from the tumor[171,172]. The fluorescent compounds studied so far have been found to be toxic, thereby limiting the clinical application of the fluorescence technique[172].

2.3.2. Radiolabelled Radiosensitizers for the Detection of Tissue Hypoxia

The development of a suitable compound for detecting hypoxic fractions in tissues, combined with a non-invasive imaging modality, represents a more recent focus of research in this field. The clinically compatible detection techniques essentially include the use of conventional gamma camera imaging, positron emission tomography (PET) and magnetic resonance imaging (MRI) techniques.

The use of radiosensitizers to measure tissue hypoxia in tumors developed after recognition of their selective adduct formation in hypoxic mammalian cells. In this regard it was predicted that misonidazole (1) might serve as a prototype marker for hypoxia within solid tumors in addition to serving as radiosensitizer[10,173]. To assess this potential, misonidazole and several of its analogs were studied both *in vivo* and *in vitro*.

^{14}C-Labelled misonidazole ([^{14}C]-1) was found to bind selectively to hypoxic cells *in vitro* in EMT-6 tumor cells and V79 chinese hamster cells[174-177], multicellular spheroids of chinese hamster cells[10,175-178] and EMT-6 multicellular spheroids[175,176,178]. These studies succeeded in identifying a radioactively-labelled marker for hypoxic cells. In addition to this, several other important observations were made;

a) The initial rate of binding increased proportionally with the square root of extracellular concentration of misonidazole[174].

b) The concentrations required to selectively label hypoxic cells was far less than the radiosensitizing or cytotoxic concentration[10].

c) The amount of binding was inversely proportional to the cellular oxygen level, as a 20 to 50 times higher binding was observed in hypoxic cells than in oxygenated cells[175-178].

In <u>in vivo</u> studies with murine EMT-6 tumors in Balb/c mice[10,179,180], artificially-induced myocardial ischemia in Balb/c mice[179] and RT-9 tumor in the brain of CD Fisher 344 rats[181], selective binding of ^{14}C-misonidazole ([^{14}C]-<u>1</u>) was observed in the hypoxic fractions. Autoradiographic analyses showed a 2-12 times higher ^{14}C activity in hypoxic tissues as compared to normal tissues[179-181]. Along with the ^{14}C-labelled (C-2 position) misonidazole ([^{14}C]-<u>1</u>), misonidazole labelled in the N^1 side chain with ^{3}H ([^{3}H]-<u>1</u>) was also studied in many systems. These included <u>in vitro</u> in V79 monolayer cells and EMT-6 spheroids[178], and <u>in vivo</u> with Balb/c mice bearing EMT-6 tumors[180], human solid tumors[182,183], and non-malignant tissue of the gerbil stroke model[184].

It was found that ^{14}C-ring labelled misonidazole

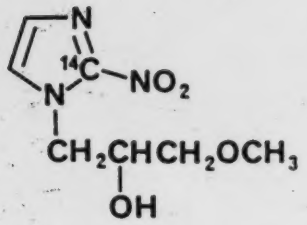

^{14}C-1

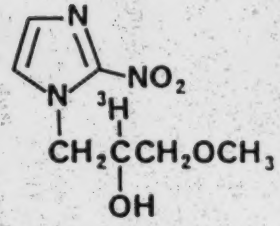

^{3}H-1

([^{14}C]-1) provided a 3 times higher *in vivo* tumor uptake than ^{3}H-side chain label ([^{3}H]-1)[180]. However, an *in vitro* study failed to show any difference in binding between the two differently labelled misonidazoles[178]. The *in vivo* differences between ^{14}C and ^{3}H radioactivity distribution was attributed to the higher retention of sidechain-labelled compound ([^{3}H]-1) than the ring label([^{14}C]-1) by normal tissue[180]. This is because the side chain is more liable to metabolic fragmentation than the ring and the fragmented side chain containing the label was retained in the normal tissue. With the ring label compound, following side chain fragmentation, the radioactivity was excluded by the normal tissue because the fragmented side chain had no label in it. Therefore, the observed tumor to normal tissue ratio of radioactivity was higher with the [^{14}C]-1) compared to ([^{3}H]-

1)[180]. Autoradiographic techniques with ([^{3}H]-1) and ([^{14}C]-1) were employed to measure hypoxia in human tumors[182,183] and in gerbil brains with severe infarct[184]. This technique provided an indirect measurement of tissue oxygen tension at the cellular level[182,183].

Although this technique using ß⁻ emitting radiolabelled compounds was invasive, it did demonstrate that sensitizer-adduct formation could be exploited for diagnosis of hypoxia in tumor[182,183] and in normal tissue[184]. Although the exact nature of adduct formation remains a matter of investigation, it is known that the sensitizer-adduct formation relies on nitro-reduction, which is several times higher under hypoxia than aerobic conditions (see Schemes 1, 3, 4, for details).

These early studies of misonidazole labelled with ^{3}H and ^{14}C further substantiated the usefulness of radiolabelled radiosensitizers as markers of tissue hypoxia. Although a radiosensitizer labelled with a ß⁻ emitter is not suitable for non-invasive diagnosis, it was predicted that misonidazole analogs could be useful for <u>in vivo</u> detection of hypoxia when gamma-emitting or positron-emitting or MRI-active elements were present.

A number of brominated and fluorinated analogs of misonidazole were studied in an effort to establish their selective uptake in hypoxic tissue. Such studies have included compounds labelled either with gamma, positron or ß⁻

emitters. β^- Emitters were used as molecular probes for biodistribution studies. The compounds studied were 4-[^{82}Br]-bromomisonidazole ([^{82}Br]-33)[185-187], ^{3}H labelled-4-bromomisonidazole ([^{3}H]-33)[187] and fluorinated misonidazole and its analogs labelled either with ^{3}H ([^{3}H]-34), [^{3}H]-35)[187-190] or ^{14}C ([^{14}C]-36)[191] or ^{18}F ([^{18}F]-34), [^{18}F]-37), [^{18}F]-38)[190,192-194].

The initial study with ([^{82}Br]-33) showed that it had some potential for imaging tumor hypoxia[185]. Two further *in vivo* studies[186,187] reported a persistently high radioactivity in blood resulting in tumor to blood ratios less than unity. The blood radioactivity was identified as bromide anion (^{82}Br$^-$) indicating that extensive *in vivo* debromination was taking place. Compound ([^{82}Br]-33) therefore appeared to have limited utility for non-invasive imaging of tissue hypoxia[186,187]. Compound ([^{3}H]-33) showed a higher tumor to blood ratio than was observed with ([^{82}Br]-33)[187]. The higher tumor to blood ratio for ([^{3}H]-33) is due to the fact that ^{3}H activity is present in the debrominated metabolite which maintains an affinity for hypoxic tissue. The ^{3}H-labelled compound ([^{3}H]-33) was interesting as a probe to demonstrate the metabolic degradation of ^{82}Br labelled compound ([^{82}Br]-33) but had no utility as an imaging agent.

^{3}H-Fluoromisonidazole ([^{3}H]-34) was studied *in vivo* with C3H mice bearing KHT tumor[188], Balb/c mice with EMT-6 tumors[187], and in spontaneous dog tumors[190], as well as *in*

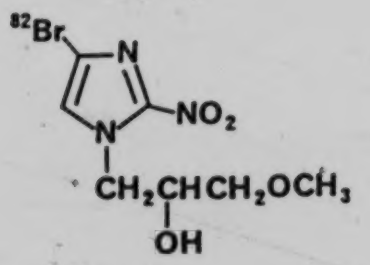

^{82}Br-33

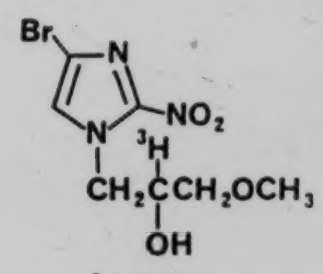

^{3}H-33

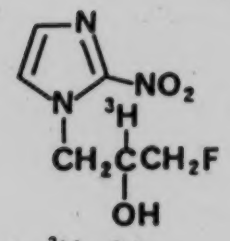

^{3}H-34

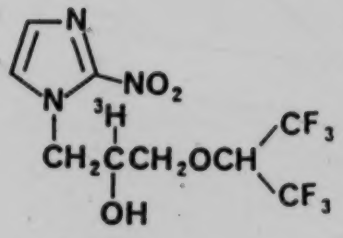

^{3}H-35

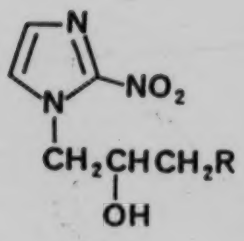

a R=F
b R=^{18}F

34

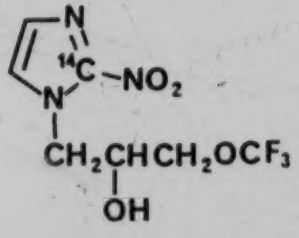

^{14}C-36

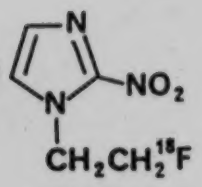

^{18}F-37

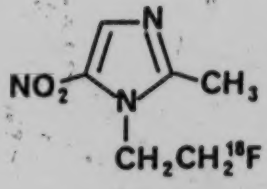

^{18}F-38

vitro in four different cell systems[190]. These studies confirmed that the binding of ([^{3}H]-34) is dependent on the oxygenation status of the cells. A higher level of radioactivity was found in larger tumors than in smaller tumors, reflecting a higher hypoxic fraction in the larger tumor[190]. However, ^{3}H-hexafluoromisonidazole ([^{3}H]-35) failed to show any favourable results, as the tumor to blood ratio was less than unity[189]. This was due to decreased in vivo stability of the hexafluoropropyl side chain. This instability was further confirmed by ^{19}F MRI analyses[189].

More recently, a study with the monofluoro compound ([^{19}F]-34) provided a detectable ^{19}F MRI signal in tumor tissue for up to 10 hours post injection in Balb/c mice bearing EMT-6 tumors[195]. ^{14}C-Labelled trifluoromisonidazole ([^{14}C]-36) showed an in vitro binding rate and a tumor uptake similar to misonidazole (1) in Balb/c mice bearing EMT-6 tumor[191]. Despite these favourable results, the utility of trifuoromisonidazole (36) as a non-invasive marker for PET imaging may be limited since a facile method of labelling this compound (36) with ^{18}F has not yet been developed.

^{18}F-Labelled fluoro nitroimidazoles have been developed with the intent that these congeners of misonidazole (1) could be useful as non-invasive markers of hypoxic cells in tumor and ischemic areas in brain and heart[190,192-194]. A series of ^{18}F labelled compounds ([^{18}F]-34), ([^{18}F]-37), ([^{18}F]-38) was tested in Sprague-Dawley rats[192]. Tissue distribution of

these compounds was similar to that of other nitroimidazoles studied earlier, such as metronidazole (12) and misonidazole (1). The potential of these compounds as *in vivo* markers of tissue hypoxia was suggested, although no PET imaging was done in this study[192].

More recently several other studies with ^{18}F-fluoromisonidazole ([^{18}F]-34) showed promise for this compound in detecting hypoxic cells in the myocardium and in tumor by PET imaging[190,193,194]. Myocardial kinetics were evaluated in isolated perfused rabbit hearts using ([^{18}F]-34). The uptake of the compound was characterized under control conditions, with ischemia, hypoxia and with reperfusion in 20 rabbit hearts[193]. The retention of ^{18}F activity in the myocardium as compared to peak radioactivity, was higher in the case of ischemia (41±7%) and hypoxia (46±8%) than the control (18±6%) and the reperfusion model (16±5%)[193]. PET studies on 5 dogs with artificially induced acute coronary occlusion were performed to validate these findings. It was found that within 30 min. of administration of ([^{18}F]-34) the accumulation of ^{18}F in ischemic myocardium was higher than in normal myocardium[193]. In another PET study, 6 dogs with osteosarcoma were imaged continuously for 4 to 5 hours after i.v. injection of ([^{18}F]-34)[190]. The PET scans showed that radioactivity in some tumor regions was higher than the radioactivity in plasma and normal tissues[190]. Some variability of uptake in different regions of the same tumor

were indicative of the heterogeneity of oxygenation status[190]. These studies suggested that the uptake of the compound ([^{18}F]-34) is due to hypoxia but not due to the diminished perfusion[190,193].

In addition to misonidazole (1) and its congeners, several other derivatives of nitroimidazoles were synthesized and tested *in vitro* and *in vivo*. The effort was devoted to identify a suitable radioiodinated compound for non-invasive detection of tissue hypoxia using conventional gamma camera imaging. The compounds investigated include iodoazomycin riboside (IAZR, 2)[12,13], 1-[2-(2-iodophenoxy)-ethyl]-2-nitroimidazole[11] and some iodo-acetophenone derivatives of 2-nitroimidazole[196]. These compounds were abandoned after preliminary *in vivo* investigations because the former compound (2), although showing a higher *in vitro* binding rate than misonidazole (1)[12], was radiochemically less stable *in vivo*[13]. The latter two compounds failed to show any potential, as their tumor to blood ratios were less than unity[11,196].

Because of the promising *in vitro* results obtained with IAZR (2), several analogs of this compound were developed in the present study, in an attempt to utilize the observed hypoxia-selective binding properties of the sugar-coupled 2-nitroimidazole and to confer greater *in vivo* stability.

The remainder of this thesis will report new radiobiological data and biodistribution/gamma-camera imaging

data for several novel (radio)iodinated sugar-coupled 2-nitroimidazoles. The effort is completely devoted to analyze the potential of the four novel (radio)iodinated sugar-coupled 2-nitroimidazoles as non-invasive markers of hypoxic tumor tissue.

3. EXPERIMENTAL

3.1. MATERIALS

3.1.1. Chemicals, Solvents, Gases and Equipment

All chemicals used were reagent grade unless otherwise specified. Solvents were distilled prior to use. Where dry solvents were required these were dried by standard methods. Gases were purchased from LINDE Union Carbide, Canada and were of research grade purity. Thin layer chromatography (TLC) was carried out on silica gel Whatman MK6F microplates. A Büchi rotavapor (model HB-K10) was employed for vacuum drying. Radiochemical syntheses were generally carried out in Pierce Reacti-vials$^{T.M.}$ sealed with teflon-rubber septa, with heating by a Pierce Reactitherm$^{T.M}$ block heater. Eppendorf micropipettes were used for measuring micro quantities of solvents. Eppendorf micro centrifuge tubes were used for micro centrifugation with a Brinkman Model 5412 centrifuge.

3.1.2. Instruments

High Pressure Liquid Chromatography (HPLC) was used to purify radiolabelled compounds, for partition coefficient studies and also for phosphorolysis studies. Analytical and small scale preparative HPLC separations were performed

using a Waters C-18 Radial-Pak reverse phase column (8mm I.D., 10 µm, Waters Assoc. Inc.) (Column A) on a Waters system (model 680 Automated Gradient Controller, models 510 and M-45 solvent pumps, model U6K injector, 480 LC ultraviolet (uv) detector and model 3390A Hewlett Packard integrator). Large scale radiochemical synthesis products were purified by using a preparative Whatman Partisil M9 10/25 ODS reverse phase column (Column B). Radioactive column effluent (radiochromatography; Radio-HPLC) was monitored by a NaI(Tl) 5 cm crystal scintillation detector fitted with a single channel analyzer (BNC Portanim model AP-2), high voltage power supply (Ortec model 456) Amp and CSA (Ortec model 490A) and log/lin ratemeter (Ortec model 449), integrator (Waters 740 data module). The single channel analyzer was calibrated for the desired photopeak of the radionuclide. The activity of radioactive compounds was measured with a Capintec Radioisotope Calibrator model CRC-30BC.

Tissue samples and filter papers containing acid-insoluble fractions for <u>in vitro</u> binding studies were counted in a Beckman Gamma 8000 gamma scintillation counter.

Whole-body scintigraphy was performed using a pin-hole collimator fitted to a Searle gamma camera (Pho/Gamma III) that was interfaced to an ADAC (CAM III) computer for storing the image. Dysan$^{T.M.}$ floppy disks were used for electronic storage of the whole-body scintigrams.

3.1.3. Radioisotopes

Radioiodines were the radionuclides used in these studies. ^{123}I was purchased from Nordion International Inc., Vancouver, Canada, and ^{125}I and ^{131}I were purchased from Nordion International Inc., Toronto, Canada, through the Edmonton Radiopharmaceutical Center, Alberta, Canada.

The radioiodines were purchased as no-carrier-added solutions of NaI in 0.1N NaOH.

3.1.4. Animals

Male Balb/cCr/Alt mice weighing 20-25 g were purchased from the Health Sciences Small Animal Program, University of Alberta. All animals were maintained ad lib with rodent food pellets and tap water in standard plastic cages (5 mice per cage).

3.1.5. Tumor Cell Line

EMT-6 tumor cells were used for both in vivo and in vitro studies. Tumor cells were obtained routinely from the Radiobiology Department of the Cross Cancer Institute. The tumor cell line was usually maintained in the laboratory by alternate in vivo and in vitro passage. The cells were cultured as monolayers and transferred twice weekly into Waymouth's medium complete with 12.5% fetal Calf serum for regrowth. EMT-6 cells grown to near confluence in flasks

were trypsinised, centrifuged and resuspended in normal saline.

For *in vivo* studies, EMT-6 cell suspensions contained approximately $1x10^6$ viable cells per mL of normal saline.

3.2 METHODS

3.2.1. Synthesis of 1-(5-Iodo-5-deoxy-β-D-arabinofuranosyl)-2-nitroimidazole <Iodoazomycin Arabinoside:IAZA>.(45)[b]

The title compound was synthesized in six steps as described in detail elsewhere[197]. The blocked arabinofuranosyl bromide (42) was prepared in three steps from the pyranose sugar according to the published procedures[198,199]. Coupling of the blocked sugar with 2-nitroimidazole was accomplished by treatment of an approximately equimolar mixture of the two reagents with mercuric cyanide in dry acetonitrile using the method of Sakaguchi[113]. Coupled product (43) was obtained in 70% yield after workup and chromatographic purifications.The title compound (IAZA, 45) was obtained in 75% yield following deblocking and iodination.

[b]The initial syntheses of IAZA (45), IAZG (49), IAZP (54) and FIAZP (60) were performed by Dr. V.V. Somayaji, as part of the development of this project.

3.2.2. Synthesis of 1-(6-Iodo-6-deoxy-β-D-galactopyranosyl)-2-nitroimidazole <Iodoazomycin Galactoside:IAZG> (49)

Details of the synthesis and product characterization are reported elsewhere[200]. The title compound (IAZG, 49) was obtained in three steps. A coupling procedure similar to that described for IAZA (above) was employed. The blocked, coupled product (47) was obtained in 73% yield. Deblocking of this product followed by iodination yielded the title product (IAZG, 49) in 78% yield from AZG (48).

3.2.3. Synthesis of 1-(4-Iodo-4-deoxy-β-L-xylopyranosyl)-2-nitroimidazole <Iodoazomycin Pyranoside:IAZP>. (54)

The title compound (IAZP, 54) was synthesized in five steps[201]. Blocked arabinopyranosyl bromide (51) was synthesized in two steps from the pyranose sugar (39) using the published procedure[202]. Coupling, deblocking and iodination procedures similar to those employed for the synthesis of IAZA and IAZG were used. The coupled product (52) was isolated in 60% yield based on the starting blocked sugar (51). Deblocking of (52) and subsequent iodination of (53) gave the title compound in 48% yield.

3.2.4. Synthesis of 1-(2-Fluoro-2-deoxy-4-iodo-4-deoxy-β-L-xylopyranosyl)-2-nitroimidazole <2'-Fluoro-iodoazomycin Pyranoside:FIAZP> (60)

The synthesis of the title compound (60) was similar to that used for the preparation of IAZP, except that two additional intermediate steps were required to incorporate the xylo configuration fluorine in the sugar. Fluorination of the blocked arabinopyranosyl bromide (57) was performed prior to the coupling step[201]. The iodination reaction was performed by adding triphenylphosphine (212 mg, 0.8 mmol) and iodine (101 mg, 0.4 mmol) to a stirred solution of FAZP (59) (100 mg, 0.4 mmol) in dry pyridine. The reaction mixture was then heated to 60 °C for 48 h. The final product (FIAZP, 60) was obtained in 50% yield.

3.2.5. Exchange Radioiodination of 1-(5-Iodo-5-deoxy-β-D-arabinofuranosyl)-2-nitroimidazole <IAZA>. ([^{125}I-IAZA]), ([^{123}I-IAZA])

3.2.5.1. Solvent Exchange Method

No-carrier-added <^{125}I>-NaI (55.5 MBq), as a solution in 10 µL of 0.1N NaOH, was supplied in 1.0 mL Reacti-vials. One drop (0.04 mL) of glacial acetic acid was added to the vial and the solvent was evaporated over 15 minutes with a stream of nitrogen . A solution of 2.2 mg (6.2 µmol) of IAZA in 100 µL of dry dimethyl formamide was added to the Reacti-vial.

The vial was sealed with a teflon-rubber septum and heated at 70 °C for 3.5 h in a heating block.

The vial was cooled and a 5 µL sample was analyzed by Radio-HPLC using column A, 60:40 water: MeOH, flow rate 2 mL/min., 350 nm uv detector setting. Under these conditions the retention time of IAZA was found to be about 6.85 min.

The labelling efficiency as determined by radioactivity at IAZA elution volume, expressed as a function of total activity, was calculated to be 70%, with the non-bound radioiodine present as polar components. The 70% radiochemical yield has been confirmed by TLC on several occasions. HPLC always has the danger that some non-polar material will not be eluted from the column during the chromatogram trace. The chemical yield was approximated by determining the area under the uv trace of the HPLC effluent corresponding to IAZA, compared with total peak areas. At 350 nm the HPLC detection is fairly sensitive and specific to 2-nitroimidazoles. The major impurity after reaction appeared to be deiodinated starting compound (AZA, 44). Based on this rough estimate, the chemical yield in the reaction was approximately 80% and the specific activity at the end of synthesis was 7.8 GBq/mmol.

The crude product was purified in portions by preparative HPLC using column B, 60:40 water: MeOH, flow rate 2 ml/min., retention time 10.60 min. The radioactivity after purification was 26.8 MBq representing a chemical recovery of about

1.1 mg of the original IAZA as ^{125}I labelled product ([^{125}I]-IAZA). The final product was 99% chemically and radiochemically pure by HPLC analysis. Similar reactions with the other isotopes of iodine (^{131}I and ^{123}I) gave comparable yields (68% and 73% radiochemical yield respectively).

3.2.5.2. Pivalic Acid Melt Method

No-carrier-added <^{123}I>-NaI (185 MBq), supplied in 21 µL of 0.1N NaOH solution, was treated with 3 drops of glacial acetic acid. The solvent was then evaporated to dryness by a stream of nitrogen over 30 min. A 50 µL portion of 98% v/v aqueous ethanol was added to the vial and then evaporated to dryness by a stream of nitrogen. Pivalic acid (2 mg) and a solution of IAZA (2.4 mg in 100 µL of 30% v/v aqueous methanol) was added to the Reacti-vial, and the solvent was again evaporated to dryness with a stream of nitrogen. The radioactivity measured at this point was 166.5 MBq. The Reacti-vial was sealed with a teflon-rubber septum and heated at 65 °C for 1 h in a heating block.

The contents of the vial were then dissolved in 100 µL of 30% v/v aqueous methanol and allowed to cool. A 1.0 µL sample was analyzed by Radio-HPLC using column B, 30:70 water: MeOH, flow rate 2 ml/min. The retention time was about 6.62 min. under these conditions. The labelling efficiency and chemical yield were determined by the methods mentioned earlier, and were found to be 70% and 85% respectively.

The crude product was purified in portions by preparative HPLC (column B) under similar elution conditions. The radioactivity after purification was 115 MBq, representing a chemical recovery of about 2.1 mg (85%) of the original IAZA as ^{123}I labelled product. The specific activity at the end of purification was approximately 20 GBq/mmol. The time required to prepare and purify the ^{123}I-IAZA was approximately 3.5 h.

3.2.6. Exchange Radioiodination of 1-(6-Iodo-6-deoxy-β-D-galactopyranosyl)-2-nitroimidazole <IAZG>. ([^{125}I]-IAZG), ([^{123}I]-IAZG])

Radiolabelling of the title compound was carried out by the two procedures described above for IAZA. Solvent exchange iodination was used to prepare <^{125}I>-IAZG and the melt method was used to prepare <^{123}I>-IAZG.

HPLC analysis and purification conditions were similar to those used with IAZA. Retention times were 4.98 min. on an analytical column (column A) and 8.75 min. on a preparative column (column B). Radiochemical purity of ^{125}I labelled product at the end of synthesis was about 65% and chemical yield was estimated to be 75%. The melt method yielded ^{123}I-IAZG in radiochemical and chemical yields of approximately 71% and 90% respectively.

The HPLC purified product from both the methods was found to be more than 99% chemically and radiochemically pure by HPLC analysis.

3.2.7. Preparation of <^{125}I> 1-(4-Iodo-4-deoxy-ß-L-xylo-pyranosyl)-2-nitroimidazole (<^{125}I>-IAZP)

The title compound was prepared by radioiodination of the synthetic precursor compound AZP (53).

No-carrier-added <^{125}I>-NaI (120 MBq) was transferred to a Reacti-vial and evaporated to dryness under a stream of nitrogen gas. The dried sample was sealed and heated at 40 °C under vacuum for 2 h. The vial was cooled and filled with dry nitrogen gas at atmospheric pressure. Iodogen (0.3 mg) dissolved in 50 µL of dry pyridine was added to this vial. The reaction mixture was allowed to stand for 30 min. A solution of 216 µL of dry pyridine containing 3.05 mg (0.024 mmol) of iodine was added to the Reacti-vial. After standing for 20 min. this solution was transferred to a Reacti-vial containing a desiccated mixture of 6.2 mg (0.024 mmol) of AZP (53) and 12.9 mg (0.048 mmol) of triphenylphosphine. The vial was sealed and heated for 16 h at 70 °C. At the end of the reaction the vial was allowed to cool. Isolation and purification of the labelled product (^{125}I-IAZP) was performed by Radio-HPLC using column A; (50:50 water: MeOH, 350 nm, 2 ml/min. flow rate, retention time 4.85 min.).

The radiochemical yield at the end of synthesis was estimated at 15%, with 32% chemical yield. The purified product had a specific activity of 2.5 GBq/mmol, and was 99% chemically and radiochemically pure.

3.2.8. Preparation of <^{125}I> 1-(2-Fluoro-2-deoxy-4-iodo-4-deoxy-β-L-xylopyranosyl)-2-nitroimidazole <^{125}I>-FIAZP)

The title compound was prepared as described for IAZP. HPLC analysis and purification conditions were similar to those used with IAZP; the retention time was 4.59 min. Radiochemical yield at the end of the synthesis was 15% and the chemical yield was calculated to be 35%. The specific activity of the final product was 2.1 GBq/mmol. The final product was 99% chemically and radiochemically pure.

3.2.9. Purification of Radiolabelled Compounds.

HPLC was employed to isolate and purify the radiolabelled compounds. An analytical column (column A) was used to separate those compounds which were used in biodistribution and <u>in vitro</u> binding studies. For scintigraphic studies with either ^{123}I or ^{125}I labelled compounds, purification was done with a preparative HPLC column (column B). The general procedures for either purpose are as follows.

An aliquot of the reaction mixture (25-50 μL) was injected into the HPLC. The solvent system used was the same as mentioned earlier. The uv detector was set at a wavelength

of 350 nm in all cases. Authentic non-radioactive samples of the compounds were used to determine the retention time, prior to purification of the radiolabelled analogs. Radiolabelled products eluting at the correct retention times were collected into vials and evaporated to dryness by a stream of nitrogen gas or by using a small scale rotary evaporator at 40 °C under vacuum. Samples were dissolved in a small volume of 95% ethanol, transferred to multi-dose sterile vials and taken to dryness by stream of nitrogen. The radioactivity present in these vials was measured by the dose calibrator. These samples were stored at -5 °C until further use.

Compounds labelled with ^{123}I were not stored but were dissolved immediately in saline after the preliminary drying step and then transferred to multi-dose vials. Additional dilution was carried out by saline as required. These products were used immediately.

3.2.10. Measurement of Partition Coefficient.

Partition coefficients of the compounds used in this study were determined by their equilibrium distribution between 1-octanol and water.

3.2.10.1. Preparation of solvents.

1-Octanol (Aldrich Chemical Co. Inc.) was refluxed over calcium hydride overnight followed by distillation to obtain dry pure 1-octanol. Equal volumes of 1-octanol (200 mL) and

distilled water (200 mL) were stirred together in a one liter brown bottle overnight. The water-saturated 1-octanol and 1-octanol-saturated water thus produced were separated and stored in brown glass bottles at room temperature until further use.

3.2.10.2. Preparation of Calibration Curve.

A stock solution of the test substrate was prepared by dissolving 1.0 mg of test sample in 1.0 mL of 1-octanol-saturated water. From this solution, 10,20,30,40 and 50 µL volumes were pipetted into two sets of numbered test tubes. These tubes were then made up to 1.0 mL with 1-octanol-saturated water. The concentration of test substrates in these tubes was therefore 10,20,30,40 and 50 µg/mL respectively.

HPLC analyses of 20 µL aliquots were performed using column A, a uv detector set at 350 nm, solvent system 60:40 water: MeOH and a flow rate of 2 mL/min.

The standard curve was prepared by plotting elution peak area versus concentration in µg/mL.

3.2.10.3. Determination of Partition Coefficient.

Test substrate from the stock solution (10,20,30,40 and 50 µL) was transferred to test tubes (3 sets of 5 tubes in each set). The volume in each tube was then made up to 1.0 mL by adding 1-octanol-saturated water to give a final concentration of 10,20,30,40 and 50 µg/mL of substrate, respectively. Then 1.0 mL of water-saturated 1-octanol was

added to each tube to give a final volume of 2.0 mL. These tubes were allowed to stand for 30 min., after which they were partitioned by a mechanical shaker (Dubnoff metabolic shaking incubator, Precision Scientific Co. Chicago, U.S.A.). After shaking at room temperature for 3.5 h the equilibrated phases were separated and the water layers were analyzed. An aliquot of 20 µL, taken from the water fraction, was injected into the HPLC and analyzed under the same conditions used to generate the standard curve. Peak area and standard curve data were used to calculate the amount of substrate in the water fraction after partitioning.

The partition coefficient (P) was then determined according to the formula; $P = C_1/C_2$, where C_1 is the concentration of substrate in octanol phase and C_2 is the concentration of substrate in water phase.

Concentration of substrate in octanol was calculated by mass balance, ie. (concentration of substrate in water before partitioning) - (concentration of substrate in water after partitioning).

Direct analysis of the octanol phase was also done with selected samples to confirm that the substrate had partitioned without any mass loss due to decomposition.

3.2.11. Study of Phosphorolysis of Test Compounds.

An *in vitro* phosphorolysis study of IAZA ,IAZG, IAZP and FIAZP was carried out by incubating the test substrates with the enzyme thymidine phosphorylase from *E.coli* (Sigma Chemical Co.) for various times ranging from 10 min. to 2 h at a temperature of 37 °C. Deoxyuridine and deoxythymidine were used as reference compounds. A general procedure for this study is given below.

3.2.11.1. Preparation of Tris Buffer Solution (10 mM Tris-HCl, pH 7.3 at 22 °C)

One liter of Tris buffer solution was made by dissolving 1.41 g Tris base (Trizma) and 0.744 g Na EDTA.$2H_2O$ in 900 mL of distilled water. The pH was measured by a standard pH meter (Radiometer Copenhagen, Model pHM 82) and adjusted to 7.3 with 10 M HCl and the solution made up to one liter with water. This solution was stored at 4 °C until further use.

3.2.11.2. Preparation of Potassium Phosphate Buffer (100 mM, pH 7.1)

KH_2PO_4 (13.6 g) was dissolved in 900 mL of water. The pH of the solution was measured by a pH meter and adjusted to 7.1 with 10 M KOH and the solution volume was made up to one liter with water. This solution was also stored at 4 °C until further use.

3.2.11.3. Preparation of Enzyme

Thymidine phosphorylase from E.coli was purchased from the Sigma Chemical Co. (T-7006). This product contains thymidine phosphorylase 1200 U/mL in 0.5 M potassium phosphate buffer, with 2.0 mM uracil and 0.02% sodium azide and bovine serum albumin. Immediately before use, 5 µL of stock enzyme solution was diluted with 3.9 mL of Tris-buffer solution to produce an enzyme dilution of 1 : 780. This working enzyme was stored in an ice bath until use.

3.2.11.4. Solutions of Substrates

Each of the test substrates, dThd and dUrd were dissolved and diluted to 5 mM in Tris-buffer. These solutions were stored at -20 °C until further use.

3.2.11.5. Enzymatic Reaction Procedure.

Each reaction was done in triplicate with an additional triplicate set of controls (without enzyme). Diluted enzyme solution (130 µL) was transferred to a 1.5 mL Eppendorf micro centrifuge tube and mixed thoroughly with 20 µL of potassium phosphate buffer (Vortex-Genie model K-550-G). Control sets were prepared in the same manner using 130 µL of Tris-buffer in place of enzyme solution. The tubes were then incubated at 37 °C for 2 min. in a water bath incubator (Haake E3, W. Germany). Test substrate was added to both the experimental and control sets (50 µL, 250 nmol). The solution was mixed thoroughly by vortexing and then incubated at 37 °C for the desired time (10 min. to 2 h).

The reaction was terminated by addition of 200 µL of ice-cold methanol followed by vortex mixing and storage in an ice bath for 10 min. After centrifuging for 3 min. at 4 °C, 350 µL of clear supernatant was transferred from each tube to another set of clean tubes. These tubes were stored at -20 °C until analysis by HPLC.

3.2.11.6. Analytical Procedure.

Stored samples were thawed and 50 µL of the supernatant from each tube was injected into the HPLC. A reverse phase analytical column (column A) was used for analysis. The solvent system was 60:40 water: MeOH at a flow rate of 2 mL/min. The uv detector was operated at a wavelength of 350 nm for all substrates except dThd and dUrd, where 270 nm was used.

The peak area and retention time of each of the test substrates at different times of incubation were compared to the corresponding control substrates.

3.2.12. Animal Studies

3.2.12.1 Preparation of the Animal Model

Murine EMT-6 tumor cells were obtained as a suspension in normal saline from the Cross Cancer Institute, at a concentration of about $1x10^6$ cells/mL. The cell suspension (0.1 mL; $1x10^5$ cells) was injected subcutaneously into the left flank of each recipient Balb/c mouse. The mice were

caged in standard plastic cages (5 mice per cage) and maintained with water and rodent food pellets ad lib. After 12 to 14 days, when the tumors reached the desired size of 300 to 500 mg (8-10 mm diameter), the animals were used for biodistribution or whole-body scintigraphic study.

3.2.12.2. Administration of Radiopharmaceuticals.

Radiolabelled compounds were stored dry and frozen, and were reconstituted with physiological saline just prior to injection. The radioactivity of the vials was measured by an isotope dose calibrator and the appropriate dilutions were made so that each mouse would receive the required activity in about 0.1 mL. For biodistribution studies, the radioactivity present in 0.1 mL solution was 50-60 kBq (1.35 - 1.62 μCi) and for whole-body scintigraphic study it was 3.7 to 4.44 MBq (100 - 120 μCi). Reconstituted radiopharmaceuticals were injected via the dorsal tail vein in a single bolus injection.

3.2.12.3. Collection of Tissue Samples.

Tissue samples of the mice that received a single bolus injection of radiopharmaceuticals were collected by the following general procedure.

The mice were sacrificed by asphyxiation with carbon dioxide, followed by cardiac puncture and exsanguination.

In addition to the blood, other samples recovered were heart, lung, liver, kidney, spleen, gastrointestinal tract (GIT), stomach, muscle, bone, tumor, thyroid, skin and tail. Entire organs of the above mentioned samples were dissected and collected into small plastic vials and weighed wet using a taring balance. Stomach and GIT samples were emptied of their food contents. Other organs were blotted to remove surface blood contamination. The muscle sample was taken from the upper hind leg, and the femur of this leg was removed as a representative sample of long bone. A skin sample containing fur was taken from the upper back. The thyroid was collected with trachea containing surrounding tissue. The remaining carcass was divided into two portions and placed into large counting vials (Beckman Poly-Q-vials) and weighed by a taring balance.

3.2.12.4. Biodistribution Study.

Balb/c mice bearing EMT-6 tumors were given an i.v. dose of the radiopharmaceuticals and were then sacrificed at various time intervals after injection. Biological samples were collected by the procedure outlined in section 3.2.12.3.

The tissue samples containing ^{125}I were counted in a Beckman Gamma 8000 gamma scintillation counter. The count per min. value (cpm) for each tissue sample was determined

in the preset ^{125}I counting window, with correction for background. The cpm of ^{125}I radiopharmaceutical administered to each animal was determined by counting a known volume of diluted injected dose. No attempt was made to correct for counting efficiency. Cpm values were used for all calculations.

The data from six animals at each time period were analyzed with the help of an animal distribution computer program[c].

3.2.12.5. Whole-Body Scintigraphy.

Whole-body scintigraphic studies were performed on Balb/c mice bearing EMT-6 tumors, at set time periods chosen on the basis of the biodistribution and preliminary imaging studies with ^{125}I-IAZA. IAZG imaging time period was chosen on the basis of biodistribution study. Imaging was performed with a Searle gamma camera (Pho/Gamma III) and ADAC (CAM III) computer using a pin-hole collimator.

In the study, animals were dosed with 3.7 to 4.44 MBq of ^{125}I-IAZA and ^{123}I labelled IAZA or IAZG, as a bolus injection. And about 10 min. prior to imaging they were anesthesized with Rompun® and Ketamin®.

The anesthetic was prepared by adding 0.5 mL (10 mg) of Rompun® and 0.3 mL (30 mg) of Ketamin® to 6 mL of normal

---

[c]A series of programs to assist in analysis of biodistribution data were written in-house by Dr. Richard Flanagan and are accessed through the University of Alberta MTS computing service.

saline. The anesthetic dose used in the study was 0.2 mL of the mixture, injected intraperitoneally (i.p).

3.2.12.6. *In vivo* Toxicity Study

In vivo toxicity studies were carried out with IAZA and IAZP in Balb/c mice. Ten male Balb/c mice weighing 15-20 g (age 30-34 days) were injected i.v. with 350 µg of the test compounds as a bolus dose in 0.1 mL normal saline. A control group of ten mice received an equal volume of saline by the same route.

The control and experimental groups were maintained separately in groups of 5 mice in plastic cages. Water and standard rodent pellets were provided *ad lib*.

The mice were weighed daily for 30 days and then sent for histopathological examination to Veterinary Laboratory, Animal Health Division of Govt. of Alberta Agriculture. The mice were euthanised upon receipt, followed by postmortem examinations. Samples of adrenal glands, kidney, lung, heart, spleen and gonads were taken for histopathological evaluation.

3.2.13. *In vitro* Study with EMT-6 Tumor Cells.

The *in vitro* tests described in this section were carried out by the technical staff of the Radiobiology Department of the Cross Cancer Institute. Short descrip-

tions of the procedures are given below, along with references to more detailed discussions.

3.2.13.1. Cytotoxicity

The cytotoxic effect of the test substrates was determined by *in vitro* analysis using EMT-6 cells according to the method described by Chapman *et al*[174] and Jette *et al*[12].

EMT-6 cells were grown in monolayers in culture flasks, recovered in suspension and the suspensions were centrifuged to obtain cell pellets. The pelleted cells were resuspended in 5 to 6 mL of Spinner Minimal Essential Medium (MEM) and readjusted to $1x10^6$ cells/mL. In each glass chamber, $5x10^5$ cells were suspended, then gassed at 0.5 L /min. with air + 5% CO_2 for 10 min. for aerobic conditions and with nitrogen + 5% CO_2 for 30 min. for hypoxic conditions.

Solutions of the test substrates were prepared in sterile water at concentrations 20-30 times higher than the desired concentration, and were added to the chamber in small volumes to get the desired final concentrations. The chambers were allowed to incubate at 37 °C in a thermostat controlled water bath. Aliquots of cell samples were removed at various time periods and plated in MEM to determine their colony-forming ability upon incubation in a tissue culture incubator.

Cytotoxic effects of the test substrate were measured from the survival curves. Survival curves were constructed according to the established method described elsewhere[12,174] (see Appendix 1 for characteristic features).

3.2.13.2. Initial Binding Rate.

Suspensions of EMT-6 murine tumor cells in glass incubation chambers were prepared by procedures identical to the above, and made hypoxic under 95% nitrogen and 5% CO_2 or aerobic with 95% air and 5% CO_2 . The cells were equilibrated for 30 min. under gas flow prior to addition of test substrates.

Solutions of test substrates labelled with ^{125}I were added to the vessel as described above. The vessels were allowed to incubate at 37 °C in a water bath incubator. Aliquots of the samples were drawn at various time intervals and treated with 5% trichloroacetic acid (TCA) according to the method described by Jette et al[12].

The amount of ^{125}I activity bound to the acid-insoluble macromolecular fraction was counted by Beckman Gamma 8000 gamma counter.

The initial binding rate of each test substrate was calculated according to the procedure given in Appendix 2. The binding rate was expressed as pmol/10^6 cells/h against substrate concentrations.

A closer examination of the binding-dependency on oxygen concentration was carried out by the procedures used above, by substituting various concentrations of oxygen (0.03%, 0.1%, 0.3%, 1% and 3%) in nitrogen for air.

3.2.13.3. Radiosensitization.

Suspensions of EMT-6 murine tumor cells were prepared and suspended in glass irradiation chambers by processes similar to those described above. Preparation of hypoxic and aerobic conditions in the glass chambers was carried out by similar methods as described above. Detail procedures for this study are described by Jette et al[12].

Test substrate solutions in Hanks balance salt solution (HBSS) were added to the vessels which were in the hypoxic condition; no test substrate was added to the chamber in the aerobic condition or in hypoxic control chamber. The cells in the chamber were irradiated at 37 °C by an ^{137}Cs irradiator at a dose rate of 1.2 Gy/min. An aliquot of cell suspension was collected after each fraction of radiation dose and plated in petri dishes. These dishes were incubated for one week to determine the colony forming ability of the cells.

Radiation survival curves were constructed for various concentrations of test substrates by plotting cell survival fractions as a function of radiation doses (see Appendix 3 for characteristic features).

4. RESULTS AND DISCUSSION

4.1. 1-(5-Iodo-5-Deoxy-β-D-Arabinofuranosyl)-2-Nitroimidazole (Iodoazomycin Arabinoside:IAZA) (45)

4.1.1. Chemistry

The title compound (IAZA, 45) was synthesized by the general procedure in section 3.2.1. and as described in detail elsewhere[197]. The synthesis is outlined in Scheme 6.

Scheme 7 shows the two methods of exchange radioiodination of IAZA (45) used in this study. Method A employed dimethyl formamide (DMF) as a solvent while Method B was a 'melt method' using pivalic acid. Detailed radiosynthesis by these two methods is described in section 3.2.5. The radiochemical yields by both methods were similar (~70%).

An aliquot of the reaction mixture from Method A was analyzed using column A (60:40 H_2O: MeOH, flow rate 2 mL/min., 350 nm). The chemical yield of IAZA (45) as indicated by the uv chromatogram was 80%. The radiochemical yield was calculated by Radio-HPLC, based on the amount of radioactive compound corresponding to the uv trace at IAZA (45) retention time of about 6.85 min. The other peaks observed in the chromatogram indicate deiodinated product (AZA, 44) and some unidentified impurities. The identity of the former product (AZA, 44) was confirmed by analyzing pure AZA (44), which under the same conditions had an identical

Scheme 6. Synthesis of 1-(5-iodo-5-deoxy-β-D-arabinofuranosyl)-2-nitroimidazole (IAZA, 45).

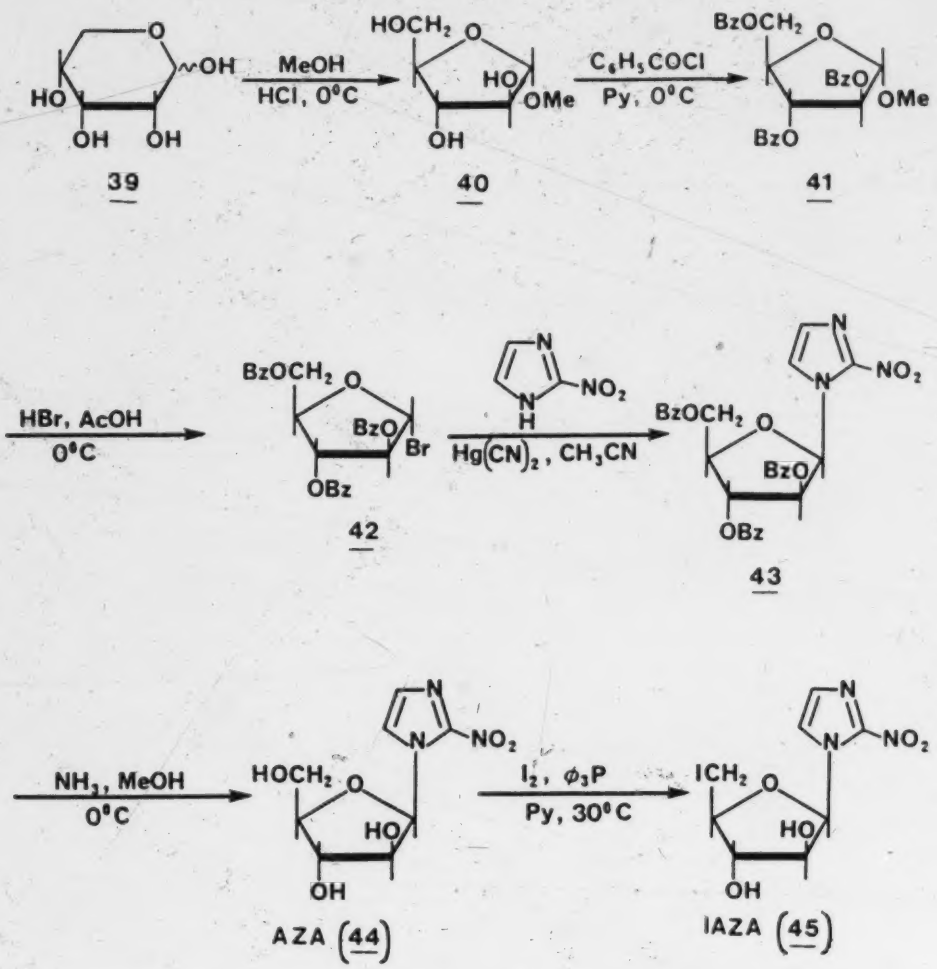

Scheme 7. Synthesis of radioiodinated 1-(5-iodo-5-deoxy-ß-D-arabinofuranosyl)-2-nitroimidazole.

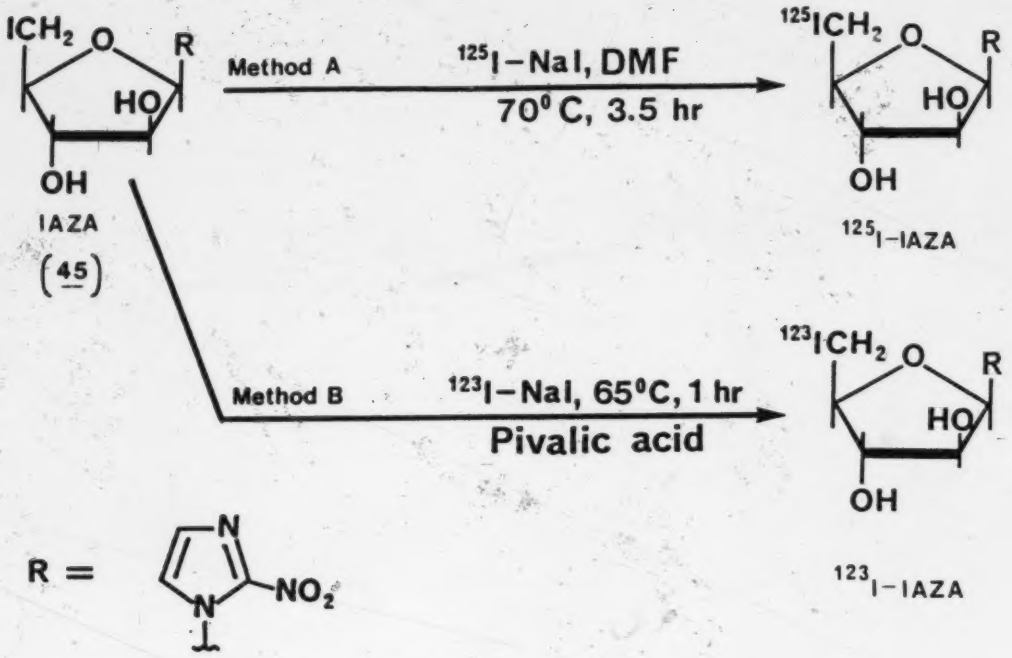

retention time (2.79 min.). The radioactive peaks other than ^{125}I-IAZA detected by Radio-HPLC appeared to be free iodide (18-20%) and unidentified compounds (8-10%). No attempt was made to improve radiochemical or chemical yield except for one instance, where the reaction was carried out for 4.5 h and showed a similar yield as above. The crude product, purified using column B (60:40 H_2O: MeOH, flow rate 2 mL/min., 350 nm), showed a retention time of 10.60 min. for

^{125}I-IAZA. This product was synthesized and purified routinely under the conditions mentioned above and was used for *in vitro*, biodistribution and preliminary scintigraphic studies.

Method B (Scheme 7) was used in an attempt to synthesize ^{123}I-IAZA with higher chemical and radiochemical yields in shorter reaction times. Although no improvement was realized in terms of yields, Method B was preferred for the ^{123}I synthesis due to the shorter reaction time required compared to Method A. The initial reaction was performed using 5 mg of pivalic acid, with 2.4 mg of IAZA (45), which provided 60% radiochemical yield after 80 min. reaction time at 70 °C. Several attempts were made to improve the radiochemical yield with same amount of IAZA by varying the temperature, the amount of pivalic acid and the reaction time. With 2 mg of pivalic acid at 65 °C for a 1 h reaction time, a radiochemical yield of 70% was achieved, although no improvement on product decomposition was achieved. The HPLC analysis and purification of the reaction mixture were performed using column B (30:70 H_2O: MeOH, flow rate 2 mL/min.,350 nm). The chromatogram showed a product retention time of 7.76 min. The chemical yield was 85% and the radiochemical yield as detected by Radio-HPLC was 72%. The other uv peaks appeared to be deiodinated compound (AZA, 44) and some undetermined impurities. Free radioiodide seemed to be the major contaminant found in Radio-HPLC, at about 3.29 min.

retention time. The product (^{123}I-IAZA) synthesized routinely by the Method B (melt method) was used for scintigraphic studies only. The purified product from both of these two methods, when analyzed by HPLC, showed chemical and radiochemical purity greater than 99%.

4.1.2. *In vivo* Toxicity

The *in vivo* toxicity of IAZA (45) was studied in healthy Balb/c mice. The amount of IAZA (45) injected per mouse, in a single bolus dose, was about 100 times higher based on body mass than the anticipated dose required for imaging in humans. The human dose is expected to be 10 mg/70 kg. Each animal, weighing approximately 20 g, was injected with 350 µg of the test compound (IAZA).

In 30 days of observation after dosing, there was no death, no weight loss and no unusual behaviour among the treated mice as compared to the control group. Both the groups showed usual normal weight gain and the physical appearance of all mice was normal.

On the 31st day after dosing the mice were sacrificed for histopathological examination. The histopathological report provided by the veterinary pathologist (based on a double blind model) suggested no toxicity. Evidence of silent myocarditis in one treated mouse was believed to be due to a non-related infection. The non-toxic nature of IAZA (45) at this dose was subsequently confirmed by a second study

performed by another group[203]. The results suggested that at this dose IAZA is totally non-toxic *in vivo* to mice for this period of time (30 day).

4.1.3. Cytotoxicity

The cytotoxic effect of AZA (44) and IAZA (45) was studied *in vitro* with hypoxic EMT-6 cells, as described in detail earlier in section 3.2.13.1. The cytotoxic effect of IAZA (45) on the cell cultures at various concentrations (0.1, 0.3 and 1.0 mM), when incubated for upto 6 h at 37 °C, is given in Figure 1. The data show that IAZA (45) exerts a cytotoxic effect on the EMT-6 cells in culture under hypoxic conditions. The toxicity increases with time and with concentration of the substrate (IAZA). The time required to kill 90% of the cells was found to be 1.65 h at a concentration of 1.0 mM. At lower concentrations (0.1 or 0.3 mM) the 90% cell kill was not reached during an incubation period of 6 h. Figure 2 shows the cytotoxic effect of AZA (44) at concentrations of 1.0 and 5.0 mM. At 5.0 mM, 90% cell kill was achieved in 5.2 h; at 1.0 mM, the 90% cell kill was not reached during a 6 h incubation period.

However, neither IAZA nor AZA showed cytotoxic effects under aerobic conditions at these concentrations in the same cell line. Other electron-affinic compounds including misonidazole (1) and IAZR (2) have also shown selective toxicity to hypoxic cells[12,72,73,204-206].

Figure 1. Surviving fractions of hypoxic EMT-6 cells incubated with various concentrations of IAZA at various time intervals.

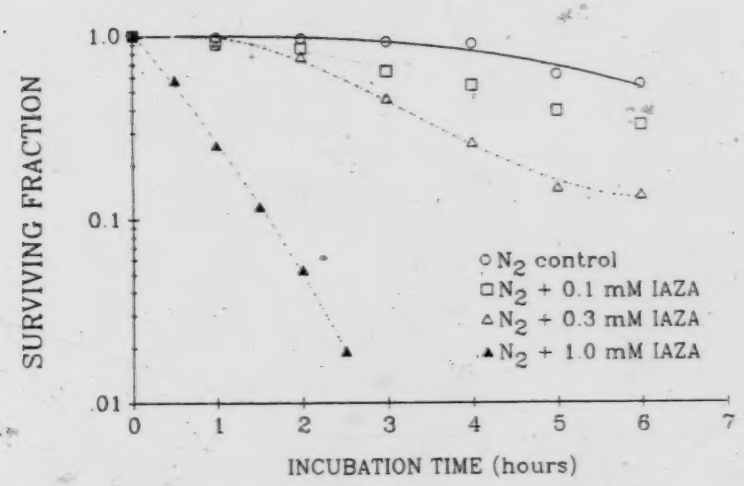

Figure 2. Surviving fractions of hypoxic EMT-6 cells incubated with various concentrations of AZA at various time intervals.

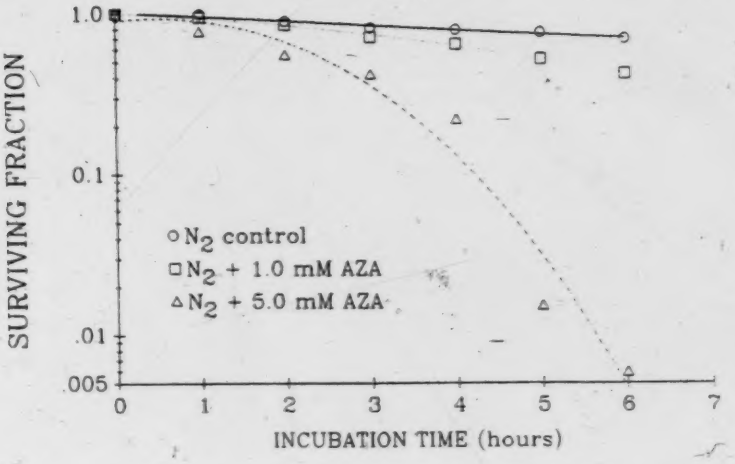

A comparison of the hypoxic cell cytotoxicity of IAZA (45) and AZA (44) is shown in Figure 3 as the reciprocal of time (hr^{-1}) required to kill 90% of cells plotted against substrate concentration. With concentrations of substrates that did not reach 90% cell kill during 6 h of incubation, the survival curve was extrapolated to determine 90% cell kill times. From Figure 3 IAZA (45) is seen to be 5.9 times more toxic than AZA (44) at equimolar concentrations (1.0 mM). IAZA was also found to be more toxic than misonidazole (1) under similar conditions[d].

The exact mechanism of this preferential hypoxic cell cytotoxicity remains a matter of further investigation. However, studies with various other nitroimidazoles have suggested that DNA damage may be the major cause of hypoxic cell toxicity[119,156,207-211]. A short-lived nitroimidazole reduction intermediate species appears to be responsible for DNA damage[119,156], by an adduct forming process[212,213]. The cytotoxic, mutagenic and radiosensitizing actions of nitroimidazoles have all been attributed to this DNA adduct forming process[212,213].

The exact reason for increased toxicity of IAZA (45) over AZA (44) and misonidazole (1) remains unelucidated. However, it is likely that partition coefficient and perhaps reduction potential may be major contributing factors[214,215].

---

[d]Detailed comparative data will be accumulated and discussed in a separate, summary Chapter (Chapter 5).

IAZA (45) is more lipophilic (P = 4.98) than AZA (44) (P = 0.52) and misonidazole (1) (P = 0.43), and it is possible that the intracellular concentration needed for peak cytotoxicity is reached much faster with IAZA. It is premature to make any comment on the effect of reduction potential, since the reduction potentials of IAZA and AZA have not been determined.

Figure 3. Comparison of hypoxic cell cytotoxicity as a function of reciprocal of time (hr^{-1}) for 90% cell kill with various concentrations of IAZA and AZA.

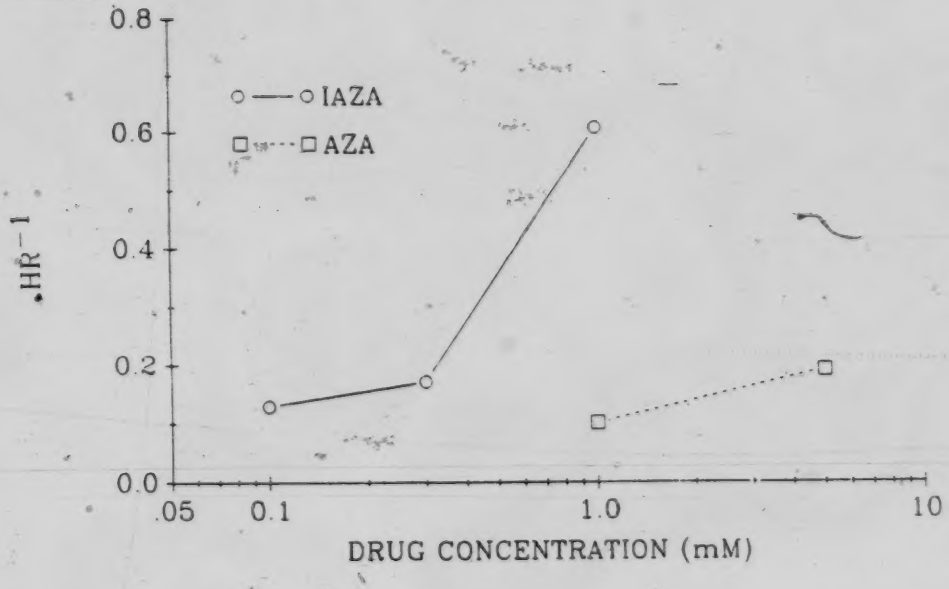

This increased toxicity of IAZA (45) over AZA (44) or misonidazole (1) was expected because IAZR (2), an analog of IAZA (45) was reported to have higher cytotoxicity than its non-iodinated analog AZR (32) or misonidazole (1) under similar conditions[12].

Compounds with high cytotoxicity toward hypoxic cells could be employed for the treatment of hypoxic cells in tumor in combination with other chemotherapeutic agents[216] and/or with radiotherapy[217]. IAZA might not be an ideal hypoxic cell cytotoxic agent for therapy. Other novel compounds are reported to be effective as cytotoxic agents at concentrations 100-1000 times lower than observed with misonidazole (1)[191,206].

4.1.4. Radiosensitization

The *in vitro* radiosensitizing property of IAZA (45) and AZA (44) was studied in hypoxic EMT-6 cells with various concentrations of the test substrates, along with air and nitrogen controls, as described previously in Section 3.2.13.3. Figures 4 and 5 show the surviving fractions of EMT-6 cells exposed to various radiation doses and various concentrations of IAZA (0.1, 0.5, 1.0 mM) and AZA (0.2, 1.0, 2.0 mM).

Under aerobic conditions, the radiation dose required for 90% cell kill is 2.8 times less than when the cells are irradiated under hypoxic conditions. This is known as the

Figure 4. Surviving fractions of EMT-6 cells at various radiation doses in air, nitrogen and nitrogen plus various concentrations of IAZA.

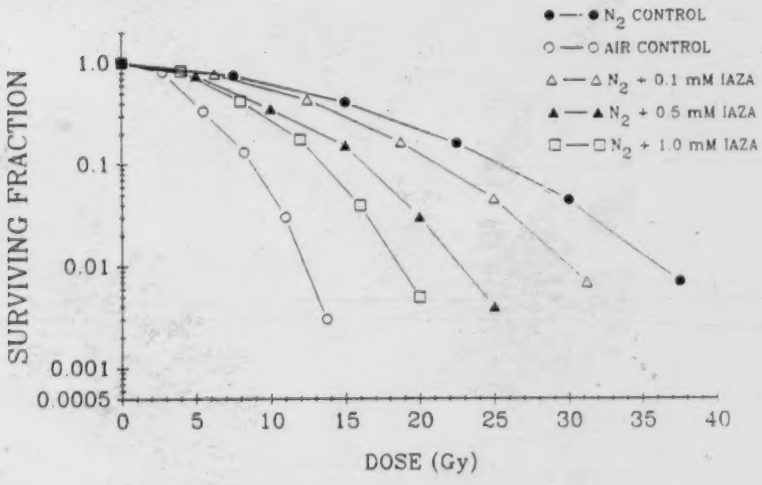

Figure 5. Surviving fractions of EMT-6 cells at various radiation doses in air, nitrogen and nitrogen plus various concentrations of AZA.

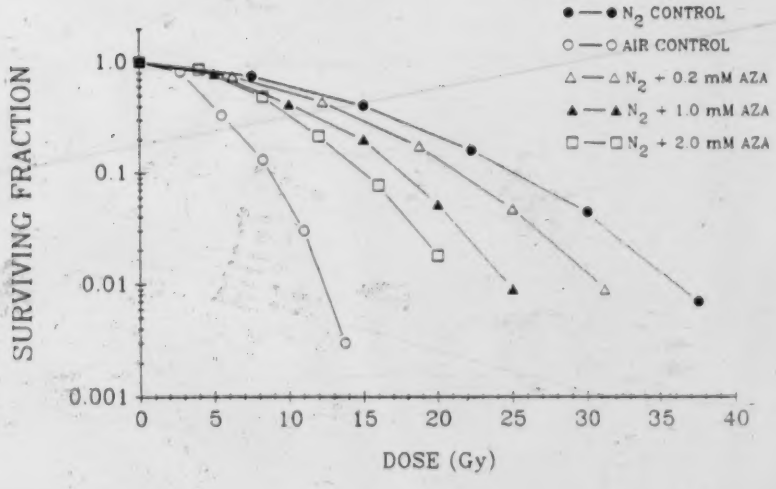

oxygen enhancement ratio (OER), defined as the ratio of the radiation dose required for 90% cell kill under hypoxia to the radiation dose required for the same level of kill under aerobic conditions. The survival curves (Figures 4 and 5) show a greater slope under hypoxic conditions as compared to aerobic conditions. This demonstrates the inherent radioresistant property of hypoxic cells.

However, when hypoxic cells are incubated with various concentrations of test substrates (IAZA, AZA), increased radiosensitivity is evident and the slope of the curve decreases as the concentration of the substrate increases.

A comparison of the sensitizer enhancement ratio (SER) of IAZA (45) and AZA (44) at various concentrations of test substrate is shown in Figure 6. The SER is calculated as the ratio of radiation dose required to achieve 90% cell kill in hypoxic cells under substrate-free and substrate-added conditions. IAZA (45) is more efficient than AZA (44) in sensitizing hypoxic EMT-6 cells to the lethal effects of ionizing radiation. IAZA is found to be 2-3 times more effective than AZA on a concentration basis to achieve the same SER. Both compounds (IAZA, AZA) have higher SER's than misonidazole (1), similar in magnitude to IAZR (2) (detail in Chapter 5).

Drug-induced hypoxic cell radiosensitivity is observed with electron-affinic compounds and is related to the reduction potential of these compounds[43,90-95]. IAZA and AZA have

radiosensitizing properties qualitatively similar to other electron-affinic compounds[12].

Figure 6. Comparison of sensitizer enhancement ratios (SER) of IAZA and AZA as a function of substrate concentration <u>in vitro</u> with hypoxic EMT-6 cells.

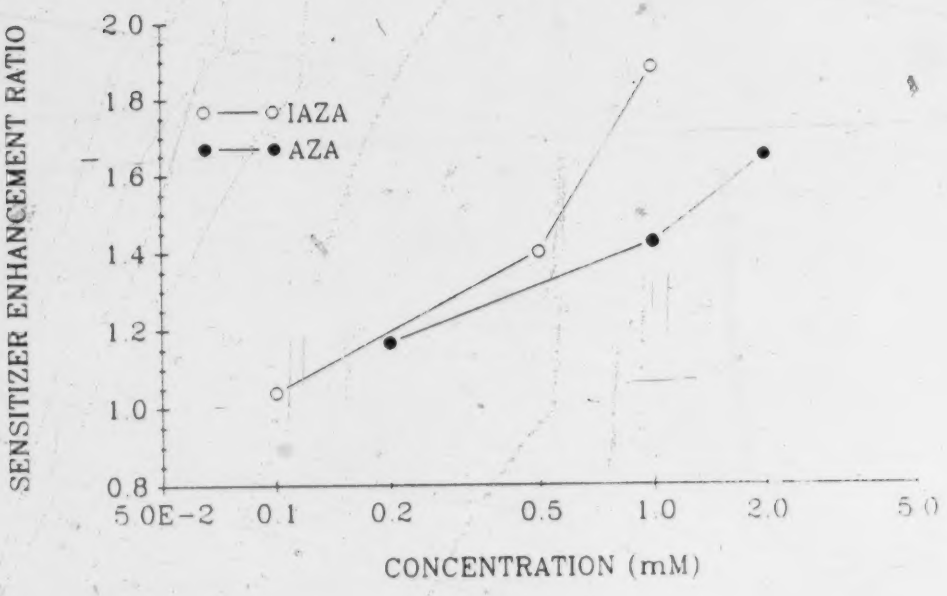

The enhanced radiosensitization by IAZA (<u>45</u>) over AZA (<u>44</u>) was expected, since IAZR (<u>2</u>), under the similar conditions, showed higher radiosensitization than the corresponding AZR (<u>32</u>)[12]. The exact reason for this effect is yet to be determined. However, several explanations could be appropriate - (a) studies with several compounds showed a general trend that compounds which are more cytotoxic are

more effective radiosensitizers[191]. (b) iodine-containing compounds are known to have better radiosensitizing properties than compounds not containing iodine[218]. This is because a transient species of iodine or iodine containing radicals are formed by reaction with radiation-induced primary water radicals. This transient species is more efficient than primary water radicals in attacking critical biological structures, and thereby enhancing radiation-induced cell death[218,219]. These explanations seem to be applicable with IAZA (45), which is more cytotoxic and a better radiosensitizer than non-iodinated compound AZA (44). Further investigations are needed to validate these hypotheses.

4.1.5. Initial Binding Rate

Figure 7 shows the amount of ^{125}I activity bound to the acid-insoluble fraction of EMT-6 cells after incubation with ^{125}I-IAZA under aerobic and hypoxic conditions, expressed as cpm/10^6 cells versus time. Under hypoxic conditions, binding of the test substrate increases linearly with incubation time and also with concentration of the substrate. Under aerobic conditions the binding is negligible and remains constant during a 3 h period of incubation. This result therefore suggests selective binding of the test drug to hypoxic cells. The initial binding rate at various concentrations of ^{125}I-IAZA to macromolecular fractions of hypoxic

Figure 7. ^{125}I Activity bound to the acid-insoluble fraction of EMT-6 cells after incubation with various concentrations of ^{125}I-IAZA at various time periods, under hypoxic and aerobic conditions.

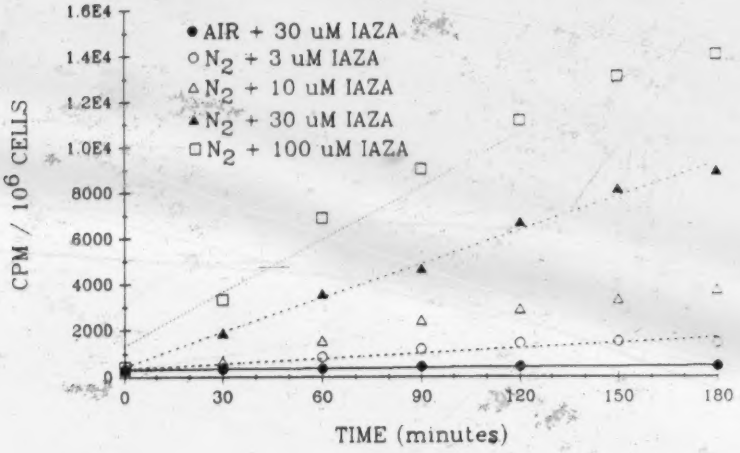

Figure 8. The initial binding rates, expressed as pmol/10^6 cells/h, of ^{125}I-IAZA to the acid-insoluble fraction of hypoxic EMT-6 cells at various concentrations of the test substrates.

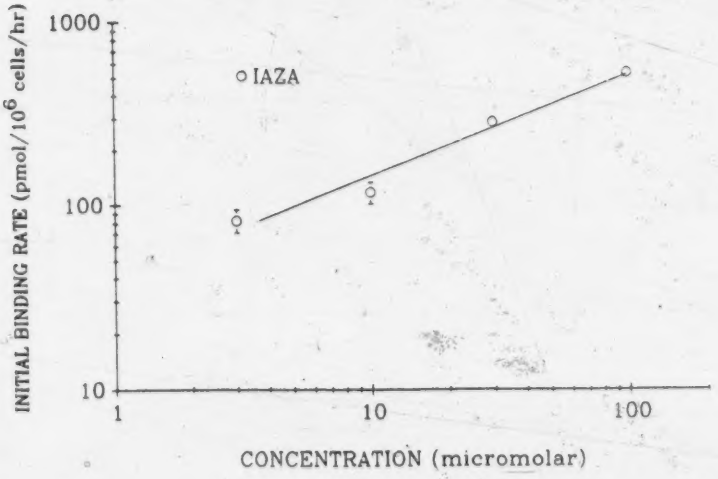

EMT-6 cells, expressed as pmol/10^6 cells/h, is given in Figure 8. The rate of binding under hypoxic conditions at a concentration of 30 μM was found to be 7.4 times greater than that observed under aerobic conditions at the same concentration. IAZA (45) was found to have a binding rate 3 to 4 times higher than misonidazole (1), a rate comparable with IAZR (2), at a concentration range between 10 and 100 μM.

The *in vitro* binding characteristics of ^{125}I-IAZA were not only studied in EMT-6 cells under hypoxia as described above, but also at different oxygen concentrations (0.03, 0.1, 0.3, 1 and 3%) (Figures 9 and 10). This study was performed to observe the relative dependence of IAZA (45) binding properties on cellular oxygen levels. As seen in Figure 9, the amount of binding of the ^{125}I activity is inversely related to the cellular oxygen levels, with the highest binding obtained in hypoxia.

The initial binding rate measured in units of pmol/10^6 cells/h versus oxygen concentration is shown in Figure 10. These data emphasise the oxygen dependent nature of the ^{125}I-IAZA binding *in vitro*. The rate of adduct formation drops slightly up to 0.1% oxygen and then more rapidly up to 3% oxygen.

The result indicates the potential of IAZA (45) to assess the intracellular oxygenation status of tumor tissue *in vivo* by scintigraphic analyses. The signal intensity between

Figure 9. ^{125}I Activity bound to the acid-insoluble fraction of EMT-6 cells under hypoxia and various levels of oxygen incubated with 10 μM ^{125}I-IAZA, at several time periods.

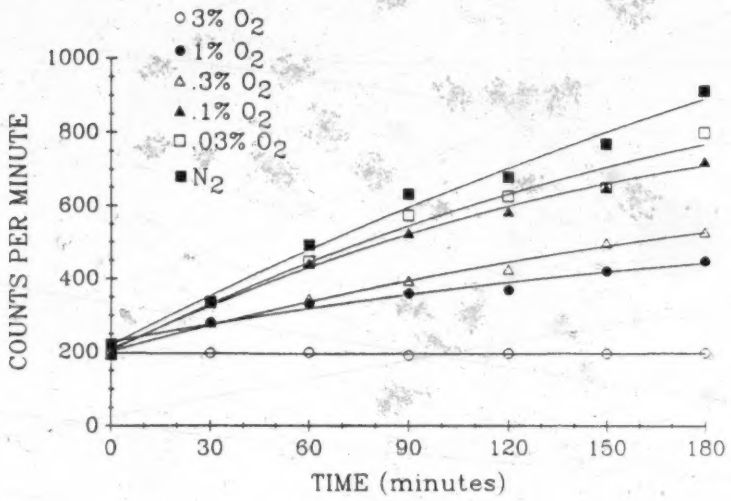

Figure 10. The initial binding rate of 10 μM ^{125}I-IAZA to the acid-insoluble fraction of EMT-6 cells under hypoxia and various levels of oxygenation.

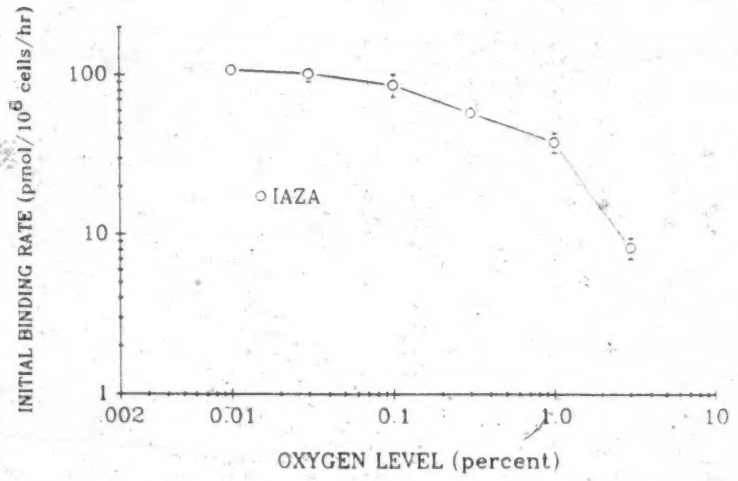

hypoxic tissues and normal tissue background is important for non-invasive analyses. It is possible at this point to predict that IAZA would have higher hypoxic signal than normal tissue background, as the binding is found to have an inverse relationship to oxygen level. However, the accuracy of this prediction will depend on the *in vivo* behaviour of IAZA in different organ systems.

4.1.6. Biodistribution and Elimination

The *in vivo* biodistribution study of ^{125}I-IAZA was carried out in Balb/c mice bearing the EMT-6 tumors. The specific activity of the injected compound (^{125}I-IAZA) was 7-9 GBq/mmol. Each animal received a dose of 50-60 kBq representing 2-3 µg of IAZA (45). The biodistribution results, as computed after measuring ^{125}I activity in each organ and in the remaining carcass, are shown in Table 2. No attempt was made to identify the metabolite(s) or the parent compound in these organs.

Table 2 reveals a rapid early distribution of ^{125}I-IAZA throughout the body with the tumor containing lower radioactivity compared to most of the other organs. This may be an indication of decreased perfusion of the tumor tissue. At longer time periods, between 4 and 24 h, tumor radioactivity, in terms of percent injected dose per gram, was found to be higher than in any other organs with the exception of thyroid. This higher tumor radioactivity is

Table 2. Biodistribution of ^{123}I-IAZA following i.v. administration in Balb/c mice bearing EMT-6 tumors at various time intervals.

Organ	Time (hours) 0.25	0.50	1	2	4	8	24
Blood	2.63 ±0.30[a]	2.17 ±0.42	1.84 ±0.67	0.91 ±0.20	0.45 ±0.32	0.14 ±0.03	0.037 ±0.007
Tumor	2.55 ±0.28 0.97 ±0.15[b]	3.48 ±0.85 1.60 ±0.42	2.70 ±0.07 1.46 ±0.45	2.55 ±1.56 2.80 ±0.85	2.08 ±1.24 4.62 ±0.52	1.22 ±0.07 8.71 ±1.39	0.206 ±0.047 5.56 ±1.10
Kidney	6.56 ±0.63 2.49 ±0.19	5.67 ±0.95 2.61 ±0.21	4.38 ±1.25 2.38 ±0.25	1.80 ±0.61 1.98 ±0.92	0.66 ±0.39 1.46 ±0.13	0.34 ±0.06 2.43 ±0.39	0.052 ±0.004 1.41 ±0.29
GIT[c]	5.42 ±1.03 2.06 ±0.41	4.44 ±0.62 2.04 ±0.41	4.63 ±1.92 2.52 ±0.36	1.73 ±0.55 1.90 ±0.36	0.81 ±0.46 1.80 ±0.34	0.77 ±0.36 5.50 ±1.77	0.041 ±0.016 1.11 ±0.74
Liver	8.65 ±1.02 3.29 ±0.31	7.14 ±1.13 3.29 ±0.41	5.63 ±2.27 3.06 ±0.41	2.18 ±0.80 2.39 ±0.55	0.95 ±0.58 2.11 ±0.20	0.47 ±0.10 3.36 ±0.52	0.098 ±0.008 2.64 ±0.31
Muscle	3.09 ±0.67 1.17 ±0.18	2.77 ±0.54 1.28 ±0.14	2.19 ±1.03 1.19 ±0.17	0.69 ±0.29 0.75 ±0.16	0.24 ±0.12 0.53 ±0.21	0.36 ±0.31 2.57 ±0.68	0.020 ±0.004 0.54 ±0.19
Bone	1.31 ±0.18 0.50 ±0.10	1.37 ±0.57 0.63 ±0.13	1.15 ±0.52 0.63 ±0.14	0.58 ±0.26 0.64 ±0.21	0.27 ±0.09 0.60 ±0.30	0.08 ±0.03 0.57 ±0.11	0.022 ±0.03 0.59 ±0.15
Lung	4.61 ±0.82 1.75 ±0.16	3.77 ±0.67 1.74 ±0.19	2.99 ±1.41 1.63 ±0.19	1.15 ±0.38 1.26 ±0.15	0.45 ±0.30 1.00 ±0.17	0.33 ±0.07 2.36 ±0.19	0.037 ±0.008 1.00 ±0.24
Heart	4.69 ±0.91 1.78 ±0.17	3.56 ±0.66 1.64 ±0.20	2.78 ±1.30 1.51 ± 0.19	1.03 ±0.43 1.13 ±0.22	0.32 ±0.24 0.71 ±0.12	0.22 ±0.05 1.57 ±0.15	0.042 ±0.019 1.14 ±0.27
Spleen	3.57 ±0.67 1.36 ±0.17	3.00 ±0.62 1.38 ±0.13	2.48 ±1.25 1.35 ±0.22	0.93 ±0.37 1.02 ±0.18	0.35 ±0.20 0.78 ±0.15	0.18 ±0.04 1.29 ±0.21	0.036 ±0.034 0.97 ±0.37
Stomach	4.36 ±0.70 1.66 ±0.16	4.75 ±1.50 2.19 ±0.29	3.95 ±0.93 2.15 ±0.37	3.30 ±0.93 3.62 ±0.84	1.81 ±1.60 4.02 ±0.78	0.87 ±0.54 6.21 ±3.53	0.067 ±0.014 1.81 ±0.41
Carcass	2.68 ±0.44 1.02 ±0.10	2.55 ±0.37 1.18 ±0.12	2.33 ±0.91 1.21 ±0.14	1.46 ±0.29 1.60 ±0.22	0.89 ±0.52 1.98 ±0.21	0.28 ±0.12 2.00 ±0.95	0.038±0.016 1.03 ±0.27

[a]The numbers represent the mean ± standard deviation for percent of injected dose per gram of wet tissue for 6 animals. [b]Tissue to blood ratio. [c]Section of intestine.

presumably because of slower clearance of radioactivity from the tumor tissue, an observation consistent with metabolic trapping of IAZA. The thyroid tissue, as shown in Table 3, indicated a gradual increment of radioactivity which reached a maximum of 38% of the total body radioactivity at 24 h.

Table 3. Thyroid radioactivity as percent injected dose of ^{125}I-IAZA/organ, in Balb/c mice bearing EMT-6 tumors (n=6; ±S.D.).

Time (hour)	Percent injected dose/organ	Thyroid radioactivity as percentage of whole-body radioactivity
0.25	0.06±0.03	0.08±0.03
0.50	0.08±0.04	0.12±0.03
1.00	0.15±0.10	0.29±0.11
2.00	0.37±0.25	1.14±0.32
4.00	0.36±0.23	1.73±0.6
8.00	0.42±0.10	3.63±0.9
24.00	0.77±0.22	38.30±2.5

The organ to blood ratio (calculated as g/g) of radioactivity (Figures 11 and 12) was highest for tumor at time periods between 4 and 24 h. The tumor to blood ratio rose gradually to a maximum of 8.7 at 8 h, then declined to 5.6 at 24 h, representing 1.2 and 0.21 percent of injected dose

Figure 11. Tissue to blood ratios of radioactivity at various time intervals following i.v. administration of ^{125}I-IAZA in Balb/c mice bearing EMT-6 tumors.

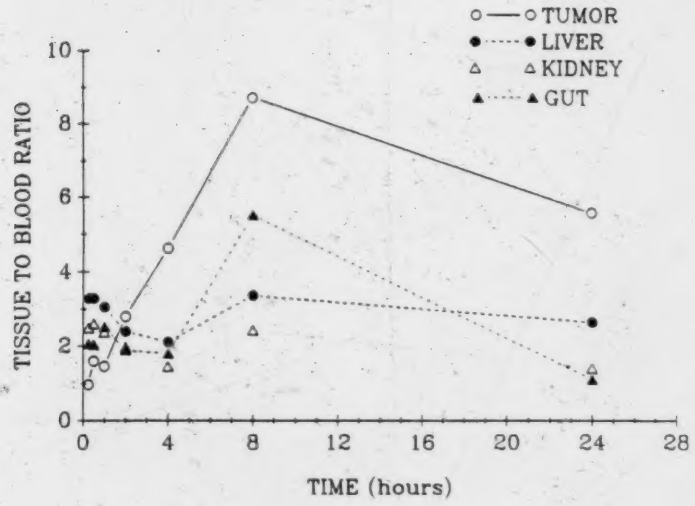

Figure 12. Tissue to blood ratios of radioactivity at various time intervals following i.v. administration of ^{125}I-IAZA in Balb/c mice bearing EMT-6 tumors.

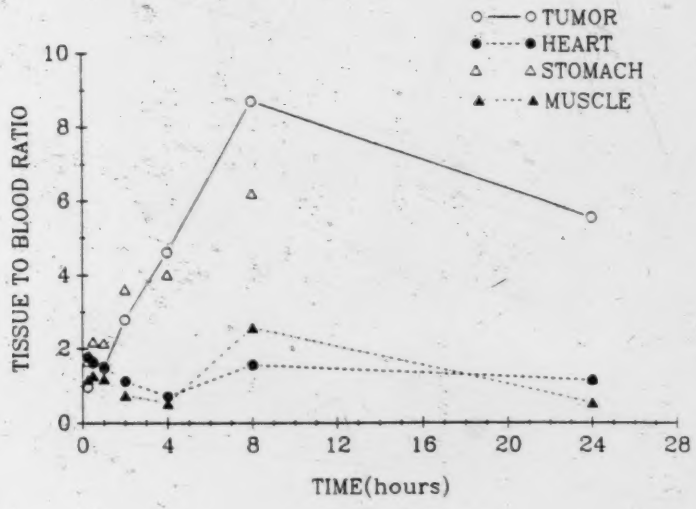

per gram of tissue, respectively. At 8 h, organ to blood ratios were relatively high in stomach, intestine, liver and kidney. These ratios were similar in magnitude to the tumor ratio when standard deviation is considered. However, the percent of injected dose per gram of tumor tissue at 8 h was higher than in these organs. At 24 h, with the exception of thyroid, only liver showed a ratio of slightly higher than 2, with 0.09% of injected dose per gram of tissue.

The gradual increase in thyroid radioactivity (Table 3) was probably due to the *in vivo* deiodination of ^{125}I-IAZA, as thyroid is known to extract and accumulate circulating iodide[220]. Elevated levels of ^{125}I activity in the stomach and intestine are also indicative of free iodide since these organs are known to take up iodide[220].

Early hepatic radioactivity is probably due to the extensive metabolism of ^{125}I-IAZA in liver. The exact nature of the metabolite(s) of the test compound is not known, nor has the mechanism of metabolism been determined. Studies with other nitroimidazoles have shown extensive oxidative metabolism in liver and predominant excretion through kidney[221,222]. These metabolites included the *in vivo* oxidative products of misonidazole (1) and metronidazole (12)[223,224]. Therefore it is reasonable to assume that similar oxidative reactions may occur with ^{125}I-IAZA, which contains a 2-nitroimidazole base.

The renal route of elimination appears to be predominant,

as suggested by kidney radioactivity and as confirmed later by bladder radioactivity in scintigraphic imaging. The nature of the urinary radioactivity was not determined in this study and probably represents both unmetabolised starting material (IAZA) and metabolic products.

The apparently higher radioactivity in tumors, yielding higher tumor to blood ratios between 4 and 24 h than other organ to blood ratios, suggests metabolic trapping of IAZA (45) in hypoxic tumor tissue. The higher tumor concentration of radioactivity relative to other organs may be due to selective hypoxia-dependent adduct formation in the tumor tissue. EMT-6 tumors are known to contain a large population (33%) of hypoxic cells[168].

The exact nature of hypoxia-mediated metabolic reactions of IAZA remains undetermined. There is reason to believe that IAZA, containing a 2-nitroimidazole base, would be preferentially activated through a series of one-electron and 2-electron transfer reduction reactions possible in hypoxic cells. This could result in selective binding of reactive reduction products of ^{125}I-IAZA with the hypoxic cells. Selective binding under hypoxic conditions was confirmed by *in vitro* binding studies as reported earlier (Section 4.1.5.).

The biodistribution data reported here suggest that the ideal time for scintigraphic imaging in this mouse model would be between 4 and 8 h post injection, when tumor signal

was higher than the background signal or the signal from other organs.

The whole-body elimination and blood clearance curves following i.v. administration of ^{125}I-IAZA into Balb/c mice bearing EMT-6 tumors are shown in Figure 13. The whole-body

Figure 13. Whole-body elimination and blood clearance of radioactivity following i.v. administration of ^{125}I-IAZA in Balb/c mice bearing EMT-6 tumors.

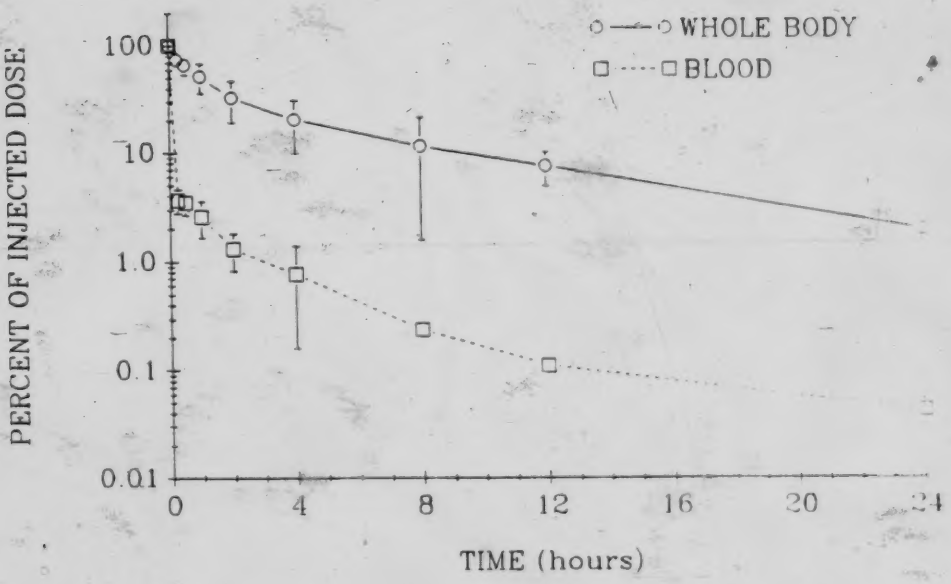

elimination curve was constructed by summing radioactivities in all organs dissected for biodistribution studies plus the radioactivity in remaining carcass (Figure 13). Whole blood radioactivity was calculated from an aliquot taken at the time of sacrifice, assuming blood to be 6.5% of the total

body weight (Figure 13).

The whole-body elimination data were analyzed as a bi-exponential function with half-lives of 0.87 h and 7.29 h. The short half-life indicates rapid initial elimination at early time periods. At longer periods the elimination was much slower presumably due to slow redistribution of radioactivity from the tissues.

Blood-radioactivity clearance data produce a more complex curve that is not resolved by simple exponential analysis. There was an initial very rapid decline in blood-radioactivity, with a half-life of approximately 5 min, indicating rapid distribution and/or elimination of ^{125}I-IAZA. This was followed by slower clearance upto 12 h. Between 12 and 24 h the clearance half-life was similar to that determined from the whole-body data.

The ^{125}I activity remaining in the blood and the whole-body at 24 h represented 0.04 and 2% of the injected dose, respectively. Rapid whole-body elimination and blood clearance data are indicative of fast tissue clearance of radioactivity with little or no specific binding of the test drug or its metabolite(s) to normal tissues or blood. Therefore, the residual radioactivity in most tissues and organs would not interfere with a tumor imaging study with an appropriately labelled (eg. ^{123}I) IAZA.

These biodistribution data and the *in vitro* binding data strongly support the potential of IAZA (45) as a clinically

useful non-invasive probe of hypoxic cells in tumor tissue.

4.1.7. Whole-Body Scintigraphy

Preliminary whole-body scintigraphy was performed with ^{125}I-IAZA in Balb/c mice bearing EMT-6 tumors. The mice were imaged at various time intervals following a bolus i.v. injection of ^{125}I-IAZA (17 GBq/mmol). Each animal received a dose of 3.7-4.7 MBq of ^{125}I-IAZA. This study was performed to establish a suitable time period for ^{123}I-IAZA scintigraphic study. For several reasons ^{123}I is the radionuclide of choice for scintigraphic study in human. These include short half-life, single gamma emission and moderate gamma energy. These features are more suitable compared to the ^{125}I, which has a long half-life and low gamma energy.

Figures 14 and 15 show the images of two mice with ^{125}I-IAZA at 2 and 14 h post injection, respectively. The thyroids of these mice remained unblocked. In these study approximately 500,000 counts were accumulated in the data acquisition mode. Other parameters of the study are given in each Figure.

It is seen from the image in Figure 14 that the radioactivity is distributed throughout the body. Among the tissues liver, stomach and intestine are prominent, whereas tumor is not visible and the thyroid is less prominent. This distribution of radioactivity is in agreement with the biodistribution study. The image shown in Figure 15 was taken

Figure 14. Static whole-body gamma scintigram of ^{125}I-IAZA at 2 hour post injection, in a Balb/c mouse bearing an EMT-6 tumor.

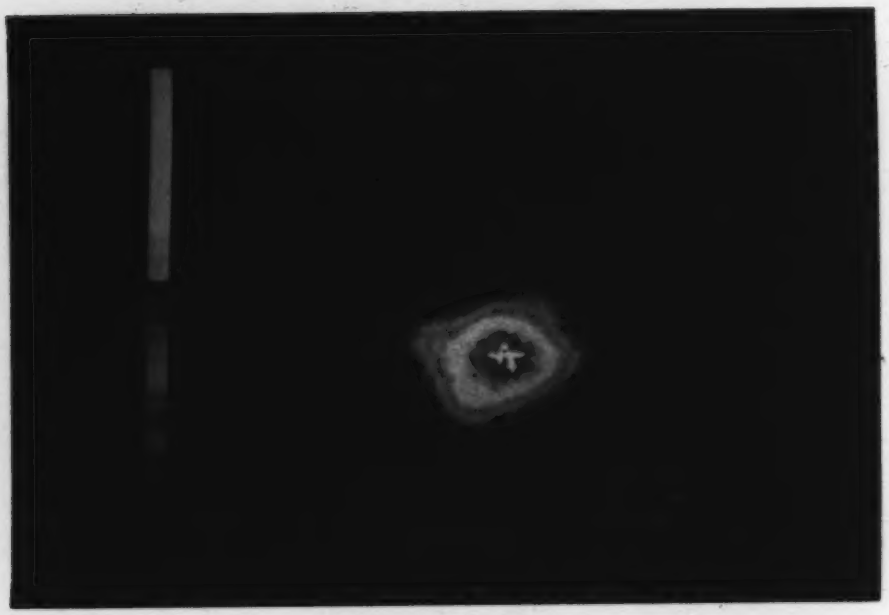

Figure 15. Static whole-body gamma scintigram of ^{125}I-IAZA at 14 hour post injection, in a Balb/c mouse bearing an EMT-6 tumor.

at 14 h post injection. The thyroid along with the bladder, stomach and intestine is prominent. Tumor is visible but less prominent in this scintigram. The thyroid radioactivity indicates the accumulation of radioiodide. All these data are in good agreement with the biodistribution study.

On the basis of these study and biodistribution data an 8-hour post injection time was chosen for ^{123}I-IAZA scintigraphic study. The whole-body scintigraphy with ^{123}I-IAZA was performed in 2 sets of Balb/c mice bearing EMT-6 tumors. In one set of mice, the thyroids were blocked by administering 0.05% w/v KI in the animals drinking water for 7 days. The other set of mice did not receive any KI and the thyroid remained unblocked. The specific activity of the injected ^{123}I-IAZA was about 20 GBq/mmol. Each animal received a bolus i.v. injection of 3.7-4.7 MBq of ^{123}I-IAZA, representing 65-70 µg of IAZA (45). In this study approximately 100,000 counts were accumulated in data acquisition mode. Other parameters of the scintigram are given in each Figures.

Figures 16 and 17 show the images of two mice with unblocked thyroid. It is seen from the images that the tumor is completely delineated from other organs. The thyroid is also prominent in the scintigrams. According to the biodistribution and preliminary scintigraphic study, thyroid visualization was expected. Among the other organs, liver, stomach, intestine and urinary bladder were visible. Although there was variation in the amount of radioactivity

Figure 16. Static whole-body gamma scintigram of ^{123}I-IAZA in a Balb/c mouse bearing an EMT-6 tumor, without thyroid block.

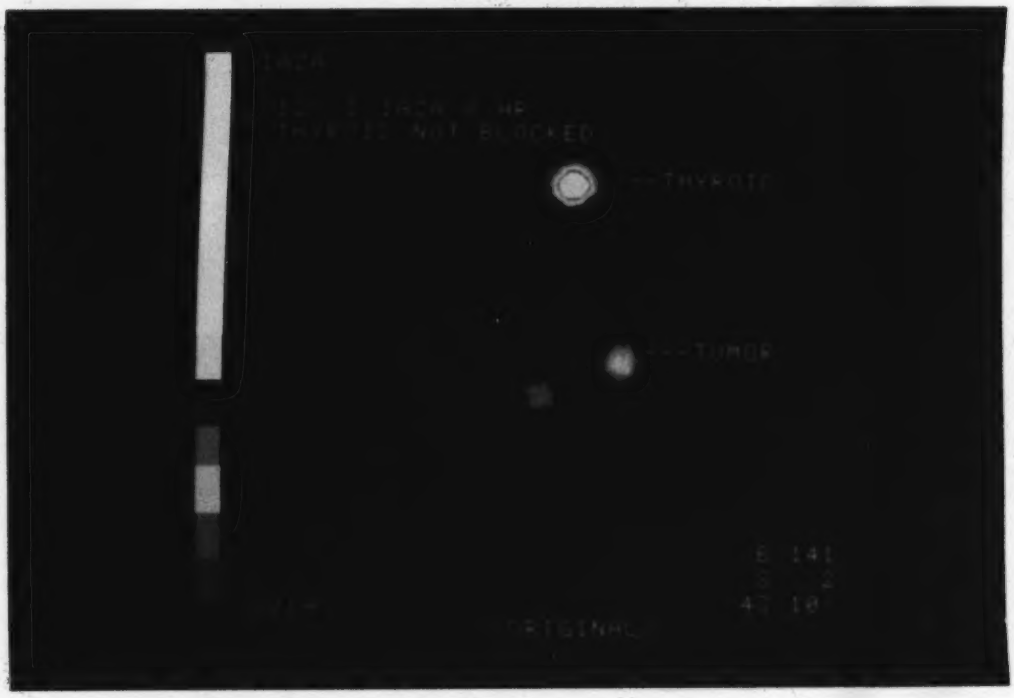

Figure 17. Static whole-body gamma scintigram of ^{123}I-IAZA in a Balb/c mouse bearing an EMT-6 tumor, without thyroid block.

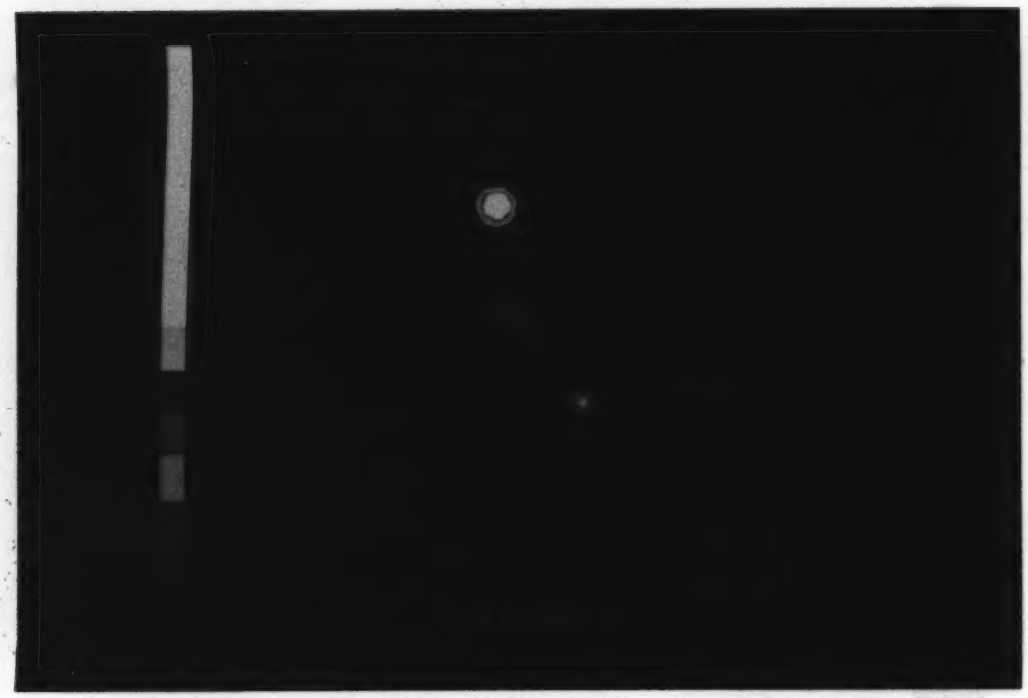

Figure 18. Static whole-body gamma scintigram of ^{123}I-IAZA in a Balb/c mouse bearing an EMT-6 tumor, with blocked thyroid.

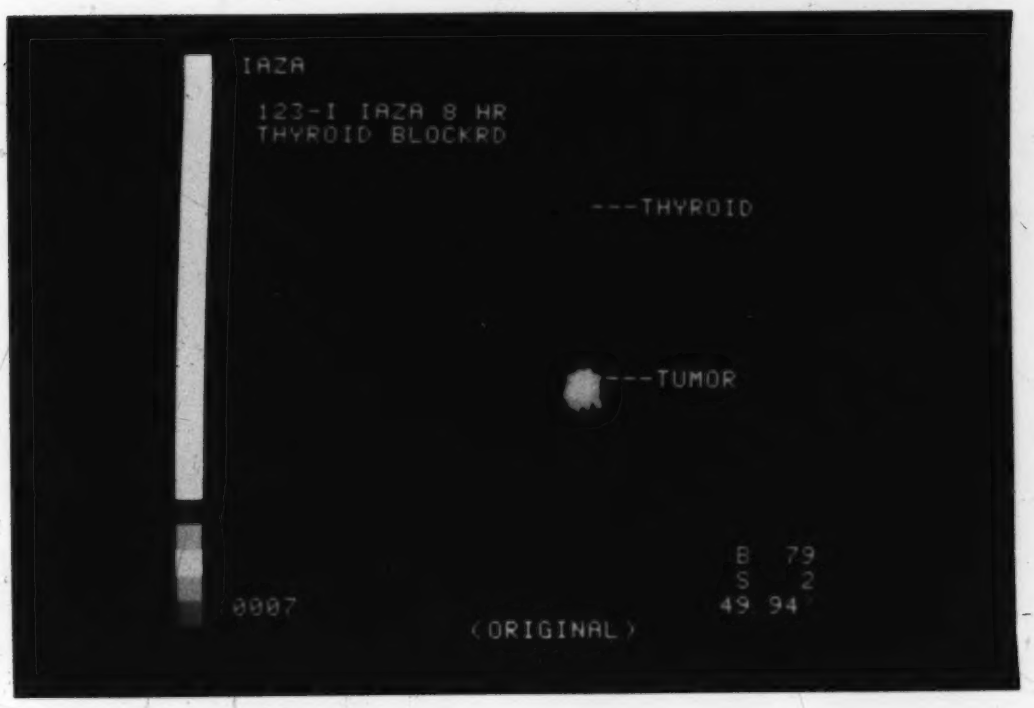

Figure 19. Static whole-body gamma scintigram of ^{123}I-IAZA in a Balb/c mouse bearing an EMT-6 tumor, with blocked thyroid.

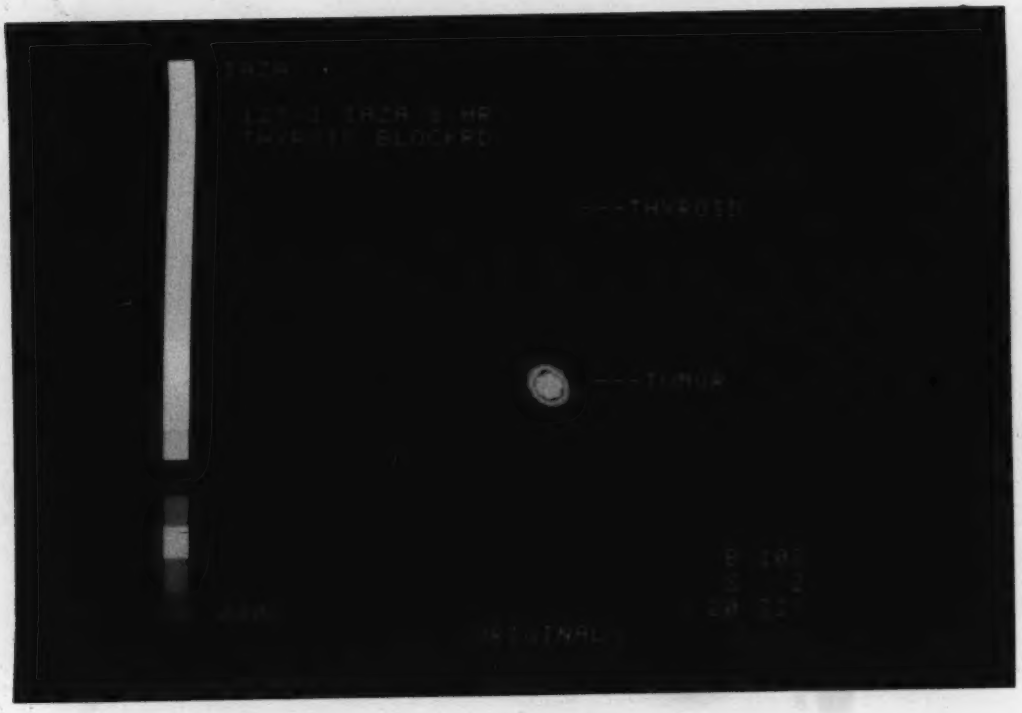

in these organs, the relative distribution seems to be in very good agreement with the quantitative biodistribution data. Several other mice injected (not shown) in this manner showed a similar trend of complete delineation of tumor and thyroid from the other organs.

Figures 18 and 19 are the images of two mice with blocked thyroid. Unlike the Figures 16 and 17, only tumor is visible in these two images. Thyroid, stomach or intestine were not visualized. This was expected because these organs appear to be saturated with the predose KI and thereby fail to pick up any free radioiodide. The liver and bladder radioactivity also seems greatly diminished. The reason for the reduced bladder radioactivity can be explained as the animal might have urinated prior to the imaging. Administration of KI has altered the distribution pattern of the compound in the liver and other organs.

The scintigraphic study further potentiates the usefulness of IAZA (45) for non-invasive evaluation of hypoxic cells in tumor tissue. The *in vitro* binding study and the *in vivo* biodistribution and scintigraphic studies all suggest hypoxia-selective binding with IAZA (45). On the basis of these results, IAZA (45) is currently under clinical trial to a limited number of cancer patients[225]. The results of the preliminary clinical-trials are very encouraging, which not only suggest the usefulness of IAZA for clinical evaluation of hypoxia in tumor tissue but also substantiates the re-

sults obtained by *in vitro* and *in vivo* investigations as reported in this section.

4.2. 1-(6-Iodo-6-Deoxy-ß-D-Galactopyranosyl)-2-Nitroimidazole (Iodoazomycin Galactoside:IAZG) (49)

4.2.1. Chemistry

The title compound was synthesized by the general procedure described previously (Section 3.2.2.). The detailed synthesis has been described elsewhere[200]. The synthesis is outlined in Scheme 8. Radioiodination of IAZG (49) was accomplished by an isotope exchange procedure as described previously for IAZA (45) (Section 4.1.1.). Scheme 9 outlines the two different methods of exchange labelling used in this study. ^{125}I-IAZG was used *in vivo* for mouse biodistribution and for all *in vitro* investigations, while ^{123}I labelled IAZG (49) was used for whole-body scintigraphic studies with mice.

Method A represents the radiosynthesis of ^{125}I labelled IAZG (49). The chemical purity of the product (^{125}I-IAZG), as evidenced from the HPLC uv trace (column A, 60:40 H_2O: MeOH, 2 mL/min., 350 nm, retention time 4.98 min.), was 75%. The radiochemical yield was calculated by Radio-HPLC as described in Section 3.2.5. and was found to be 65%. The other major peak observed in the uv trace was identified as AZG (48) (eg. deiodinated IAZG). This was confirmed by analyzing an authentic sample of AZG (48) under identical HPLC conditions, to give the same retention time (1.75 min). Besides AZG (48), several other minor peaks were observed in

Scheme 8. Synthesis of 1-(6-iodo-6-deoxy-β-D-galactopyranosyl)-2-nitroimidazole (IAZG, 49).

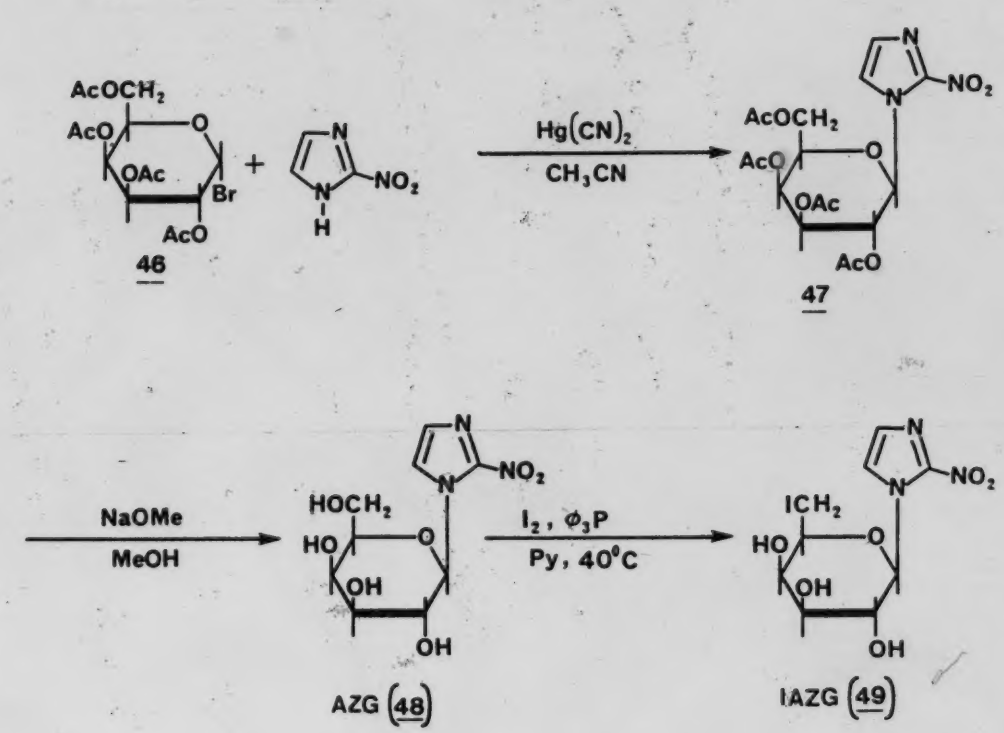

the uv trace. The single radioactive peak other than ^{125}I-IAZG which was observed in the radioactive trace (radio-HPLC) was assumed to be free iodide (33-35%), which has a short retention time (1.37 min.) in this HPLC system. Changing the reaction time influenced the radiochemical yield and loss of starting material (IAZG) (Table 4). It appeared that at 3.5 hour reaction time the exchange

Scheme 9. Synthesis of radioiodianated 1-(6-iodo-6-deoxy-ß-D-galactopyranosyl)-2-nitroimidazole.

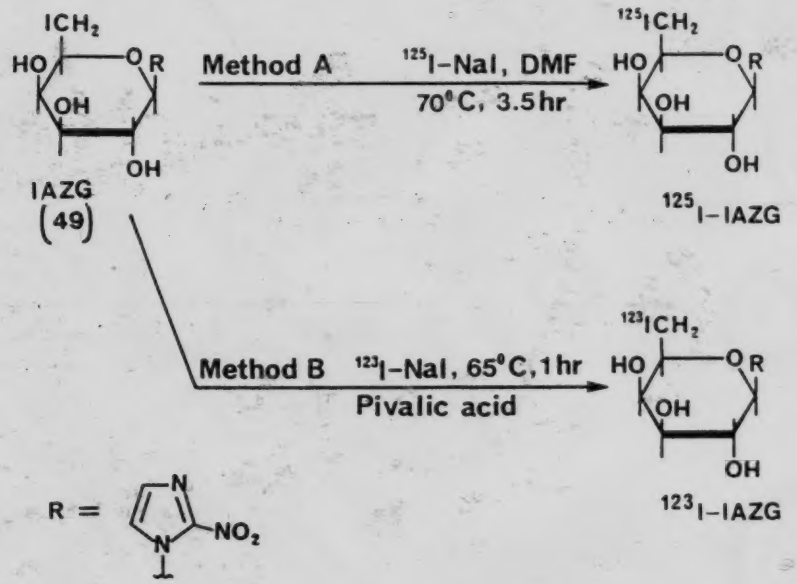

labelling reached an optimal radiochemical yield (65%) with 25% loss of starting material (IAZG) (Table 4). The reaction

time periods longer or shorter than this resulted in lower chemical or radiochemical yields.

The crude reaction product was purified by HPLC using column A under similar conditions as above. This method of synthesis and purification was employed for routine production of ^{125}I-IAZG.

Table 4. Percent radiochemical yield of ^{125}I-IAZG and percent decomposition[a] at various reaction times using Method A.

Time (hour)	% radiochemical yield	% decomposition[a]
1.0	31	16
2.0	45	21
3.0	55	22
3.5	65	25
4.0	65	28

[a]based on the loss of starting material (IAZG) during reaction.

It was found that a 1 h reaction time at 65 °C using the pivalic acid 'melt method' (Method B) gave a relatively high radiochemical yield (70.5%) with lower loss of starting material (IAZG) than Method A. The uv trace of the reaction mixture when analyzed using column B (60:40 H_2O: MeOH, 2 mL/min., 350 nm, retention time 8.75 min.), indicated ~85% chemical yield. The uv peaks other than the product (^{123}I-IAZG) were similar to those observed using Method A. The

major radioactive contaminant as shown by Radio-HPLC appeared to be the free iodide. The reaction product of Method B was purified using column B with the HPLC conditions as above. The shorter reaction time with Method B was preferred for routine synthesis of ^{123}I-IAZG due to the relatively short half-life of ^{123}I ($t_{1/2}$ = 13 h).

The final product from both methods was obtained with chemical and radiochemical purities of greater than 99%.

4.2.2. Cytotoxicity

Figures 20 and 21 show the surviving fractions of hypoxic EMT-6 cells exposed to various concentrations of IAZG (49) and AZG (48) respectively for up to 6 h at 37 °C. Both IAZG and AZG were cytotoxic to EMT-6 cells in culture under hypoxic but not under aerobic conditions. This specific cell toxicity in the absence of oxygen was expected on the basis of cytotoxicities observed for AZA (44) and IAZA (45) (Section 4.1.3.). This effect has been well documented with other electron affinic radiosensitizers[204] including misonidazole (1) and IAZR (2)[12].

With IAZG (49), the time required to kill 90% of the cells was 1.8 h at 1.0 mM. While at concentrations less than 1.0 mM (0.3 or 0.1 mM) the 10% cell survival was not reached during incubation periods up to 6 h (Figure 20). The toxicity is dependent both on time of incubation and on substrate concentration. With AZG (48), 90% cell kill was

Figure 20. Surviving fractions of hypoxic EMT-6 cells incubated with various concentrations of IAZG at various time intervals.

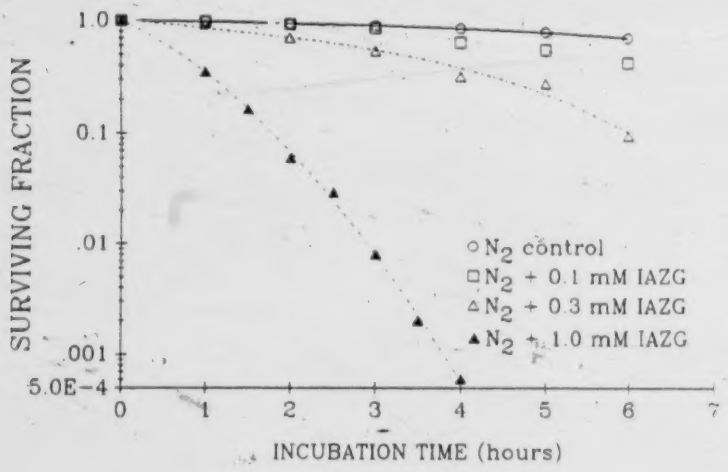

Figure 21. Surviving fractions of hypoxic EMT-6 cells incubated with various concentrations of AZG at various time intervals.

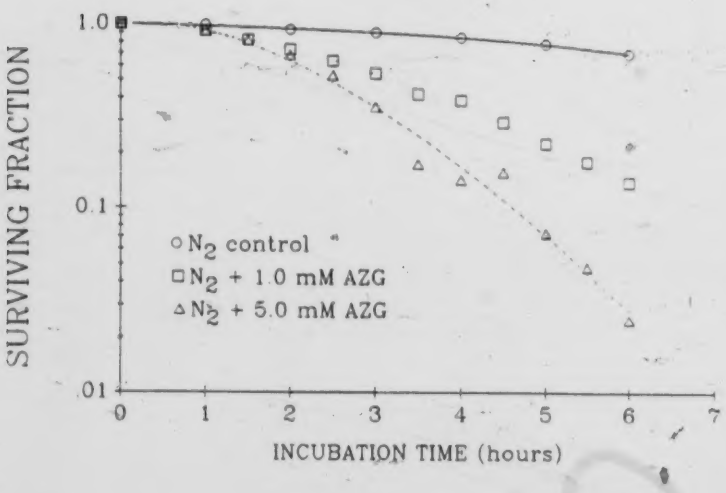

achieved at a concentration of 5.0 mM, while at 1.0 mM, 90% cell kill was not seen during the 6 h incubation period (Figure 21).

Figure 22. Comparison of hypoxic cell cytotoxicity as a function of reciprocal of time (hr^{-1}) for 90% cell kill with various concentrations of IAZG and AZG.

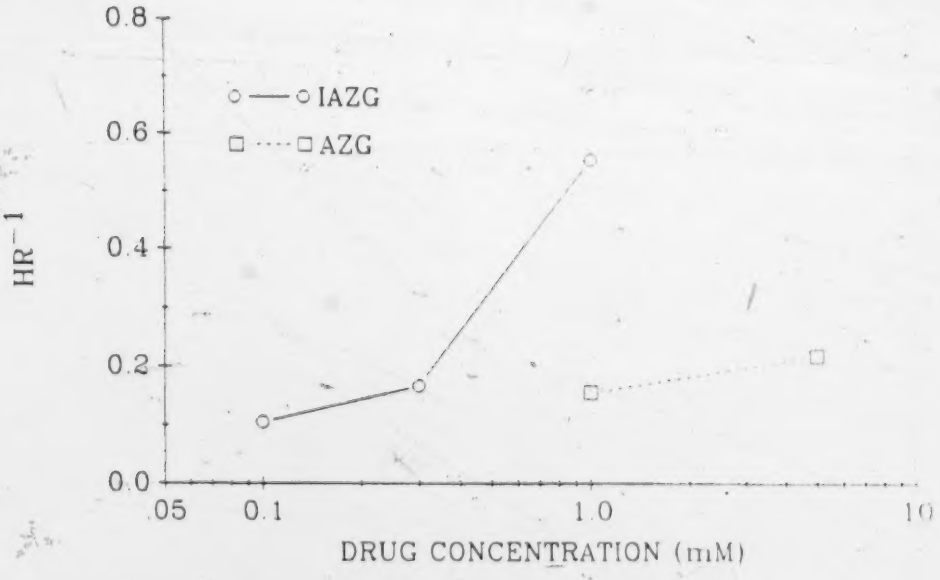

A comparison of hypoxic cell cytotoxicity of AZG (48) and IAZG (49) was made by plotting the reciprocal of time (hr^{-1}) for 90% cell kill against substrate concentration (Figure 22). The Figure was constructed as described previously (Section 4.1.3.). IAZG (49) appears to be 3.5 times as toxic

as AZG (48) at equimolar concentrations (1.0 mM). This increased toxicity of IAZG (49) over AZG (48) may be accounted for in terms of partition coefficient and reduction potential differences between the two compounds as discussed previously with IAZA (45) in Section 4.1.3.

4.2.3. Radiosensitization

The radiosensitizing abilities of IAZG (49) and AZG (48) were studied in EMT-6 cells in culture as described previously (Section 3.2.13.3.). Figures 23 and 24 show the surviving fractions of EMT-6 cells exposed to various doses of radiation at various concentrations of IAZG (49) and AZG (48) respectively. The OER at 90% cell kill was found to be 2.8. Both compounds demonstrate sensitizer enhancement (SER) values that approach this figure as their concentration is increased. This is the characteristic behaviour expected from compounds which are sensitizing cell *in vitro* to the lethal effects of ionizing radiation.

In general terms IAZG (49) is somewhat more effective as a radiosensitizer than IAZA (45). These comparisons, along with data for related compounds studied in a similar test system, are presented and discussed in Chapter 5.

A comparison of SER values of IAZG (49) and AZG (48) is shown in Figure 25. In terms of concentration of test substrate required to achieve a particular SER value, IAZG (49)

Figure 23. Surviving fractions of EMT-6 cells at various radiation doses in air, nitrogen and nitrogen plus various concentrations of IAZG.

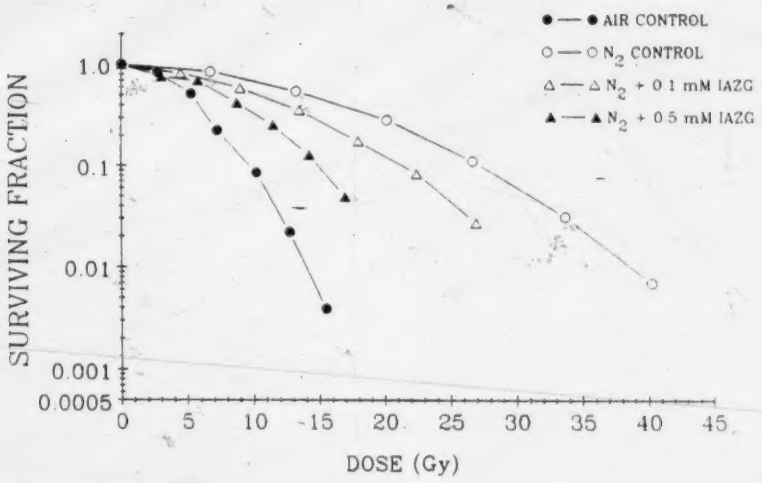

Figure 24. Surviving fractions of EMT-6 cells at various radiation doses in air, nitrogen and nitrogen plus various concentrations of AZG.

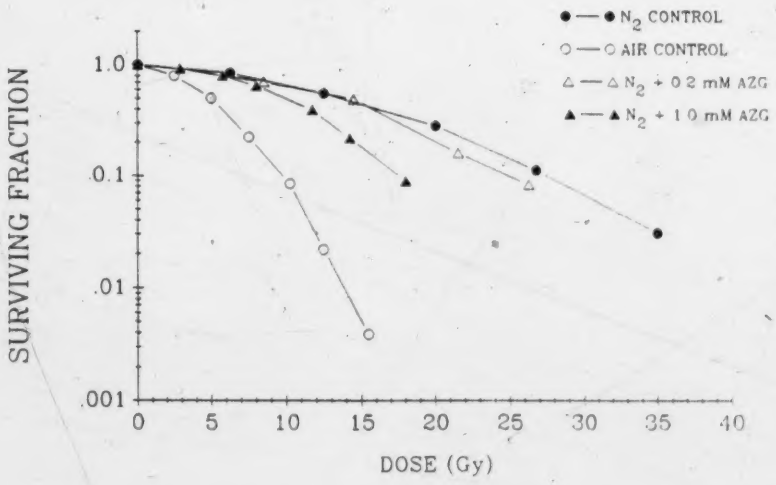

Figure 25. Comparison of sensitizer enhancement ratios (SER) of IAZG and AZG as a function of substrate concentration in vitro with hypoxic EMT-6 cells.

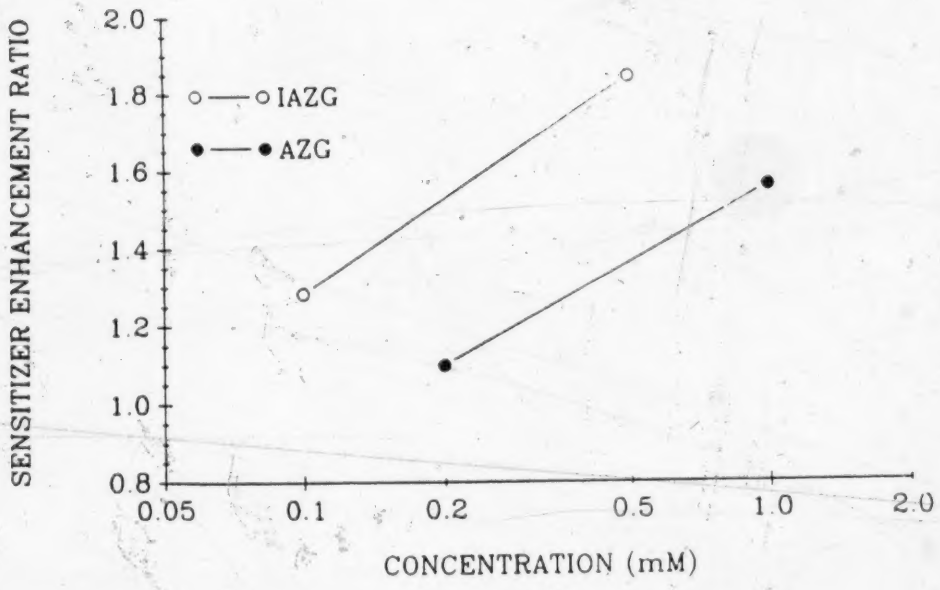

is 4-4.5 times more effective as a radiosensitizer than AZG (48). This increased SER of IAZG over AZG is probably due to the fact that iodine-containing compounds are better radiosensitizers than their non-iodinated counterparts. A detailed explanation for such prediction is described in Section 4.1.4. dealing with IAZA (45).

4.2.4. Initial Binding Rate

Figure 26 shows the amount of ^{125}I activity bound to the acid-insoluble fraction of EMT-6 cells under hypoxic and aerobic incubation with ^{125}I-IAZG, expressed as cpm/10^6 cells against the incubation time. The binding pattern of the test substrate is similar to that already observed with ^{125}I-IAZA (Section 4.1.5.), in that the bound activity increases with increased substrate concentration and that aerobic binding is minimal and remains constant over the 3 h period of incubation. These data indicate the selective hypoxic binding property of the test drug.

The initial rate of binding of ^{125}I-IAZG to the macromolecular fraction of hypoxic EMT-6 cells, expressed as pmol/10^6 cells/h versus substrate concentration, is shown in Figure 27. The binding rate increases linearly with the substrate concentration under hypoxic conditions. The binding rate at a concentration of 30 μM was found to be 665 pmol/10^6 cells/h, which is 9.9 times greater than the binding rate under aerobic conditions (67 pmol/10^6 cells/h) at the same concentration of substrate. Furthermore, The hypoxic cell binding rate of ^{125}I-IAZG is the highest binding rate measured for any 2-nitroimidazole derivative to date. This rate of binding is about 2-3 times higher than reported for IAZR (2) or IAZA (45) and much higher (4–8 times) than for misonidazole (1) (Detailed comparison in Chapter 5).

Figure 26. ^{125}I Activity bound to the acid-insoluble fraction of EMT-6 cells after incubation with various concentrations of ^{125}I-IAZG at various time periods, under hypoxic and aerobic conditions.

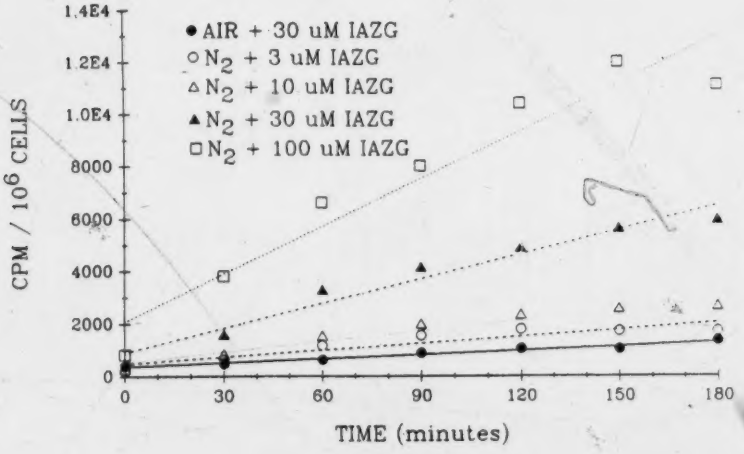

Figure 27. The initial binding rates expressed as pmol/10^6 cells/h of ^{125}I-IAZG to the acid-insoluble fraction of hypoxic EMT-6 cells at various concentrations of test substrate.

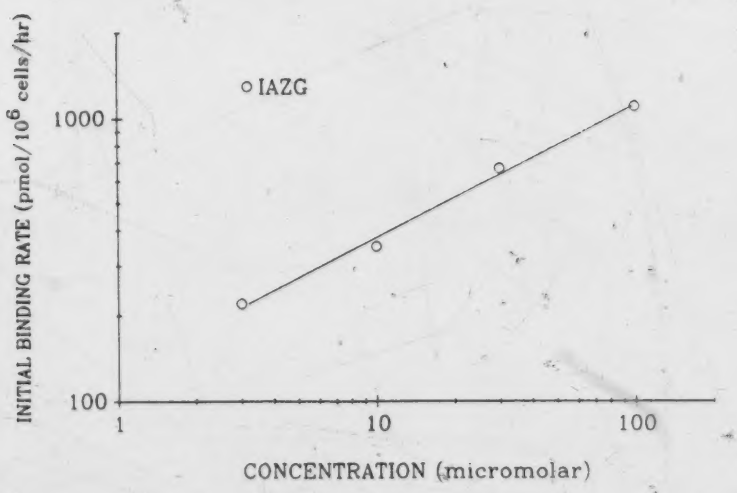

Figure 28. ^{125}I Activity bound to the acid-insoluble fraction of EMT-6 cells under hypoxia and various levels of oxygen incubated with 10 μM ^{125}I-IAZG, at several time periods.

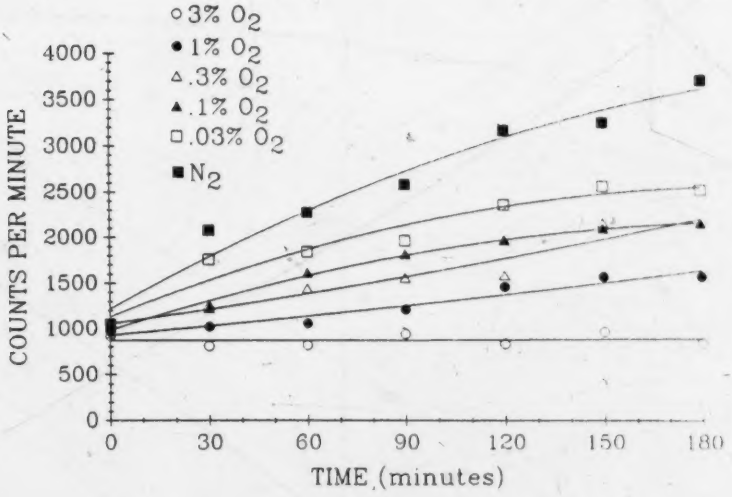

Figure 29. The initial binding rate of 10 μM ^{125}I-IAZG to the acid-insoluble fraction of EMT-6 cells under hypoxia and various levels of oxygenation.

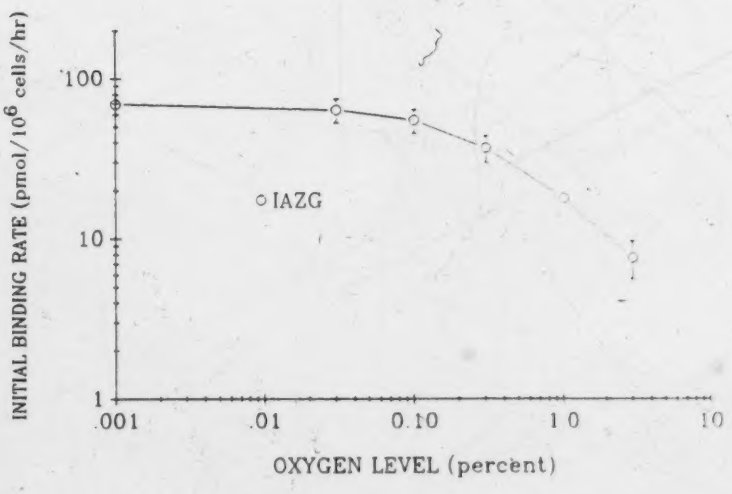

An oxygen-dependent binding study, similar to that carried out with ^{125}I-IAZA (Section 4.1.5.) was performed with ^{125}I-IAZG. The results are presented in Figure 28. The data are also expressed in terms of initial binding rate versus oxygen concentration in Figure 29.

The results are similar to those observed with ^{125}I-IAZA. The binding decreases as the oxygen concentration of the medium increases, the binding increases linearly with time and the initial binding rate is largely dependent on the cellular oxygenation status.

These data establish the hypoxia-selective binding characteristics of ^{125}I-IAZG. The cellular oxygenation status can be seen to have a profound influence on the binding properties of the test compound. It is important here to note that the "degree" of hypoxia may have significant influence since the binding is greatly reduced even at relatively low levels of cellular oxygen.

4.2.5. Biodistribution and Elimination.

Table 5 shows the <u>in vivo</u> biodistribution of ^{125}I-IAZG at several time intervals in Balb/c mice bearing EMT-6 tumors. The specific activity of the injected compound was between 6 and 7 GBq/mmol. Each animal received an intravenous bolus injection of 50–60 kBq containing 2.5 to 3.0 µg of IAZG (<u>49</u>). The data are presented as percent injected dose per gram of tissue and as tissue to blood ratios of ^{125}I

Table 5. Biodistribution of ^{123}I-IAZG following i.v. administration in Balb/c mice bearing EMT-6 tumors at various time intervals.

Organ	Time (hours)						
	0.25	0.50	1	2	4	8	24
Blood	1.83 ±0.17[a]	1.11 ±0.16	0.86 ±0.26	0.53 ±0.10	0.28 ±0.07	0.16 ±0.03	0.06 ±0.02
Tumor	1.75 ±0.46	1.45 ±0.24	1.21 ±0.21	0.77 ±0.17	0.43 ±0.09	0.23 ±0.09	0.08 ±0.01
	0.95 ±0.19[b]	1.31 ±0.22	1.41 ±0.23	1.45 ±0.37	1.56 ±0.25	1.43 ±0.20	1.33 ±0.48
Kidney	15.64 ±1.15	8.94 ±1.20	4.56 ±1.41	2.67 ±0.51	1.10 ±0.29	0.40 ±0.02	0.09 ±0.03
	8.58 ±0.91	8.07 ±0.62	5.56 ±1.57	5.06 ±1.09	4.00 ±1.09	2.47 ±0.35	1.52 ±0.38
GIT[c]	6.82 ±5.20	3.65 ±1.36	1.16 ±0.25	0.82 ±0.45	0.29 ±0.07	0.17 ±0.08	0.05 ±0.02
	3.65 ±2.71	3.19 ±1.11	1.42 ±0.39	1.48 ±0.55	1.04 ±0.29	1.05 ±0.47	0.83 ±0.48
Liver	5.50 ±0.79	2.96 ±0.49	1.48 ±0.24	1.40 ±0.56	0.43 ±0.12	0.20 ±0.02	0.08 ±0.02
	3.00 ±0.38	2.66 ±0.24	1.82 ±0.46	2.55 ±0.62	1.51 ±0.20	1.24 ±0.15	1.32 ±0.28
Muscle	1.31 ±0.21	0.70 ±0.18	0.37 ±0.19	0.34 ±0.20	0.14 ±0.03	0.06 ±0.02	0.02 ±0.01
	0.72 ±0.08	0.62 ±0.09	0.48 ±0.36	0.62 ±0.23	0.49 ±0.05	0.36 ±0.14	0.38 ±0.12
Bone	0.95 ±0.20	0.48 ±0.19	0.36 ±0.15	0.18 ±0.04	0.13 ±0.003	0.10 ±0.01	0.09 ±0.03
	0.40 ±0.13	0.41 ±0.19	0.63 ±0.49	0.46 ±0.22	0.56 ±0.30	0.46 ±0.31	0.50 ±0.21
Lung	2.77 ±0.44	1.46 ±0.24	0.74 ±0.12	0.61 ±0.17	0.33 ±0.09	0.16 ±0.02	0.07 ±0.01
	1.51 ±0.17	1.31 ±0.11	0.90 ±0.21	1.13 ±0.21	1.16 ±0.14	0.98 ±0.14	1.26 ±0.21
Heart	2.59 ±0.75	0.99 ±0.21	0.46 ±0.07	0.38 ±0.06	0.18 ±0.02	0.12 ±0.02	0.03 ±0.004
	0.99 ±0.13	0.80 ±0.10	0.61 ± 0.18	0.81 ±0.10	0.79 ±0.15	0.61 ±0.10	0.61 ±0.03
Spleen	1.80 ±0.62	0.72 ±0.15	0.35 ±0.03	0.28 ±0.05	0.13 ±0.02	0.10 ±0.009	0.016 ±0.002
	0.68 ±0.07	0.59 ±0.08	0.45 ±0.09	0.63 ±0.08	0.59 ±0.15	0.46 ±0.14	0.38 ±0.08
Stomach	3.29 ±1.07	2.14 ±1.01	1.38 ±0.42	1.49 ±1.12	0.55 ±0.30	0.42 ±0.35	0.06 ±0.04
	1.79 ±0.58	1.92 ±0.82	1.64 ±0.33	2.61 ±1.43	1.85 ±0.56	2.50 ±0.86	0.87 ±0.31
Carcass	1.78 ±0.16	1.37 ±0.24	1.37 ±0.22	0.81 ±0.25	0.33 ±0.09	0.12 ±0.04	0.03 ±0.008
	0.99 ±0.15	1.23 ±0.15	1.68 ±0.40	1.51 ±0.27	1.16 ±0.20	0.73 ±0.24	0.49 ±0.08

[a] The numbers represent the mean ± standard deviation for percent of injected dose per gram of wet tissue for 6 animals. [b] Tissue to blood ratio. [c] Section of intestine.

activity.

Soon after injection (0.25 h), the kidney has the highest concentration of radioactivity, indicating the rapid urinary excretion of the relatively hydrophillic drug (P = 0.57). The high concentration of radioactivity persists in the kidney through the first few hours and even at 24 h the kidney to blood ratio is more than 1.0 (Table 5). This suggests continued involvement of the kidney in excretion of ^{125}I-IAZG or its metabolite(s). Besides kidney, a relatively high radioactivity at early time periods was also evident in intestine and liver. This is probably due to the extensive metabolism of the compound (IAZG) in liver and possible rapid hepatobiliary excretion of the test compound. Low intestine radioactivity at longer time periods suggests that hepatobiliary elimination is not a major route of excretion of IAZG (49). Although the exact nature of metabolism of IAZG is not known, studies with other nitroimidazoles suggest that liver is the major site for oxidative metabolism[179].

Tumor radioactivity seems to be more persistent and declines less rapidly compared to other tissues. This is postulated to be due to metabolic trapping of the test drug to the tumor tissue. The EMT-6 tumor model is known to contain about 33% hypoxic cells, therefore it is reasonable to expect metabolic trapping of IAZG (49) to the hypoxic fractions of the tumor tissue. The hypoxia-selective binding

nature of the test compound was confirmed by in vitro study (Section 4.2.4.).

However, the only organ which was found to actively concentrate radioactivity was the thyroid. The thyroid radioactivity increased from 7.1% of the total body radioactivity at 8 h to 30.9% at 24 h (Table 6), probably due to deiodination of the injected compound and accumulation of the resulting radioiodide in the thyroid. The stomach radioactivity is also presumably due to the accumulation of radioiodide.

Table 6. Thyroid radioactivity as percent injected dose of ^{125}I-IAZG/organ, in Balb/c mice bearing EMT-6 tumors (n=6; ±S.D.).

Time (hour)	Percent injected dose/organ	Thyroid radioactivity as percentage of whole-body radioactivity
0.25	0.07±0.02	0.01±0.008
0.50	0.06±0.01	0.01±0.009
1.00	0.10±0.04	0.26±0.07
2.00	0.14±0.04	0.52±0.12
4.00	0.26±0.15	2.27±0.91
8.00	0.27±0.19	7.14±1.36
24.00	0.44±0.09	30.98±5.48

Figure 30. Tissue to blood ratios of radioactivity at various time intervals following i.v. administration of ^{125}I-IAZG in Balb/c mice bearing EMT-6 tumors.

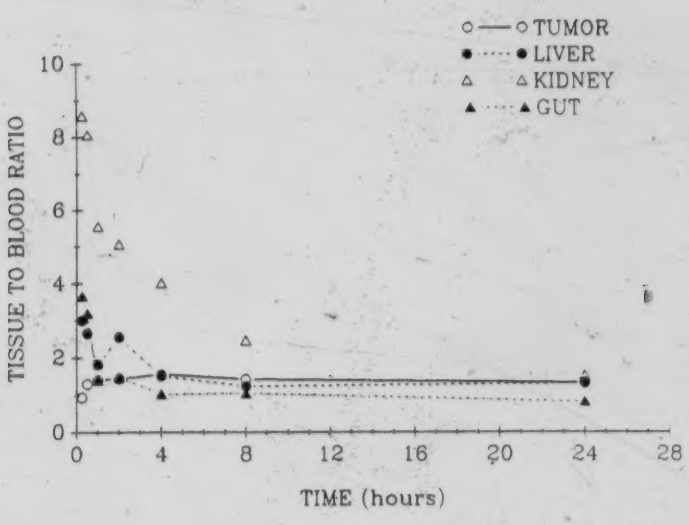

Figure 31. Tissue to blood ratios of radioactivity at various time intervals following i.v. administration of ^{125}I-IAZG in Balb/c mice bearing EMT-6 tumors.

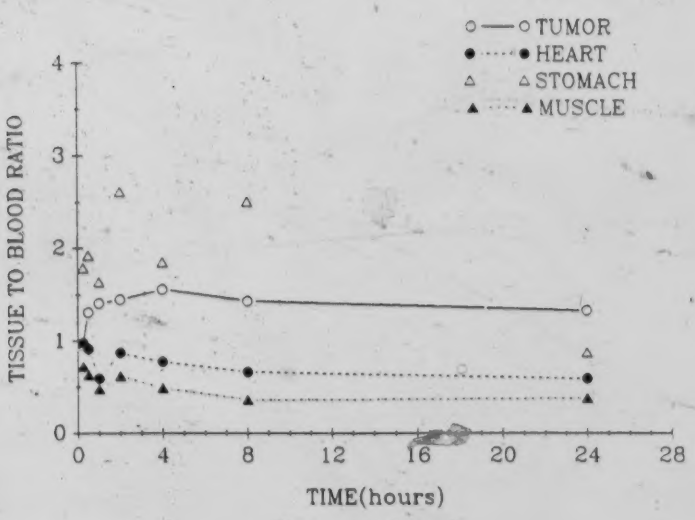

The tissue to blood ratios of radioactivity are shown in Figures 30 and 31 for tumor and selected tissues. The tumor ratio increases steadily to a maximum of 1.6 at 4 h after injection and then remains approximately constant up to 24 h.

When compared to IAZA (45), the tumor to blood ratios of IAZG (49) are much lower, and the ratios in other organs, specifically liver, kidney and stomach, are persistently higher. This suggests that IAZG is less suitable than IAZA for in vivo imaging of hypoxic tissue, at least in this mouse tumor model.

The whole-body elimination and blood clearance curves after i.v. administration of ^{125}I-IAZG into Balb/c mice bearing EMT-6 tumors are shown in Figure 32. The two curves were constructed by the methods described in Section 4.1.6.

There was a rapid decline in blood radioactivity during the distribution phase, with an estimated half-life of less than 5 minutes. This may be due to both rapid tissue distribution and renal clearance of the test drug. This curve was complex and could not be resolved by simple exponential analysis. Whole-body elimination data, however, were successfully analyzed as a biexponential function with half-lives of 0.42 h and 8.34 h. The blood radioactivity at longer times (8–24 h) shows a slower clearance with a half-life approximately equal to whole-body half-life over this time interval.

Figure 32. Whole-body elimination and blood clearance of radioactivity following i.v. administration of ^{125}I-IAZG in Balb/c mice bearing EMT-6 tumors.

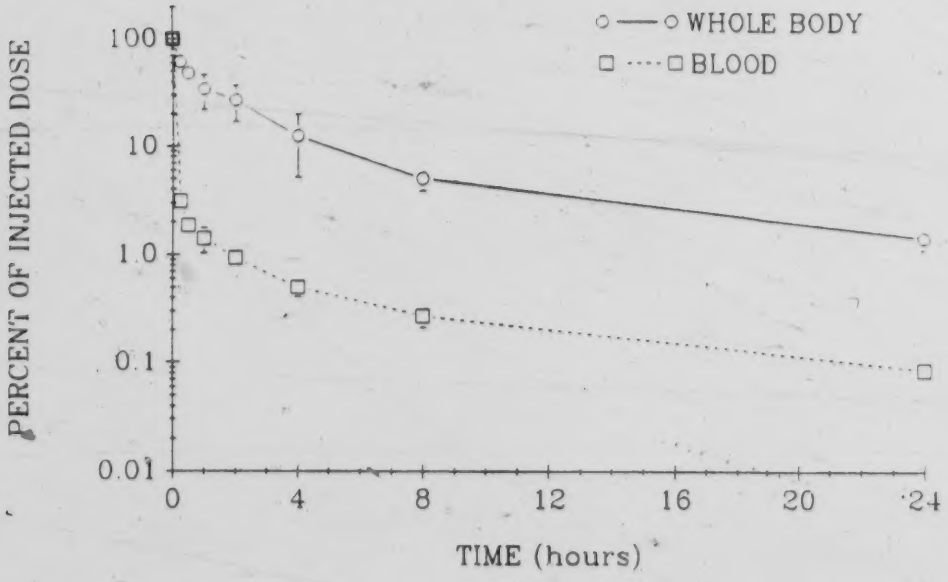

At 24 h the ^{125}I activity remaining in the blood and whole-body is 0.09 and 1.42 percent of the injected dose respectively. This rapid blood and whole-body clearance of radioactivity is quantitatively similar to that of IAZA (45). However, this compound (IAZG) may not be suitable as non-invasive marker of tissue hypoxia. The higher ratios of radioactivity in excretory organs and liver may interfere with the imaging, leading to poor diagnosis of hypoxic cells in tumor tissue.

4.2.6. Whole-Body Scintigraphy

Whole-body scintigraphy was carried out in Balb/c mice bearing EMT-6 tumors. The mice were injected with ^{123}I-IAZG (12–15 GBq/mmol) i.v. via the tail vein. Each animal received a single bolus dose of 3.7 to 4.7 MBq of ^{123}I-IAZG containing 94 µg to 100 µg of IAZG (49). An imaging time of 4 h post injection was chosen, based on biodistribution data in order to maximize tumor to blood ratios.

Figure 33 presents the scintigraphic image for an animal in which the thyroid was not blocked by pre-administration of KI. Tumor and thyroid are clearly visible whereas the other organs are not visible except for stomach. Thyroid and stomach visualization was expected on the basis of the biodistribution study.

Figure 34 shows the scintigram of an animal in which the thyroid was blocked with KI (0.05%) administered in drinking water for 7 days prior to imaging. In this image (Figure 34) only the tumor is clearly visible. Little or no radioactivity is seen in any other organ including the thyroid and stomach.

The image shown in Figure 33 is different than expected based on biodistribution data. The tumor is clearly visible with no interference from liver or kidney. The clear delineation of tumor tissues suggests a tumor to blood ratio greater than the 1.6 maximum obtained from biodistribution data. Reasons for such variability remain unexplained.

Figure 33. Static whole-body gamma scintigram of ^{123}I-IAZG in a Balb/c mouse bearing an EMT-6 tumor, without thyroid block.

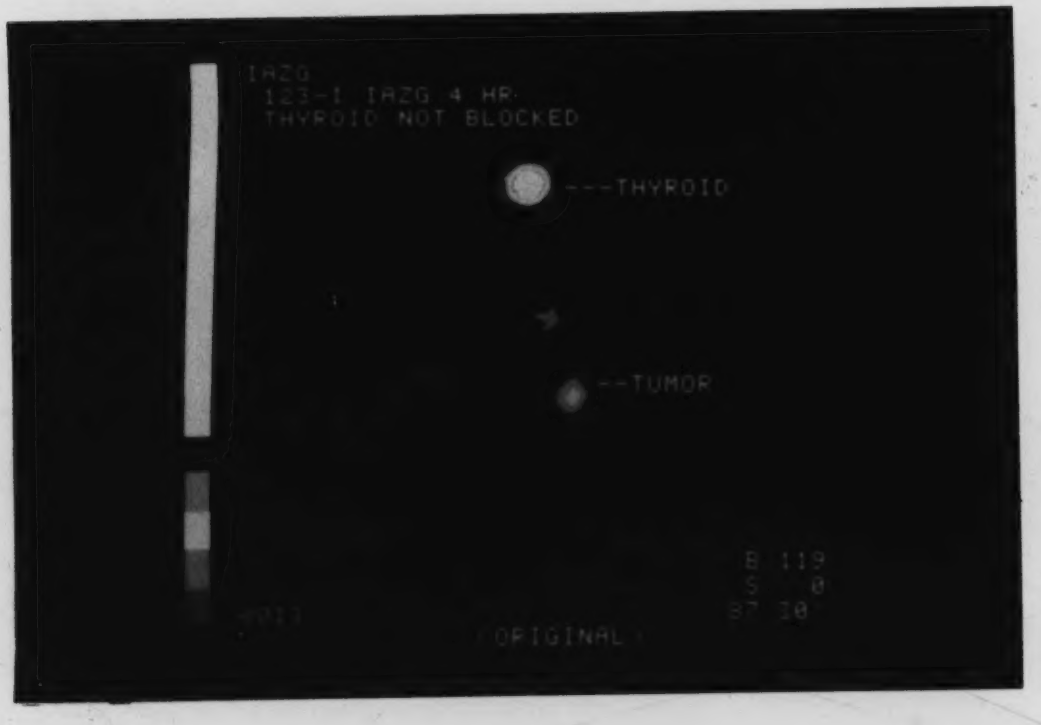

Figure 34. Static whole-body gamma scintigram of ^{123}I-IAZG in a Balb/c mouse bearing an EMT-6 tumor, with a thyroid block.

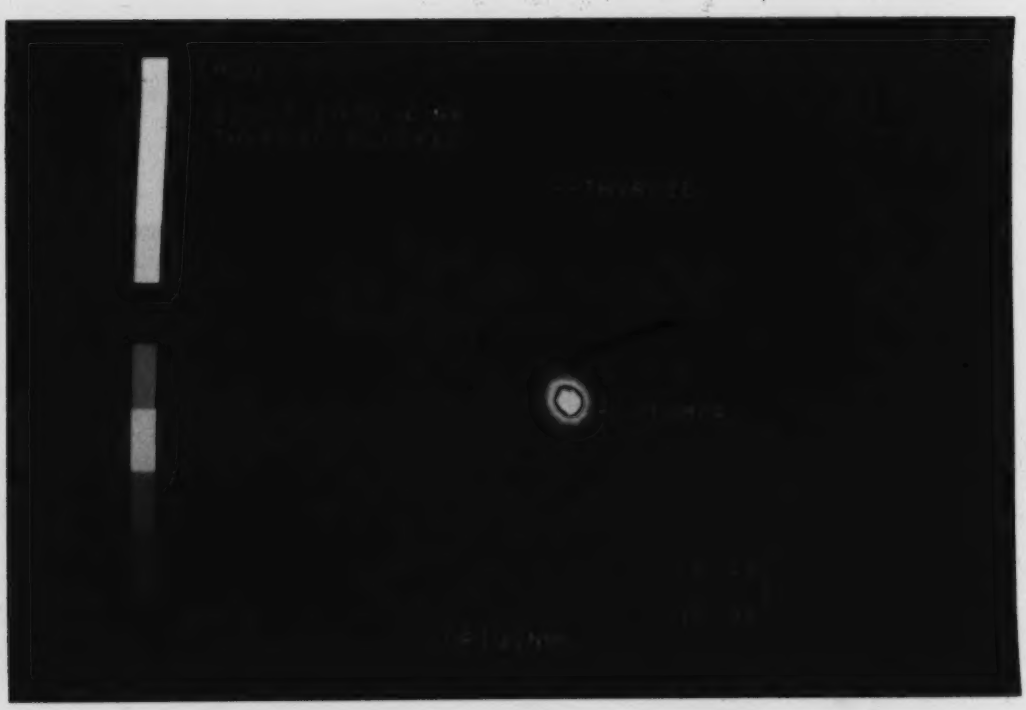

However, it is assumed that tumor size and the drug dose used in the imaging study may have some bearing on tumor uptake. The size of the tumor used in imaging study was 2-3 times bigger than the tumor used in biodistribution study. In addition the amount of IAZG injected for the imaging study was 35 to 40 times higher than that used for biodistribution study. In biodistribution study the radioactivity in whole tumor was measured. Hypoxia may only occur in regions of tumors while surface or core region are not responsible for uptake of radioactivity. Thus the 1.6 ratio could be higher for certain cells within tumors.

Although there is no firm evidence that the hypoxic fraction depends on tumor size at the macroscopic level, it is suspected that small, microscopic tumors may have smaller hypoxic fractions[226]. The hypoxic fraction might, therefore, be lower in the small tumors used in the biodistribution study compared to larger tumors used in scintigraphic study. A series of other images taken with animals bearing smaller tumors seem to agree with the biodistribution data. This indirectly supports the proposed relationship between hypoxic fraction and tumor size. An example of such image is shown in Figure 35. The smaller sized tumor (<100 mg) is less prominent in the scintigram compared to thyroid, liver, stomach and urinary bladder.

Figure 35. Static whole-body gamma scintigram of ^{123}I-IAZG in a Balb/c mouse bearing an EMT-6 tumor, without thyroid block.

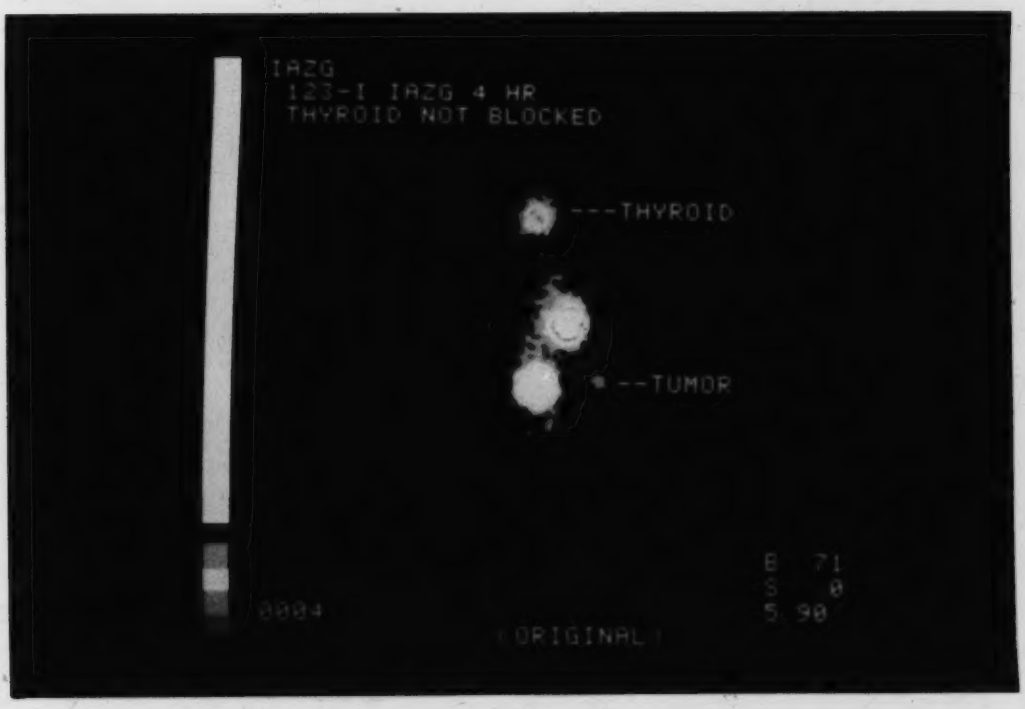

4.3. 1-(4-Iodo-4-Deoxy-ß-L-Xylopyranosyl)-2-Nitroimidazole (Iodoazomycin Pyranoside:IAZP) (54)

4.3.1. Chemistry

The title compound was synthesized by the general procedure described in Section 3.2.3. The synthesis is outlined in Scheme 10. The radiosynthesis of ^{125}I-IAZP is shown in Scheme 11. Direct iodination of the synthetic precursor (AZP; 53) was chosen because of the failure of several attempts to radiolabel IAZP (54) by iodine for iodine exchange reactions. Among the exchange reactions attempted were the solvent exchange iodination in dimethyl formamide (DMF), pivalic acid melt method as described for IAZA (45) /IAZG (49), and a reaction via NaI and triphenylphosphine with IAZP (54) at 130 °C for 5 h. It appears from these reactions that IAZP (54), unlike IAZA (45) or IAZG (49), is resistant to exchange iodination. This may be due to a greater chemical stability of the secondary iodine present in IAZP (54) than the primary iodine present in IAZA/IAZG molecule.

The radioiodination technique shown in Scheme 11 gave a relatively low radiochemical (15%) and chemical yield (32%). No further improvement on the yields was obtained despite a variety of modifications of the reaction conditions. The low yield may be due to several unresolved factors including water sensitivity of the iodinated product leading to

Scheme 10. Synthesis of 1-(4-iodo-4-deoxy-β-L-xylo-pyranosyl)-2-nitroimidazole (IAZP, 54)

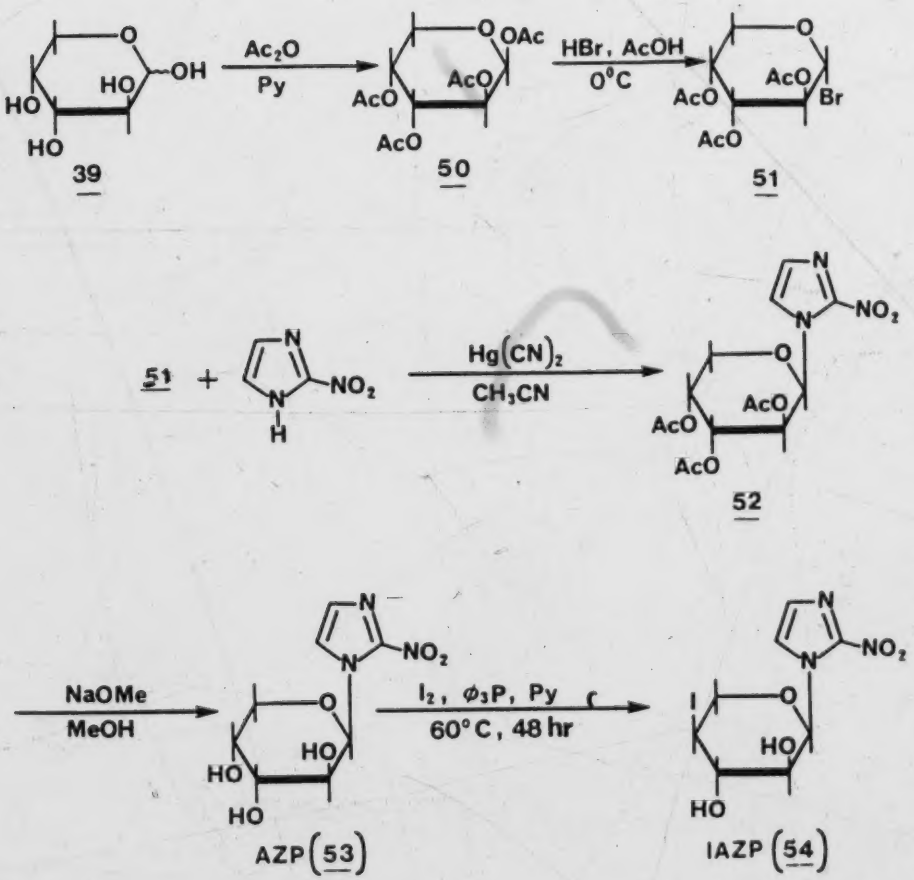

Scheme 11. Synthesis of radioiodinated 1-(4-iodo-4-deoxy-ß-L-xylopyranosyl)-2-nitroimidazole (^{125}I-IAZP).

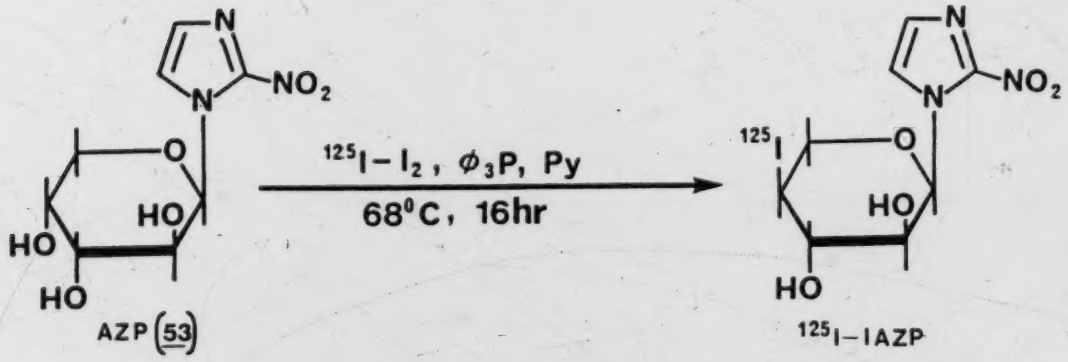

hydrolysis of IAZP (54) back to AZP (53).

HPLC purification was performed as described for IAZA (45). ^{125}I-IAZP had a retention time of 4.85 min. while unreacted precursor (AZP) had a retention time of 2.18 min. (column A, 50:50 H_2O: MeOH, 2 mL/min., 350 nm).

The specific activity of the purified product was determined to be 2.5 to 3.0 GBq/mmol. This specific activity was suitable for *in vivo* biodistribution and *in vitro* studies. An improved synthesis with higher radiochemical yield and shorter reaction time would be desirable for the preparation of ^{123}I-IAZP as an *in vivo* imaging agent. This may not be possible with the present reaction conditions, because the

reaction requires substantial carrier iodine (I_2) which would limit the specific activity of the final product. Also, the time to complete the reaction (16 h) is unsuitable for ^{123}I radiosynthesis.

4.3.2. *In vivo* Toxicity

An *in vivo* toxicity study of IAZP (54) in healthy young Balb/c mice indicated no toxicity at a dose of 350 µg/mouse. This suggests that a clinical study in humans could be performed at non-toxic drug levels. The mouse toxicity results were obtained at a dose level of about 100 times higher, in terms of mg of drug per kg of body weight, than the speculated human dose required for a scintigraphic evaluation study.

4.3.3. Cytotoxicity

Figures 36 and 37 show the cytotoxic effect on EMT-6 cells under hypoxic conditions, at various concentrations of IAZP (54) and AZP (53). Both compounds exert a cytotoxic effect on hypoxic EMT-6 cells in culture proportional to the concentration of substrate and to the incubation time. The time required to kill 90% of the cells was found to be 2.32 h at an IAZP (54) concentration of 1.0 mM (Figure 36). At lower concentrations (0.3 or 0.1 mM) the 90% cell kill was not realized during the 6 h incubation time. With AZP (53) at 5.0 mM, 90% cell kill was reached after 5.3 h of incuba-

Figure 36. Surviving fractions of hypoxic EMT-6 cells incubated with various concentrations of IAZP at various time intervals.

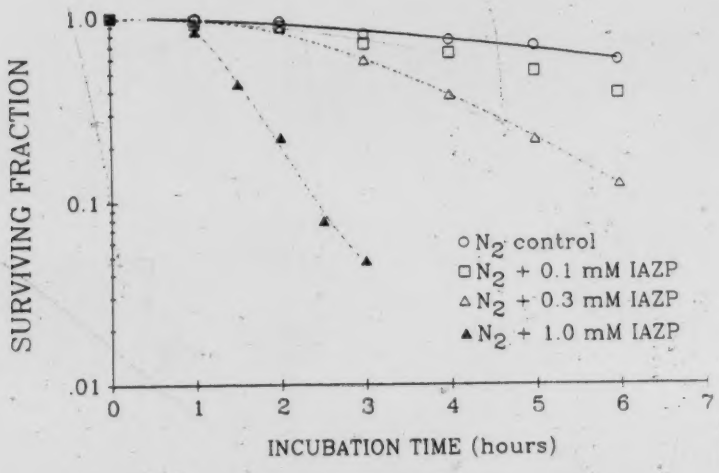

Figure 37. Surviving fractions of hypoxic EMT-6 cells incubated with various concentrations of AZP at various time intervals.

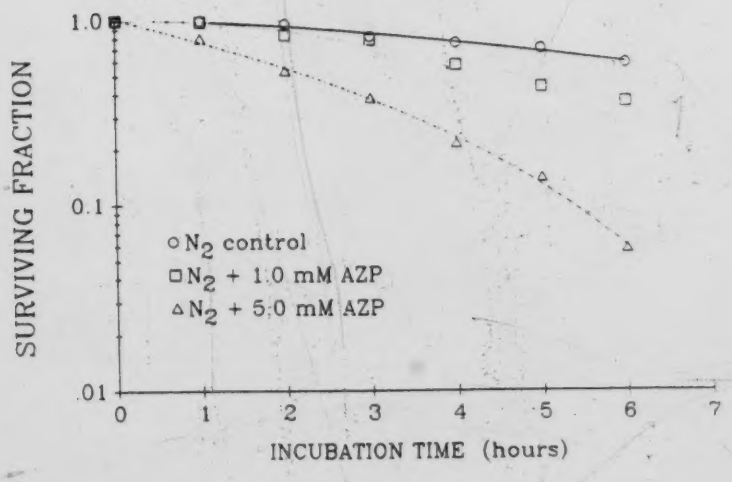

tion (Figure 37), while at a concentration of 1.0 mM much reduced cell kill was achieved during the 6 h of incubation.

Figure 38. Comparison of hypoxic cell cytotoxicity as a function of the reciprocal of time (hr^{-1}) for 90% cell kill, with various concentrations of IAZP and AZP.

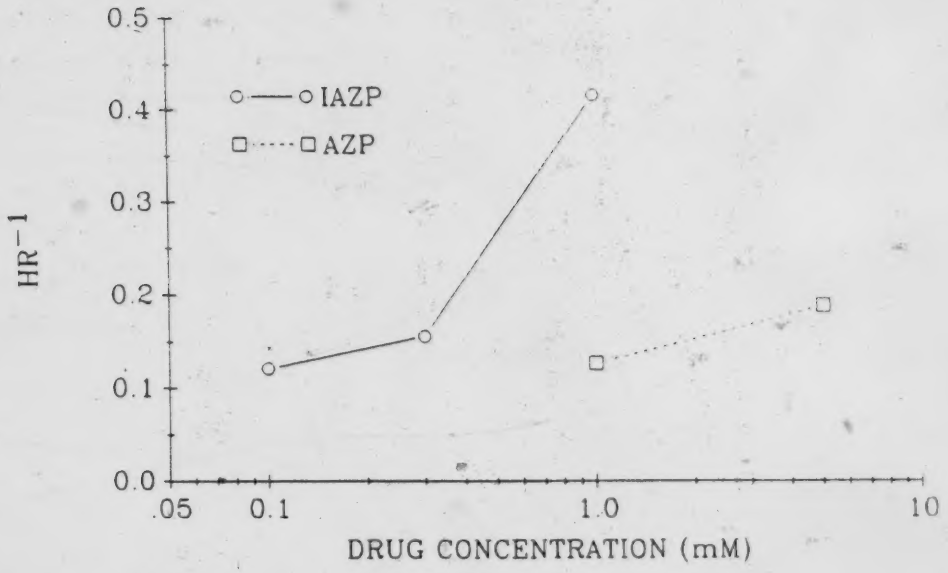

Like IAZA (45) and IAZG (49), these two test substrates (IAZP, AZP) also show selective toxicity toward hypoxic cells. No cytotoxic effect was observed under aerobic conditions in the same cell line.

A comparison of the cytotoxicity of IAZP (54) and AZP (53) is shown in Figure 38, expressed as reciprocal of time

(hr^{-1}) required to kill 90% of the cells as a function of substrate concentration. From the Figure 38, it appears that IAZP (54) is 3.3 times as toxic as AZP (53) at equimolar concentrations (1.0 mM). This type of increased toxicity with the iodinated analog IAZP over AZP was also observed with IAZA and IAZG. A number of factors are likely to be associated with the hypoxic cell cytotoxicity, of which lipophilicity and electron affinity may have an essential role.

4.3.4. Radiosensitization

The radiosensitizing properties of IAZP (54) and AZP (53) were studied *in vitro* with hypoxic EMT-6 cells at various concentrations of the test substrates. At the same time a drug-free air control and nitrogen control were also studied. Surviving fractions of EMT-6 cells following various doses of radiation at various concentrations of IAZP (54) and AZP (53) are shown in Figures 39 and 40. Hypoxic cells (nitrogen control) required 2.7 times more radiation than cells irradiated under aerobic conditions, to achieve 90% cell kill (OER = 2.7). Hypoxic cells, when irradiated together with various concentrations of IAZP or AZP showed increased radiosensitivity, evident in Figures 39 and 40, where the slope of the survival curve decreases compared to that of the nitrogen control curve. Both IAZP and AZP have radiosensitizing properties which increase as the concen-

Figure 39. Surviving fractions of EMT-6 cells at various radiation doses in air, nitrogen and nitrogen plus various concentrations of IAZP.

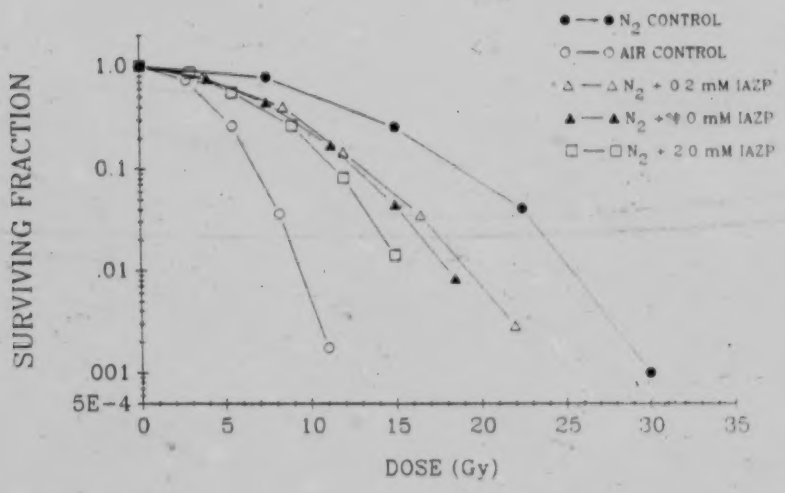

Figure 40. Surviving fractions of EMT-6 cells at various radiation doses in air, nitrogen and nitrogen plus various concentrations of AZP.

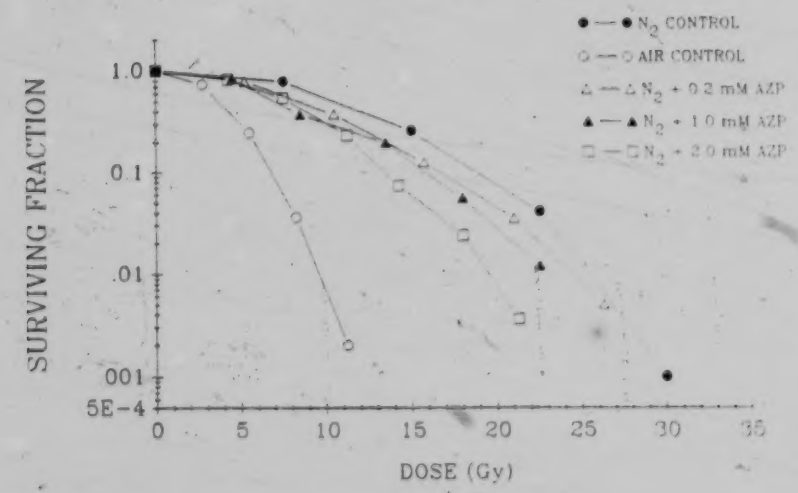

Figure 41. Comparison of sensitizer enhancement ratios (SER) of IAZP and AZP as a function of substrate concentration in vitro with hypoxic EMT-6 cells.

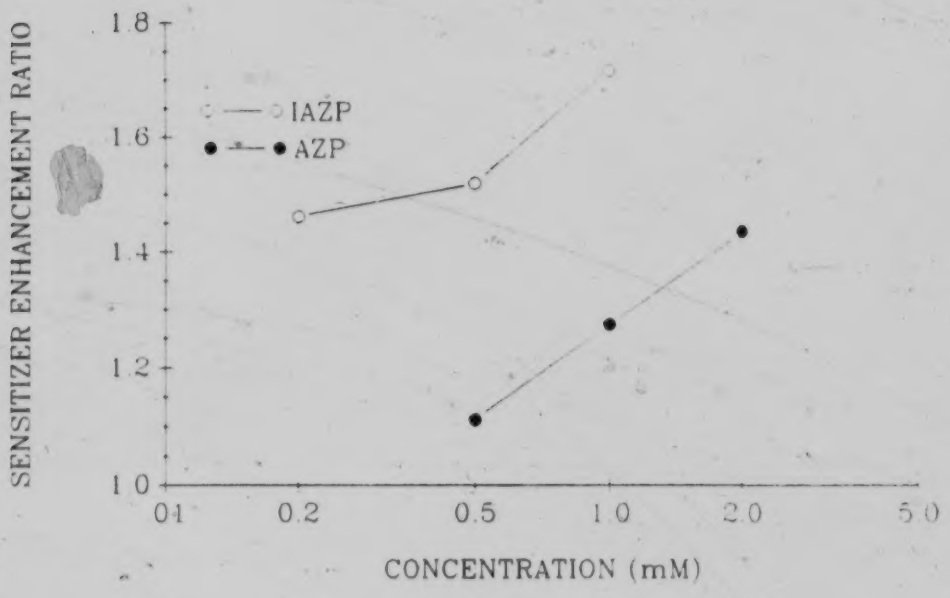

tration of the substrate increases.

A comparison of the SER's of these two compounds (IAZP, AZP) as a function of concentration is shown in Figure 41. The SER values were calculated at 10% survival, as described in Section 4.1.4. In terms of a concentration required to achieve the same SER value, IAZP (54) was found to be approximately 10 times more efficient than AZP (53) in sensitizing hypoxic EMT-6 cells (Figure 41). This increased radiosensitization with IAZP (54) over AZP (53) was expected as the former (IAZP) was seen to have increased cytotoxicity

compared with AZP. Other 2-nitroimidazoles such as IAZR (2) and AZR (32) show that higher hypoxic cell cytotoxicity correlates with greater radiosensitivity[12]. The reasons for such an effect have been discussed previously for IAZA (Section 4.1.4). Chapter 5 presents a further analysis of these relationships.

4.3.5. Initial Binding Rate

Figure 42 presents the amount of ^{125}I activity bound to the acid-insoluble fraction of EMT-6 cells under hypoxic and aerobic incubation with ^{125}I-IAZP. The data are presented as cpm/10^6 cells against incubation time. Under hypoxic conditions the ^{125}I activity bound to the macromolecular fraction of EMT-6 cells increases linearly as the concentration of substrate and incubation time increase. Under aerobic conditions, even at a concentration of 30 μM, the binding is negligible and remains constant during the 3 h of incubation. This suggests selective binding of ^{125}I-IAZP to hypoxic cells.

The initial rate of binding of ^{125}I-IAZP to the macromolecular fractions of hypoxic EMT-6 cells, expressed as pmol/10^6 cells/h as a function of substrate concentration, is shown in Figure 43. Under hypoxic conditions the initial binding rate increases linearly with the increasing substrate concentration. It is found that at 30 μM, the binding rate under hypoxic conditions is 30 times higher than under

Figure 42. ^{125}I Activity bound to the acid-insoluble fraction of EMT-6 cells after incubation with various concentrations of ^{125}I-IAZP at various time periods under hypoxic and aerobic conditions.

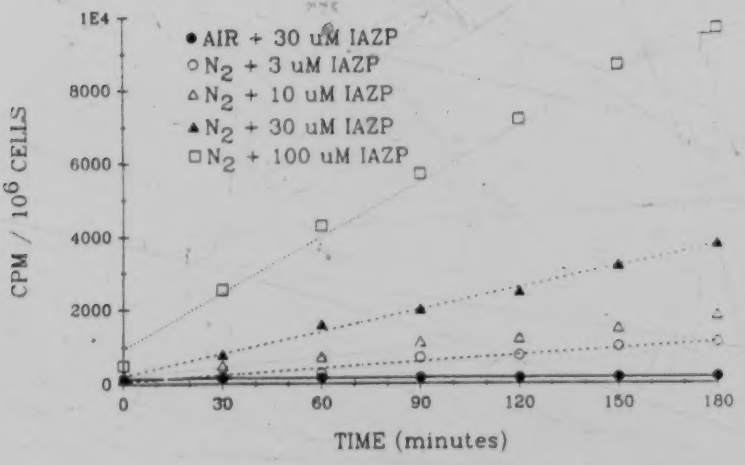

Figure 43. The initial binding rates expressed as pmol/10^6 cells/h of ^{125}I-IAZP bound to the acid-insoluble fraction of hypoxic EMT-6 cells at various concentrations of the test substrate.

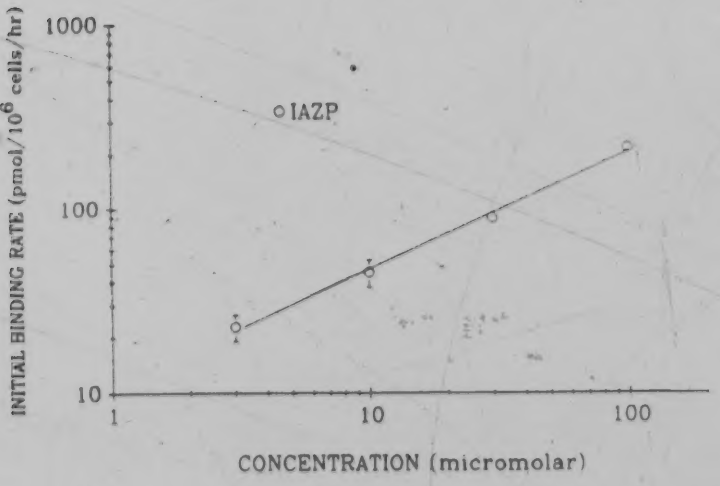

aerobic conditions. This hypoxia-selective binding property of IAZP (54) is similar to that of other electron-affinic nitroimidazoles including misonidazole (1) IAZR (2) and trifluoromisonidazole (36) as measured under similar conditions[12,191]. A comparison of the initial binding rate with those of misonidazole (1) and IAZR (2) as well as other test compounds is given in Chapter 5.

The relative dependence of binding characteristics of the test compound (^{125}I-IAZP) on the cellular oxygen level was studied in EMT-6 cells. Figure 44 shows the amount of ^{125}I activity bound to the acid-insoluble fraction of the EMT-6 cells at various oxygen levels as well as under hypoxia. The data are presented as cpm/10^6 cells against incubation time. The radioactivity bound to the macromolecular fraction of EMT-6 cells shows a general pattern similar to that observed for IAZA (45) and IAZG (49) in that; a) the binding is linear with incubation time in hypoxia and at various levels of oxygen, b) that the binding depends on the cellular levels of oxygenation and c) that the lower the level of oxygen the greater the binding.

Figure 45 presents the binding rate of ^{125}I-IAZP, as function of pmol/10^6 cells/h, versus various oxygen levels. There is a 48 times decrease in binding rate between the hypoxic condition and the 3% oxygen level. This rapid decline in binding rate further indicates the hypoxia-selective binding nature of the test compound (^{125}I-IAZP), as well

Figure 44. ^{125}I Activity bound to the acid-insoluble fraction of EMT-6 cells under hypoxia and various levels of oxygen incubated with 10 μM ^{125}I-IAZP at several time periods.

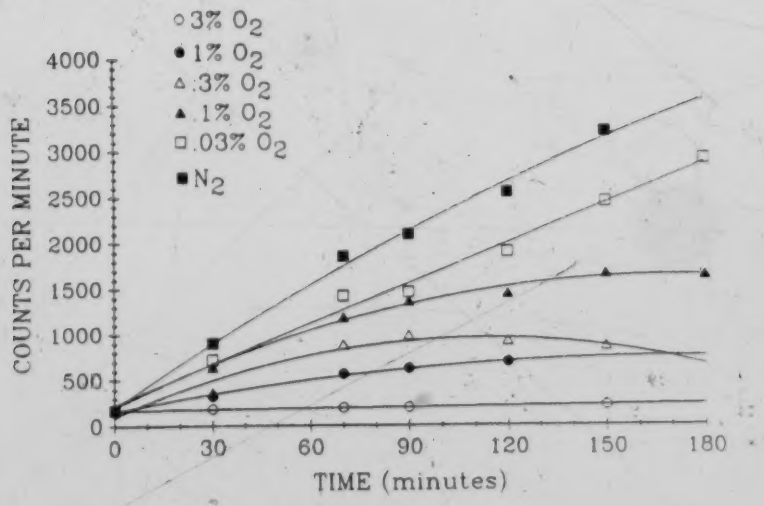

Figure 45. The initial binding rate of 10 μM ^{125}I-IAZP bound to the acid-insoluble fraction of EMT-6 cells under hypoxia and various levels of oxygenation.

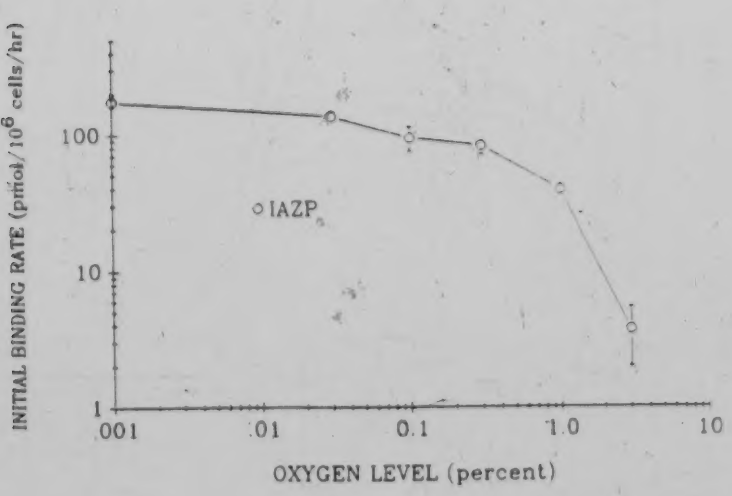

as the relative dependence of binding on the degree of hypoxia.

4.3.6. Biodistribution and Elimination

Table 7 shows the *in vivo* biodistribution data for ^{125}I-labelled IAZP (54) in Balb/c mice bearing EMT-6 tumors. Each animal received a single, i.v. bolus injection of 50 to 60 kBq of ^{125}I-IAZP (2.5 to 3.0 GBq/mmol). The results were computed by measuring ^{125}I activity in each organ as well as in the remaining carcass. Radioactivity was distributed throughout the body after injection of ^{125}I-IAZP with most of the organs showing higher radioactivity at early time periods (Table 7). A somewhat lower tumor radioactivity is probably an indication of poor vascularization/perfusion in this tissue.

The organ to blood ratios of radioactivity are shown in Figures 46 and 47. The tumor to blood ratio, which was found to be lower than other organ to blood ratios at early time periods, rose gradually and reached a maximum of 13.9 at 24 h. The tumor to blood ratios, between 4 and 24 h post injection, were found to be higher than any other organ ratios and therefore suggest that these time periods would be suitable for an imaging study. The higher tumor ratio is probably due to slower clearance of radioactivity from the tumor than from other organs. This slow clearance can be rationalized through a mechanism involving metabolic trap-

Table 7. Biodistribution of ^{123}I-IAZP following i.v. administration in Balb/c mice bearing EMT-6 tumors at various time intervals.

Organ	Time (hours) 0.25	0.50	1	2	4	8	12	24
Blood	2.06 ±0.58[a]	1.87 ±0.33	1.55 ±0.58	1.02 ±0.44	0.55 ±0.19	0.21 ±0.07	0.07 ±0.03	0.03 ±0.004
Tumor	2.62 ±0.47	2.68 ±0.87	3.01 ±0.85	2.16 ±0.36	1.93 ±0.90	1.20 ±0.24	0.58 ±0.15	0.47 ±0.009
	1.00 ±0.24[b]	1.31 ±0.43	2.24 ±0.32	2.53 ±0.77	5.37 ±2.08	5.93 ±0.85	8.42 ±2.71	13.88 ±3.13
Kidney	10.50 ±1.56	9.42 ±1.51	6.68 ±1.10	4.28 ±0.57	2.78 ±0.88	0.56 ±0.24	0.32 ±0.09	0.22 ±0.05
	4.44 ±0.69	4.48 ±0.41	5.35 ±0.73	5.47 ±1.09	5.29 ±1.00	4.37 ±0.64	5.43 ±0.76	6.36 ±0.97
GIT[c]	5.84 ±1.37	5.20 ±1.02	3.81 ±1.29	2.64 ±1.04	1.90 ±0.79	0.73 ±0.26	0.18 ±0.05	0.06 ±0.02
	2.46 ±0.52	2.54 ±0.31	2.97 ±0.62	3.30 ±1.29	3.45 ±0.70	4.68 ±1.52	2.95 ±1.79	1.80 ±0.51
Liver	9.79 ±1.56	8.55 ±2.47	5.42 ±1.17	3.64 ±1.09	2.42 ±0.69	0.77 ±0.14	0.58 ±0.15	0.21 ±0.05
	4.13 ±0.68	4.09 ±0.57	4.27 ±0.25	4.12 ±1.17	4.29 ±0.60	3.85 ±0.77	6.38 ±2.25	6.38 ±1.78
Muscle	3.51 ±1.67	3.85 ±1.07	2.19 ±0.23	1.52 ±0.42	0.59 ±0.30	0.22 ±0.07	0.10 ±0.06	0.04 ±0.01
	1.80 ±0.47	1.84 ±0.44	1.96 ±0.29	1.69 ±0.67	1.57 ±0.35	1.07 ±0.13	1.31 ±0.64	1.16 ±0.35
Bone	1.57 ±0.74	1.60 ±0.84	1.44 ±0.65	1.32 ±0.31	0.40 ±0.18	0.13 ±0.09	0.23 ±0.01	0.03 ±0.001
	0.86 ±0.29	0.75 ±0.26	0.80 ±0.42	1.62 ±0.92	1.03 ±0.17	0.63 ±0.45	2.03 ±1.42	0.84 ±0.06
Lung	4.08 ±1.32	3.68 ±0.66	3.22 ±0.85	1.36 ±0.41	0.68 ±0.26	0.35 ±0.10	0.13 ±0.05	0.08 ±0.01
	1.92 ±0.34	1.75 ±0.20	2.08 ±0.36	1.47 ±0.52	1.80 ±0.42	1.71 ±0.18	1.85 ±0.26	2.49 ±0.63
Heart	6.28 ±0.97	5.29 ±1.29	3.32 ±0.89	1.96 ±0.50	1.09 ±0.28	0.31 ±0.09	0.08 ±0.02	0.06 ±0.001
	2.64 ±0.34	2.50 ±0.26	2.60 ±0.25	2.26 ±0.67	1.98 ±0.24	1.52 ±0.32	1.12 ±0.21	1.79 ±0.24
Spleen	4.02 ±0.67	3.28 ±0.74	2.30 ±0.52	1.58 ±0.44	0.82 ±0.30	0.26 ±0.07	0.10 ±0.02	0.08 ±0.03
	1.68 ±0.18	1.55 ±0.20	1.60 ±0.26	1.80 ±0.66	1.52 ±0.24	1.27 ±0.16	1.36 ±0.38	2.39 ±1.05
Stomach	4.93 ±0.75	4.61 ±1.36	3.19 ±0.70	2.56 ±0.77	2.26 ±0.83	1.08 ±0.43	0.32 ±0.14	0.19 ±0.05
	2.30 ±0.85	2.18 ±0.32	2.53 ±0.28	2.90 ±0.64	4.17 ±0.53	5.08 ±0.72	4.57 ±1.82	5.42 ±1.11
Carcass	3.16 ±0.42	2.88 ±0.46	2.57 ±0.52	1.89 ±0.33	1.56 ±0.33	0.92 ±0.37	0.22 ±0.05	0.07 ±0.003
	1.34 ±0.21	1.37 ±0.15	1.73 ±0.30	2.16 ±0.57	2.96 ±0.58	4.38 ±0.59	3.22 ±1.98	2.14 ±0.18

[a]The numbers represent the mean ± standard deviation for percent of injected dose per gram of wet tissue for 6 animals. [b]Tissue to blood ratio. [c]Section of intestine.

Figure 46. Tissue to blood ratios of radioactivity at various time intervals following i.v. administration of ^{125}I-IAZP in Balb/c mice bearing EMT-6 tumors.

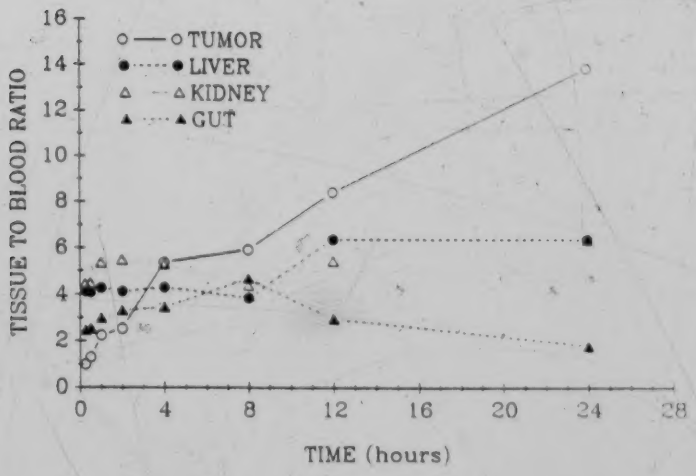

Figure 47. Tissue to blood ratios of radioactivity at various time intervals following i.v. administration of ^{125}I-IAZP in Balb/c mice bearing EMT-6 tumors.

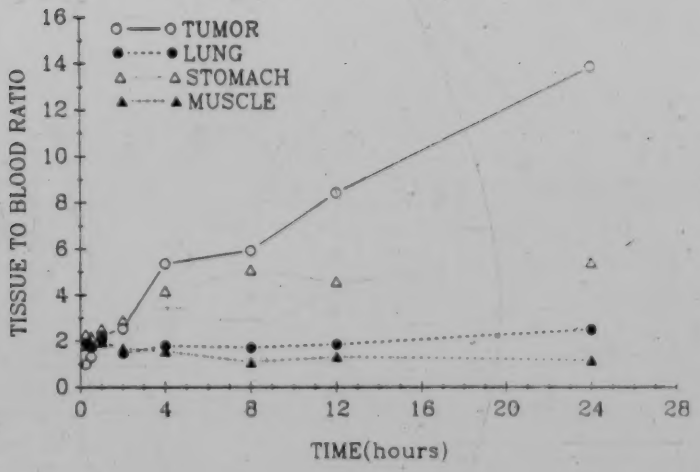

ping of the compound in the tissue, a process that has been reported for misonidazole (1) in EMT-6 tumor models[179]. It can therefore be postulated that the test compound (IAZP), once present in the hypoxic fraction of the cells, is trapped metabolically, with subsequent clearance at a slower rate than from the other tissues. Details of such a proposed metabolic process have already been discussed with reference to IAZA (45) (Section 4.1.6). The tumor to blood ratio for ^{125}I-IAZP at 24 h is the highest reported for any of the 2-nitroimidazoles tested to date in the Balb/c mice/EMT-6 tumor model.

Organ to blood ratios were relatively high in liver, kidney, intestine and stomach at the early time period (Figures 46 and 47). The persistently high liver to blood and kidney to blood ratios suggest a continuous involvement of these organs in metabolism and excretion of the test compound. The intestine to blood ratio may be an indication of hepatobiliary excretion of the compound (^{125}I-IAZP). A persistently high stomach to blood ratio may be due to the accumulation of free radioiodide in this organ. This was supported somewhat by the thyroid radioactivity, which increased to a maximum of 5.9% of the whole-body radioactivity (Table 8). Unlike the other two compounds (IAZA, IAZG) in this series presented previously, the thyroid radioactivity was relatively low (eg. compared to Table 3 and 6).

This suggests higher chemical and/or metabolic stability of ^{125}I-IAZP to deiodination.

Table 8. Thyroid radioactivity as percent injected dose of ^{125}I-IAZP/organ, in Balb/c mice bearing EMT-6 tumors (n=6;±S.D.).

Time (hour)	% injected dose/organ	Thyroid radioactivity as percentage of whole-body radioactivity
0.25	0.048±0.025	0.06±0.02
0.50	0.047±0.022	0.06±0.02
1.00	0.040±0.023	0.06±0.02
2.00	0.044±0.019	0.1±0.04
4.00	0.036±0.014	0.12±0.04
8.00	0.057±0.017	0.31±0.05
12.00	0.066±0.03	1.33±0.16
24.00	0.137±0.05	5.88±0.62

Figure 48 shows the whole-body elimination and blood clearance of ^{125}I radioactivity in Balb/c mice bearing EMT-6 tumors. These curves are complex and could not be resolved by simple exponential analysis. The whole-body radioactivity curve shows a rapid elimination at early time periods followed by an intermediate rate between 2 and 8 h. The elimination is slow at longer time periods between 12 and 24 h, with an estimated half-life of 11 h. The blood-radioactivity clearance curve shows a very rapid distribution phase, with

a half-life of less than 5 min. This is followed by clearance at an intermediate rate for up to 12 h. Between 12 and 24 h the clearance is very slow and resembles the whole-body elimination, with an approximately similar half-life.

Figure 48. Whole-body elimination and blood clearance of radioactivity following i.v. administration of ^{125}I-IAZP in Balb/c mice bearing EMT-6 tumors.

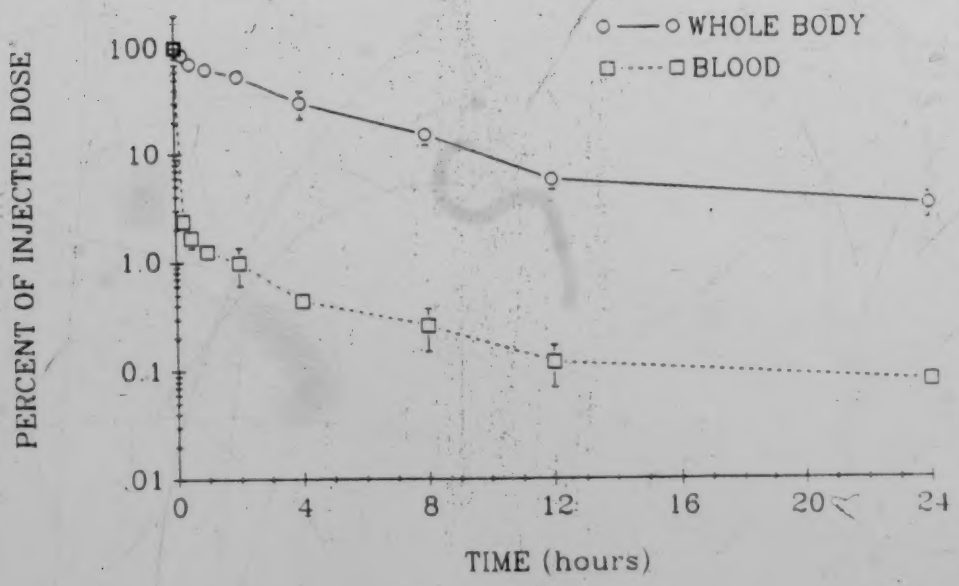

At 24 h, the ^{125}I activity remaining in blood and whole-body were 0.03 and 2.33 percent of injected dose respectively. These data show a rapid clearance and elimination of radioactivity from blood and whole-body, presumably due to

rapid clearance of radioactivity from tissues as a result of low/no specific binding with normal tissues. These properties make the compound (IAZP) a useful agent for imaging, where blood pool radioactivity and most organs and tissues would not interfere with imaging of hypoxic tumor tissue.

The *in vitro* studies and the *in vivo* biodistribution study reported in this section strongly suggest the potential of IAZP (54) as a non-invasive marker of hypoxic cells in tumor tissue. This compound may in fact prove to be a superior agent to IAZA (45) in scintigraphic studies. The major positive features are the high tumor to blood ratios and the greatly improved stability to deiodination. These factors are probably related since intact IAZP persists longer *in vivo* and likely has more opportunity to enter hypoxic cells. The major problem at the moment is the unsuitable synthesis of the radiolabelled product.

4.4. 1-(2-Fluoro-2-Deoxy-4-Iodo-4-Deoxy-ß-L-Xylopyranosyl)-2-Nitroimidazole (2'-Fluoro-Iodoazomycin Pyranoside: FIAZP) (60)

4.4.1. Chemistry

The synthesis of the title compound (FIAZP; 60) is outlined in Scheme 12 (see also Section 3.2.4).

Scheme 12. Synthesis of 1-(2-fluoro-2-deoxy-4-iodo-4-deoxy-ß-L-xylopyranosyl)-2-nitroimidazole (FIAZP, 60)

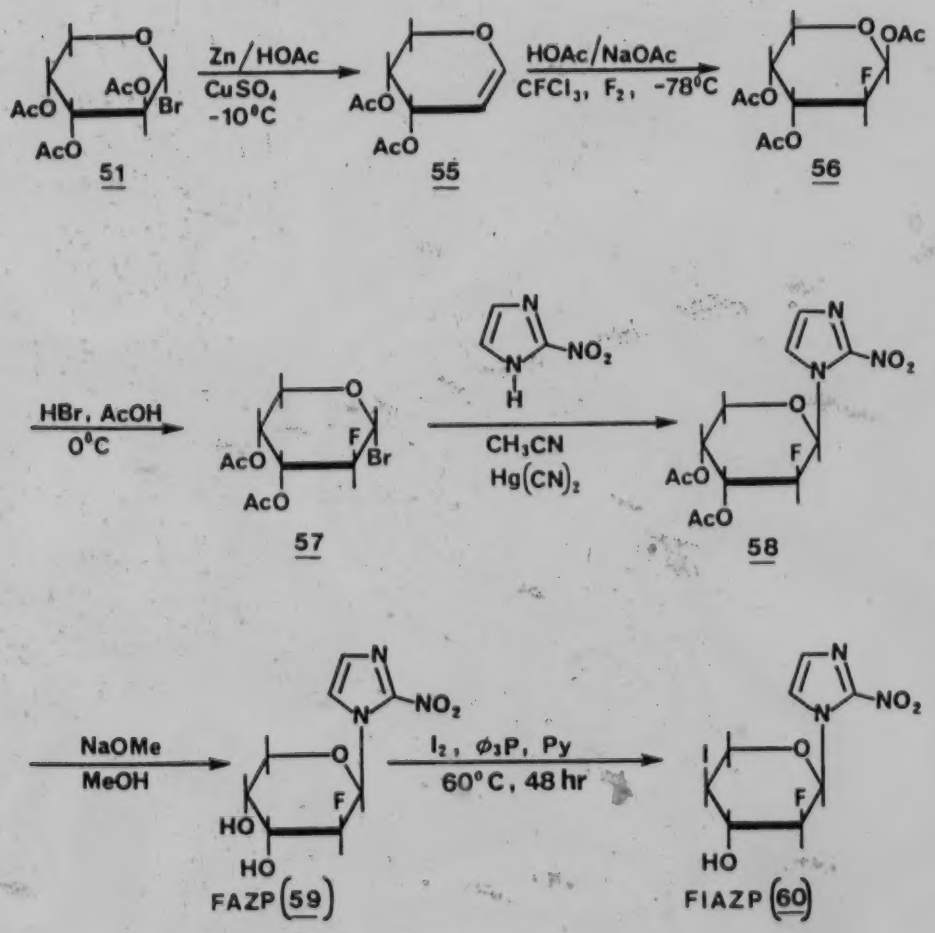

The radiosynthesis of ^{125}I-FIAZP is shown in Scheme 13. As with ^{125}I-IAZP, exchange iodination was not successful and a direct radioiodination from the synthetic precursor FAZP (59) was used to prepare the radiolabelled product. Radiochemical and chemical yields of ^{125}I-FIAZP were 15% and 35%, respectively, and the specific activity was found to be 2.1 to 2.5 GBq/mmol.

Scheme 13. Synthesis of radioiodinated 1-(2-fluoro-2-deoxy-4-iodo-4-deoxy-ß-L-xylopyranosyl)-2-nitroimidazole (^{125}I-FIAZP)

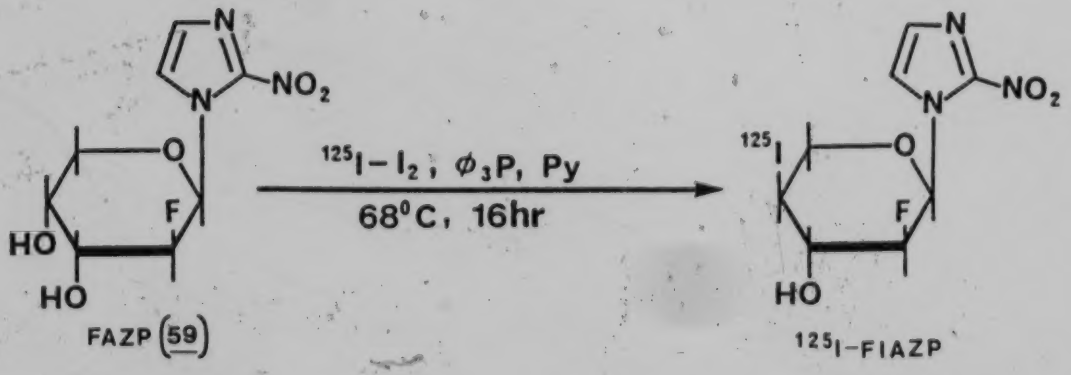

Purification of the reaction mixture was carried out by HPLC (Section 4.3.1). The retention time of the ^{125}I-FIAZP was about 4.49 min. No attempt was made to improve the radiochemical yield by increasing the reaction time.

The relatively low radioiodination yield may be due to effects similar to those described for IAZP (54) (Section

4.3.1). The compounds (IAZP, FIAZP) are structurally similar, having iodine in the 4'-position differing only in that FIAZP (60) contains a fluorine at 2'-position in place of the 2'-hydroxyl group in IAZP.

4.4.2. Cytotoxicity

The surviving fraction of EMT-6 cells incubated with various concentrations of FIAZP (60) and FAZP (59) at various time periods under hypoxia is shown in Figures 49 and 50 respectively. The time required to kill 90% of the cells was found to be 2.45 h and 5.65 h at concentrations of 1.0 and 0.5 mM of FIAZP (60), respectively. At concentrations lower than 0.5 mM, 90% cell kill was not reached during 6 h of incubation (Figure 49). With FAZP (59), the time required to achieve 90% cell kill was 2.58 h and 4.65 h at 2.0 and 1.0 mM, respectively (Figure 50). The cytotoxic effect of these two compounds is similar to the other members of this series (IAZA, IAZG, IAZP) in that cytotoxicity increases with time and substrate concentration, and that they demonstrate hypoxia-selective toxicity with little or no toxicity under aerobic conditions.

The cytotoxicity data for FIAZP (60) and FAZP (59) are presented in Figure 51. The data are expressed as reciprocal of time (hr^{-1}) required to achieve 90% cell kill as a function of substrate concentration. FIAZP (60) is seen to be

Figure 49. Surviving fractions of hypoxic EMT-6 cells incubated with various concentrations of FIAZP at various time intervals.

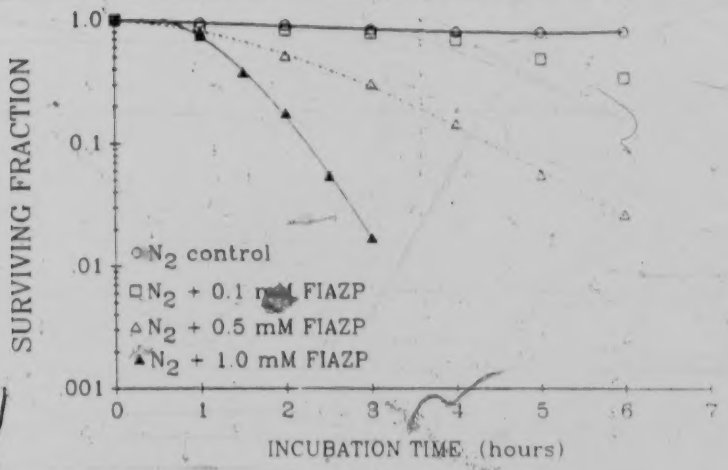

Figure 50. Surviving fractions of hypoxic EMT-6 cells incubated with various concentrations of FAZP at various time intervals.

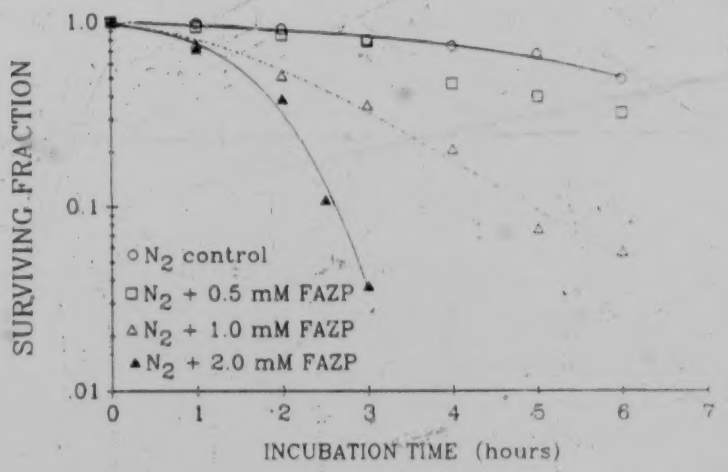

Figure 51. Comparison of hypoxic cell cytotoxicity as a function of the reciprocal of time (hr^{-1}) for 90% cell kill with various concentrations of FIAZP and FAZP

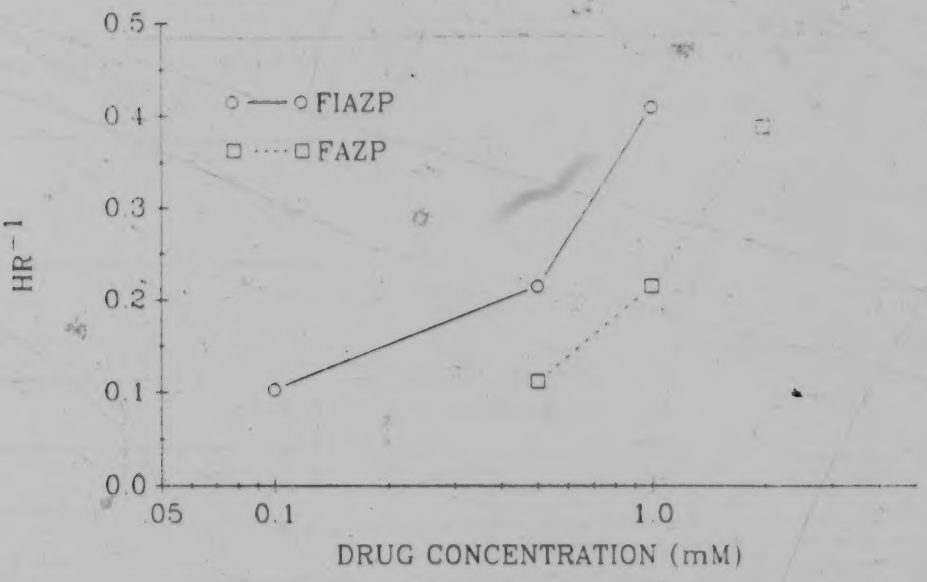

twice as toxic as FAZP (59) on a concentration basis to achieve the same level of cytotoxicity. This increased toxicity of the iodinated compound (FIAZP) over its non-iodinated precursor (FAZP) was expected on the basis of the observed behaviour of IAZA and AZA (Section 4.1.3) and other members of this series.

4.4.3. Radiosensitization

The radiosensitizing properties of FIAZP (60) and FAZP (60) were studied with hypoxic EMT-6 cells at various substrate concentrations and radiation doses. Nitrogen and air control curves were also constructed at the same time. Figures 52 and 53 show the surviving fraction of EMT-6 cells irradiated with various radiation doses following incubation with various concentrations of FIAZP and FAZP. The cells irradiated under aerobic conditions were more radiosensitive than under hypoxic conditions. The OER at 10% cell survival was calculated to be 2.7. The sensitivity of the hypoxic cells, irradiated in the presence of test substrate, increased as seen by a decrease in the slope of the survival curve. This suggests that the radiosensitizing properties of FIAZP (60) and FAZP (59) are similar to those of other compounds in this series (IAZA, IAZG, IAZP) in that cells become more radiosensitive as the concentration of the substrates increase. The SER's of FIAZP (60) and FAZP (59) at 90% cell kill are shown in Figure 54. It appears that in terms of concentration of test substrate required to achieve a particular SER value, FIAZP (60) is twice as efficient as its non-iodinated precursor FAZP (59) in sensitizing hypoxic cells to the lethal effects of ionizing radiation. The increase in SER of FIAZP (60) over FAZP (59) was expected considering the effects observed with other analogs in this series. Details of this effect have been discussed for

Figure 52. Surviving fractions of EMT-6 cells at various radiation doses in air, nitrogen and nitrogen plus various concentrations of FIAZP.

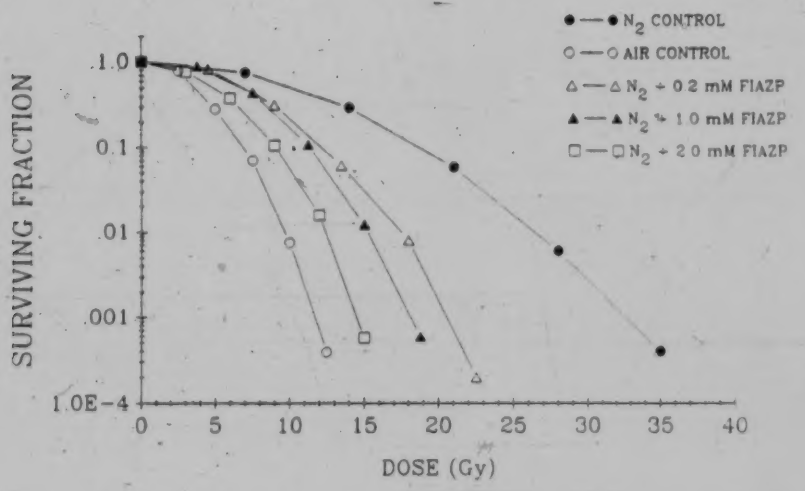

Figure 53. Surviving fractions of EMT-6 cells at various radiation doses in air, nitrogen and nitrogen plus various concentrations of FAZP.

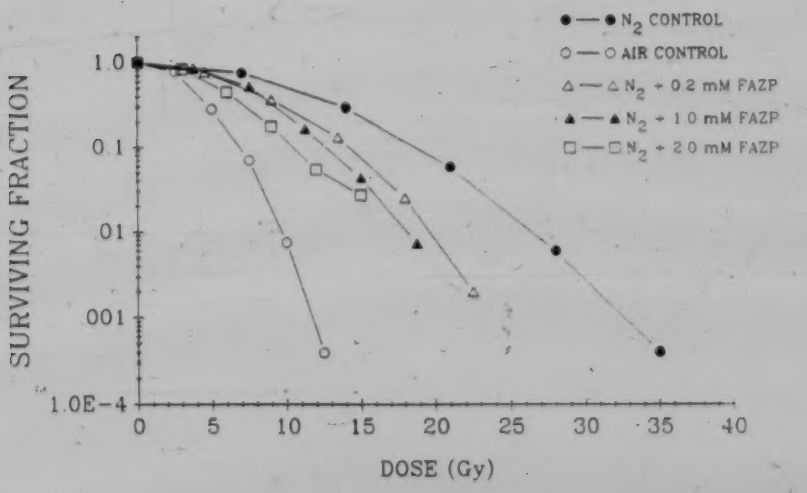

Figure 54. Comparison of sensitizer enhancement ratios (SER) of FIAZP and FAZP as a function of substrate concentration in vitro with hypoxic EMT-6 cells.

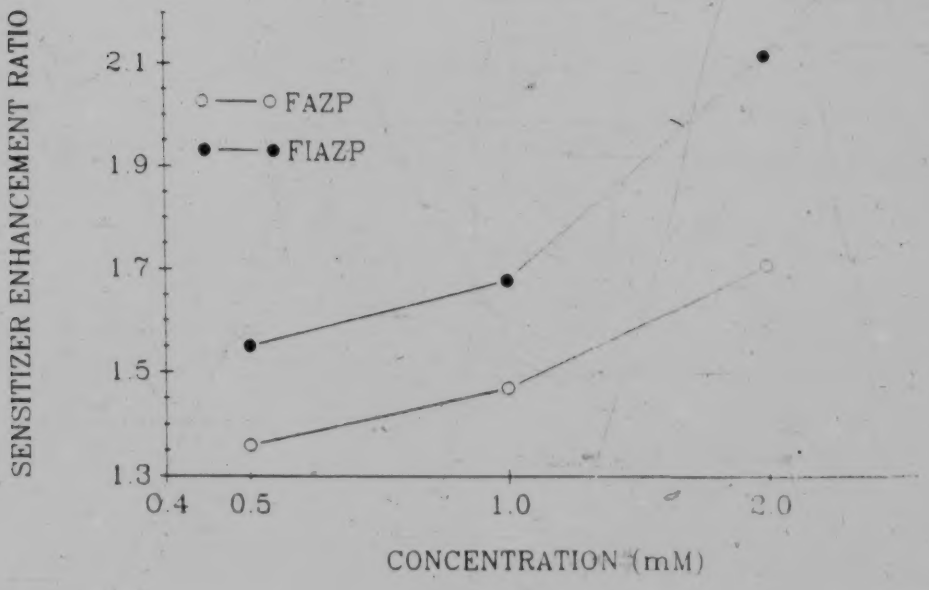

IAZA (45) (Section 4.1.4). It would appear that the higher SER of FIAZP (60) over FAZP (59) can be attributed to a number of factors including lipophilicity, electron affinity and cytotoxicity.

4.4.4. Biodistribution and Elimination

The in vivo biodistribution of ^{125}I labelled FIAZP (60) was studied in Balb/c mice bearing EMT-6 tumors. Table 9 shows the biodistribution data following i.v. injection of ^{125}I-FIAZP. Each animal received a single bolus dose of 50 to 60 kBq (2.1 to 2.5 GBq/mmol) of ^{125}I-FIAZP.

Table 9. Biodistribution of ^{123}I-FIAZP following i.v. administration in Balb/c mice bearing EMT-6 tumors at various time intervals.

Organ	Time (hours) 0.25	0.50	1	2	4	8	12	24
Blood	2.38 ±0.27[a]	1.69 ±0.33	1.26 ±0.20	0.98 ±0.38	0.44 ±0.19	0.26 ±0.11	0.12 ±0.05	0.08 ±0.01
Tumor	2.17 ±0.48	2.34 ±0.40	2.51 ±0.26	2.55 ±0.70	1.47 ±0.52	1.21 ±0.39	0.49 ±0.19	0.46 ±0.12
	0.93 ±0.25[b]	1.28 ±0.22	2.03 ±0.36	2.54 ±0.58	3.53 ±0.68	4.53 ±0.78	4.45 ±2.02	5.98 ±0.46
Kidney	6.42 ±0.60	5.21 ±0.78	4.06 ±0.66	3.02 ±1.38	1.05 ±0.48	0.56 ±0.25	0.22 ±0.09	0.15 ±0.04
	2.71 ±0.19	2.79 ±0.17	3.22 ±0.11	4.09 ±2.24	2.43 ±0.42	1.95 ±0.16	1.93 ±0.11	1.87 ±0.27
GIT[c]	5.66 ±1.96	4.57 ±1.11	4.58 ±2.49	4.70 ±2.57	1.16 ±0.66	0.83 ±0.50	0.20 ±0.12	0.07 ±0.02
	2.37 ±0.76	2.48 ±0.59	3.66 ±2.12	5.57 ±3.86	2.60 ±0.76	2.66 ±1.60	1.64 ±0.32	1.02 ±0.39
Liver	10.62 ±1.58	7.93 ±1.10	6.01 ±0.86	4.50 ±1.18	2.11 ±0.71	1.01 ±0.32	0.69 ±0.07	0.57 ±0.19
	4.49 ±0.70	4.36 ±0.96	4.80 ±0.71	4.57 ±1.11	4.70 ±0.77	3.89 ±1.23	6.45 ±1.77	7.13 ±1.22
Muscle	3.47 ±0.26	2.56 ±0.40	1.54 ±0.41	1.21 ±0.40	0.32 ±0.17	0.16 ±0.09	0.06 ±0.01	0.05 ±0.01
	1.46 ±0.10	1.37 ±0.06	1.22 ±0.14	1.20 ±0.21	0.74 ±0.20	0.52 ±0.18	0.51 ±0.06	0.67 ±0.12
Bone	1.45 ±0.54	1.02 ±0.43	0.77 ±0.29	0.95 ±0.52	0.17 ±0.12	0.21 ±0.02	0.07 ±0.06	0.02 ±0.001
	0.63 ±0.27	0.53 ±0.17	0.60 ±0.13	1.02 ±0.55	0.34 ±0.26	0.62 ±0.38	0.61 ±0.50	0.31 ±0.02
Lung	4.42 ±0.26	3.23 ±0.47	2.35 ±0.54	1.69 ±0.41	0.64 ±0.26	0.39 ±0.13	0.25 ±0.04	0.23 ±0.07
	1.87 ±0.14	1.74 ±0.12	1.86 ±0.31	1.82 ±0.34	1.52 ±0.25	1.44 ±0.31	2.24 ±0.52	2.94 ±0.54
Heart	4.49 ±0.38	3.15 ±0.49	2.06 ±0.50	1.31 ±0.32	0.69 ±0.42	0.19 ±0.07	0.09 ±0.03	0.08 ±0.02
	1.89 ±0.09	1.69 ±0.05	1.62 ±0.14	1.39 ±0.28	1.56 ±0.29	0.67 ±0.09	0.79 ±0.12	1.05 ±0.13
Spleen	3.43 ±0.29	2.57 ±0.46	1.72 ±0.31	1.04 ±0.27	0.40 ±0.15	0.21 ±0.08	0.09 ±0.02	0.05 ±0.01
	1.45 ±0.11	1.38 ±0.11	1.36 ±0.09	1.12 ±0.28	0.94 ±0.09	0.73 ±0.08	0.78 ±0.11	0.76 ±0.10
Stomach	5.91 ±1.39	3.42 ±0.48	3.23 ±0.62	3.05 ±0.91	1.79 ±1.05	1.05 ±0.37	0.48 ±0.13	0.24 ±0.05
	2.48 ±0.50	1.87 ±0.38	2.56 ±0.38	3.40 ±1.35	3.92 ±2.00	3.89 ±0.96	4.28 ±1.03	3.21 ±0.33
Carcass	3.25 ±0.28	2.74 ±0.47	2.47 ±0.46	2.32 ±0.36	1.35 ±0.51	0.76 ±0.45	0.25 ±0.19	0.08 ±0.01
	1.37 ±0.10	1.57 ±0.10	1.96 ±0.23	2.61 ±0.84	3.30 ±0.97	2.67 ±0.79	1.94 ±0.83	0.98 ±0.09

[a]The numbers represent the mean ± standard deviation for percent of injected dose per gram of wet tissue for 6 animals. [b]Tissue to blood ratio. [c]Section of intestine.

The test compound was distributed rapidly throughout the body. Most of the organs, except tumor, contained uniformly high radioactivity at the initial time period (0.25 h). The lower tumor radioactivity may be an indication of poor perfusion/vascularization of this tissue.

Organ to blood ratios of radioactivity are shown in Figures 55 and 56. The tumor to blood ratio, which was lower than most other organ to blood ratios at the early time periods, increased gradually with time to a maximum of 6 at 24 h post injection. This suggests slow clearance of tumor radioactivity relative to blood and all other organs with the exception of liver. This suggests that there is metabolic trapping within the tumor tissue.

Liver shows a higher ratio than other organs at all time periods except 8 h and increases to a maximum of 7 at 24 h. The persistently high liver ratio suggests continuous involvement of this organ in metabolism and/or hepatobiliary excretion of the metabolite(s) from FIAZP. The rate of metabolism of drugs and their uptake into liver cells appears to be dependent upon the partition coefficient[227,228]. Drugs with higher lipophilicity undergo first-pass extraction followed by binding to the lipophilic cytochrome P-450 enzyme site located in the lipoid membrane of the endoplasmic reticulum[227,228]. This may be true for the ^{125}I-FIAZP which is the most lipophilic in this series, having a P value of 6.3. The rise of the liver to blood ratio at 12 h and the gradual,

Figure 55. Tissue to blood ratios of radioactivity at various time intervals following i.v. administration of ^{125}I-FIAZP in Balb/c mice bearing EMT-6 tumors.

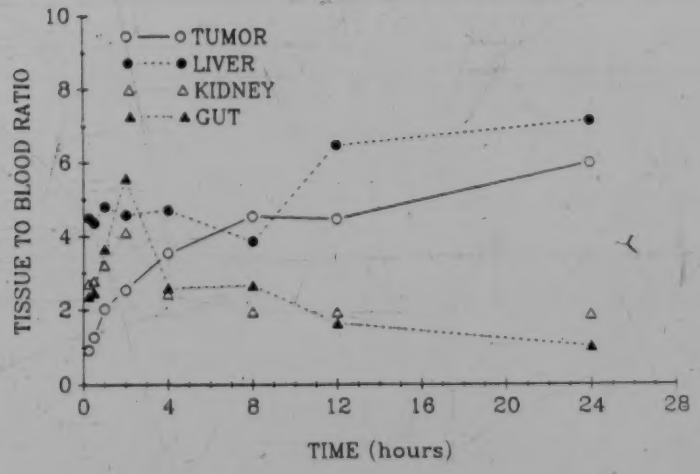

Figure 56. Tissue to blood ratios of radioactivity at various time intervals following i.v. administration of ^{125}I-FIAZP in Balb/c mice bearing EMT-6 tumors.

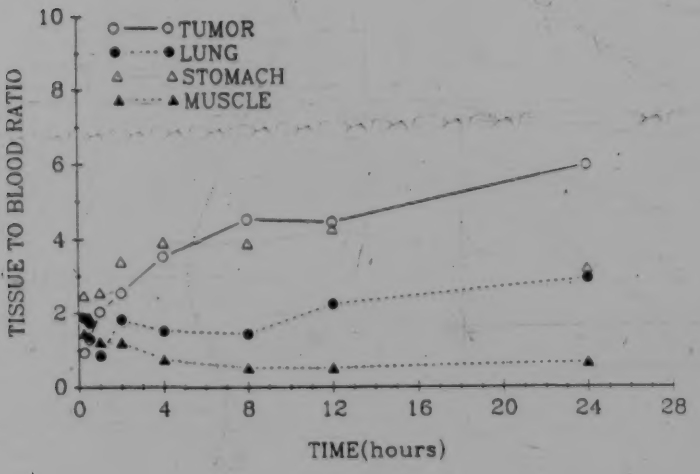

continued rise between 12 and 24 h is probably due to entero-hepatic circulation of the test drug (^{125}I-FIAZP). These assumptions remained unverified since no study to identify the metabolite(s), the site of metabolism or the elimination of radioactivity via the bile was performed.

Relatively high organ to blood ratios were also found for kidney, intestine and stomach. The kidney to blood ratio remains approximately constant, while the intestine to blood ratio decreases further between 8 and 24 h. The stomach to blood ratio seems to rise up to 12 h and then remains more or less constant up to 24 h. The kidney and intestine to blood ratios may be an indication of urinary and hepato-biliary excretion of ^{125}I-FIAZP. The increase in stomach to blood ratio presumably due to deiodination of the radio-labelled compound (^{125}I-FIAZP) and subsequent accumulation of free radioiodide in the organ. This speculation of deiodin-ation was supported by the gradual increase of thyroid radioactivity (Table 10), which reaches a maximum of 3.4% of total body radioactivity at 24 h. The amount of deiodin-ation as suggested by these values is much lower than IAZA (45) or IAZG (49) and is comparable to IAZP (54).

Figure 57 shows the whole-body elimination and blood clearance of ^{125}I-FIAZP. The whole-body elimination and blood clearance curves are complex and could not be resolved by simple exponential analysis.

Table 10. Thyroid radioactivity as percent injected dose of ^{125}I-FIAZP/organ, in Balb/c mice bearing EMT-6 tumors (n=6;±S.D.).

Time (hour)	% injected dose/organ	Thyroid radioactivity as percentage of whole-body radioactivity
0.25	0.043±0.03	0.05±0.01
0.50	0.042±0.03	0.06±0.01
1.00	0.039±0.02	0.06±0.01
2.00	0.029±0.02	0.06±0.02
4.00	0.096±0.05	0.32±0.04
8.00	0.11±0.05	0.74±0.06
12.00	0.107±0.05	1.88±0.25
24.00	0.11±0.07	3.36±0.55

The whole-body elimination pattern of this compound (^{125}I-FIAZP) is similar to that of ^{125}I-IAZP with an estimated half-life of 15 h between 12 and 24 h post injection. The blood clearance curve for ^{125}I-FIAZP is also similar to that of ^{125}I-IAZP in that it shows a very rapid decline of radioactivity in the distribution phase with a half-life of less than 5 min., a relatively slow clearance up to 12 h, and between 12 and 24 h the blood clearance is slow and resembles the whole-body elimination curve.

At 24 h post injection the radioactivity remaining in the whole-body and blood represented 3.3 and 0.08 percent of the injected dose respectively. This rapid elimination and blood

clearance suggests that the blood pool activity would not interfere with an imaging study provided sufficient radioactivity were trapped in tumor tissue. Little specific uptake of the compound occurs in normal tissues other than liver and thyroid.

Figure 57. Whole-body elimination and blood clearance of radioactivity following i.v. administration of ^{125}I-FIAZP in Balb/c mice bearing EMT-6 tumors.

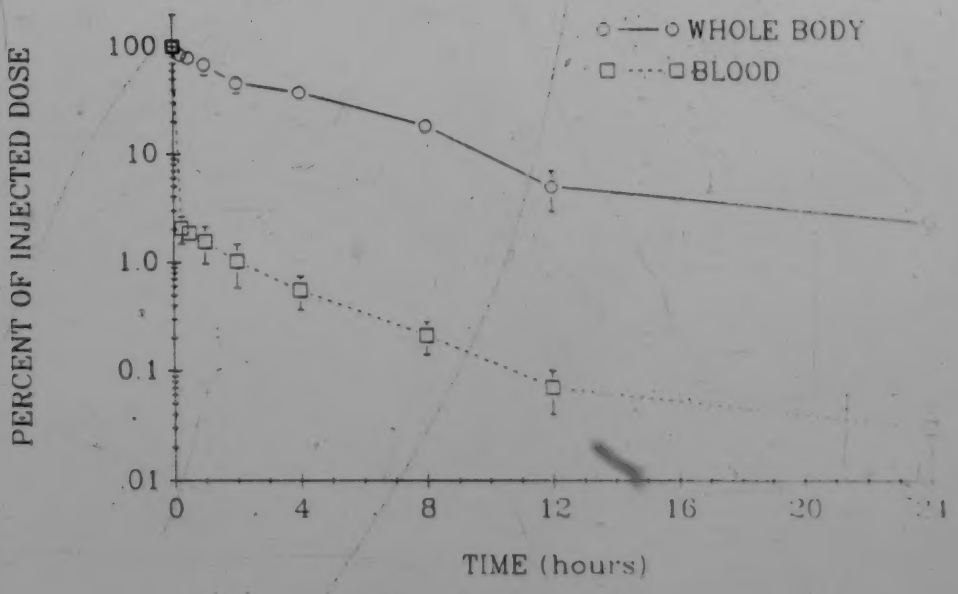

On the basis of the results discussed in this Section, it appears that this compound (FIAZP) like others in the series is trapped in EMT-6 tumors, presumably due to the large fraction of hypoxic cells. Despite these favourable results

FIAZP (60) may not be an ideal agent for non-invasive diagnosis of hypoxic cells in tumors especially those present in the abdomen, due to the elevated liver radioactivities up to 24 h. No time period was found to be suitable for an imaging study, as the liver to blood ratio was higher than tumor to blood ratio and stomach showed a persistently high ratio throughout the 24 h period.

5. COMPARATIVE SUMMARY OF PHYSICO-CHEMICAL AND BIOLOGICAL PROPERTIES OF VARIOUS SUGAR-COUPLED 2-NITROIMIDAZOLES

This chapter presents a comparative summary of the results obtained from *in vitro* (cytotoxicity, radiosensitization, and binding rate) and *in vivo* (biodistribution) studies with the four iodinated sugar-coupled 2-nitroimidazoles described in earlier chapters. Whenever possible the results are also compared with published data for misonidazole (1) and IAZR (2). Reports on partition coefficients and phosphorolysis studies with the iodinated and non-iodinated compounds are also included in this chapter.

5.1. Partition Coefficient

Table 11 presents the octanol-water partition coefficient (P) values of the four main compounds and their non-iodinated counterparts along with a number of reference compounds. In general the iodinated compounds are 6-10 times more lipophilic than their non-iodinated counterparts. This is presumably due to substitution of the hydroxyl group by an iodine atom in the sugar moieties of these compounds. Studies with several novel pyrimidine nucleosides also showed that the replacement of the hydroxyl group by iodine in the sugar moiety increases P values[229,230]. These studies showed that in general, replacement of a sugar hydroxyl group by any halogen increased lipophilicity, with iodine

increasing P values to a greater extent than other halogen when present at the 5' position of the sugar moiety[229].

Table 11. Partition coefficient (P) for the sugar-coupled 2-nitroimidazoles and reference compounds.

Compound	P (n=3;±S.D.)	Reference
AZA (44)	0.52±0.02	
IAZA (45)	4.98±0.67	
AZG (48)	0.07±0.002	
IAZG (49)	0.57±0.02	
AZP (53)	0.18±0.03	
IAZP (54)	0.89±0.12	
FAZP (59)	1.52±0.22	
FIAZP (60)	6.26±1.01	
AZR (32)	0.04	12
IAZR (2)	2.1±0.30	12
Misonidazole (1)	0.43	12
Trifluoromisonidazole (36)	2.6	191

Among the iodinated 2-nitroimidazole analogs studied, the lipophilicity is in order FIAZP > IAZA > IAZP > IAZG. The differing P values of these compounds may be attributed to the sugar moiety attached to the 2-nitroimidazole base. The galactoside is less lipophilic than the furanoside or pyranosides. Among the pyranosides, FIAZP is 7 times more

lipophilic than IAZP. This is due to the insertion of a fluorine atom at the 2'-arabino position in place of hydroxyl group of IAZP, presumably with accompanying electronic and conformational changes. The replacement of an hydroxyl group at the 2'-arabino position has been shown to increase the lipophilicity of a variety of pyrimidine nucleosides[229,230]. Furthermore, it was also shown that fluorine at the 2'-arabino position increased lipophilicity more than that of fluorine at the 2'-ribo position[229,230]. The arabino sugar moieties are known to have greater P values than their ribo counterparts, possibly due to their (arabino) intramolecular bonding or other steric and electronic effects[229]. Within the nitroimidazole furanoside group, the P value of IAZA was found to be twice as high as the P value for the ribo analog (Table 11).

The increment of lipophilicity by fluorine was also evident with the trifluoromisonidazole (36)[191]. This fluorinated analog of misonidazole was 6 times more lipophilic than the parent compound (Table 11).

The effect of the substituents on the P values of parent compounds was determined according to the formula given by Fujita et al[231].

$$\pi_x = \log P_x - \log P_H$$

Where, π_x refers to the substituent constant, $\log P_x$ is the partition coefficient of the compound containing x substituent (in this case it would be either iodine or fluorine),

log P_H is the partition coefficient of the parent compound (in this case it would be either non-iodinated or non-fluorinated compounds). The result of this analysis is presented in Table 12.

Table 12. Calculated values of the substituent constants (π_x) for various sugar-coupled 2-nitroimidazoles.

Compound	Substituent	Substituent constant (π_x)
IAZA vs. AZA	I	0.981
IAZG vs. AZG	I	0.911
IAZP vs. AZP	I	0.694
FIAZP vs. FAZP	I	0.615
FIAZP vs. IAZP	F	0.848

The substituent constants of iodine on partition coefficient of IAZA and IAZG are similar (0.98 and 0.91); with IAZP and FIAZP the π_x values are also similar (0.69 and 0.62), although lower than those of IAZA and IAZG (Table 12). The higher π_x values for IAZA and IAZG compared to IAZP and FIAZP are presumably due to the position of iodine atom in the sugar moiety. In case of IAZA/IAZG the iodine is attached at the primary carbon position, while with IAZP/FIAZP it is at a secondary carbon position. The substituent present in the primary position obviously has a greater

influence on partition coefficient than those present at the secondary position.

The fluorine atom in FIAZP, which replaced the hydroxyl group of IAZP at the 2'-arabino position, appears to have greater influence on the lipophilicity than that of iodine at 4' position, although both are attached to a secondary carbon atom. This is apparent in the case of FIAZP vs IAZP, where the π_x for fluorine is 0.85 while with FIAZP vs FAZP, the π_x for iodine is 0.62 (Table 12). The exact reason for this effect is not known. The results thus indicate that the effect of the substituent on the partition coefficients of parent compounds are in order of 1° iodine at 5' or 6' position > 2° iodine at 4' position and 2'-arabino fluorine > 2° iodine at 4'position.

5.2. Phosphorolysis

The *in vitro* phosphorolytic cleavage of the glycosidic bond between the N^1 of 2-nitroimidazole and the sugar moiety of the four major compounds in the series (IAZA, IAZG, IAZP, FIAZP) was studied. The test substrates were incubated with thymidine phosphorylase from *E. coli* as described in Section 3.2.11. All four of these test compounds have demonstrated greater *in vivo* stability than the corresponding analog IAZR (2). It was therefore postulated that the decreased *in vivo* stability of IAZR may be due to the phosphorolytic cleavage of the glycosidic bond.

There exists some precedent for the enzymatic cleavage of glycosidic bonds in sugars coupled with non-physiological nitrogen heterocycles. For example ribavirin (1,2,4, triazole-3-carboxamide-1-ß-D-ribofuranosyl) showed in vivo cleavage of the N^1-glycosidic bond[232]. Although the exact nature of this cleavage remained undetermined, 1,2,4, triazole-3-carboxamide was identified in rat urine, serum, kidney and liver as a major metabolite[232].

In the present study no cleavage of the glycosidic bond was observed for any of the test substrates, for incubation up to 2 h. However, control studies with deoxythymidine and deoxyuridine showed cleavage at 10 and 30 min. of incubation to 35% and 38%, respectively. These results demonstrated that the bacterial pyrimidine phosphorylase was active and that the four test compounds were not substrates for phosphorolytic cleavage by this enzyme preparation. Furthermore, when IAZR was tested, it also did not show any cleavage of the glycosidic bond. The increased in vivo stability of these four compounds compared to IAZR remains unexplained.

5.3. Cytotoxicity

A comparison of cytotoxic effects of the test compounds studied in hypoxic EMT-6 cells is given in Figure 58. The data are presented as the reciprocal of time (hr^{-1}) required to kill 90% of the cells at various substrate concentrations.

Figure 58. Comparison of cytotoxicity, defined as reciprocal of time (hr^{-1}) to kill 90% of the hypoxic EMT-6 cells, as a function of substrate concentration for sugar-coupled 2-nitroimidazoles and reference compounds.

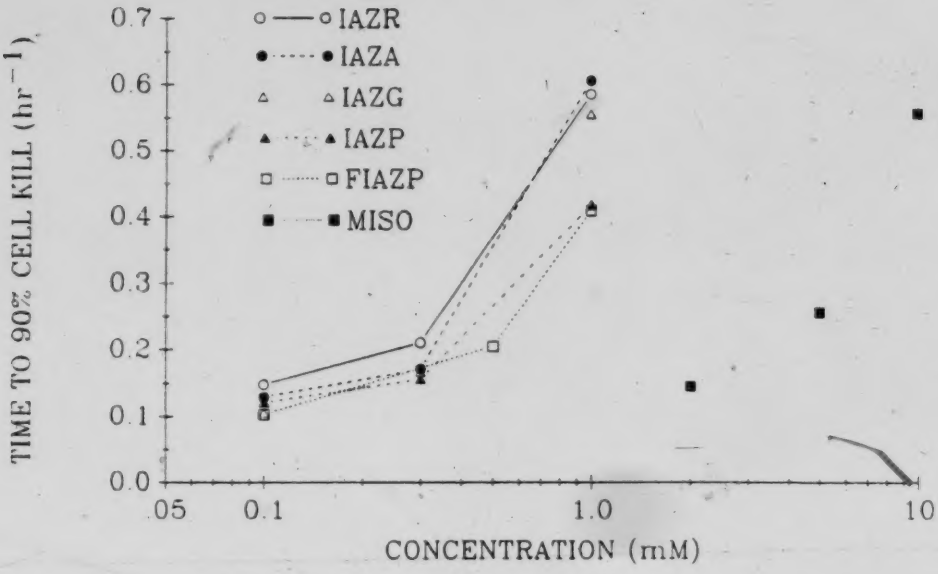

At lower concentrations (0.1 mM) all the compounds (IAZA, IAZG, IAZP, FIAZP) exert approximately similar cytotoxicity to the hypoxic EMT-6 cells. However, at higher concentrations (1.0 mM), IAZA and IAZG showed somewhat greater toxicity than IAZP and FIAZP. The cytotoxic effects of these compounds were in order of IAZA > IAZG > IAZP > FIAZP. In this study IAZA was found to be 1.1, 1.5 and 1.6 times more toxic, respectively, than IAZG, IAZP and FIAZP. However, IAZP and FIAZP showed similar patterns of toxicity at both lower (0.1 mM) and higher (1.0 mM) conentrations.

It appears from these results that partition coefficient values of these compounds have little effect on the *in vitro* cytotoxicity. For example, although FIAZP has a higher P value than the other compounds in the series, it shows the lowest cytotoxicity. To validate this assumption a linear regression analysis was performed for the reciprocal of time (hr^{-1}), at a substrate concentration of 1.0 mM, required for 90% cell kill as a function of their respective P values (Table 13). The analysis yielded correlation coefficients, $r^2 = 0.003$ and $r = 0.05$, which show that for partition coefficient values ranging from 0.57 to 6.26, there was no direct correlation to the cytotoxicity observed in this study with hypoxic EMT-6 cells. However, when the same analysis was done with the non-iodinated compounds (AZA, AZG, AZP, FAZP) (Table 13), the values of r^2 and r were 0.54 and 0.74, respectively, suggesting that for partition coefficients ranging from 0.07 to 1.52 there is some correlation to the observed cytotoxicity.

The cytotoxic effects of these four iodinated compounds are compared to the reference values of IAZR and misonidazole[12] (Figure 58). At lower concentrations (0.1 mM) there is no apparent difference in toxicity between IAZR and four test compounds. However, at higher concentrations (1.0 mM) IAZR is approximately as toxic as IAZA and IAZG and 1.5 to 1.7 times as toxic as IAZP and FIAZP. In comparison to

Table 13. Partition coefficient and cytotoxicity (hr^{-1}) of sugar-coupled 2-nitroimidazols.

compound	P	Cytotoxicity[a]
AZA	0.52	0.102
AZG	0.07	0.156
AZP	0.18	0.126
FAZP	1.52	0.215
IAZA	4.98	0.606
IAZG	0.57	0.555
IAZP	0.89	0.417
FIAZP	6.26	0.409

[a]Cytotoxicity expressed as reciprocal of time (hr^{-1}) required for 90% cell kill at 1.0 mM, for EMT-6 cells in culture.

misonidazole, IAZA and IAZG are at least 10 times, and IAZP and FIAZP about 7 times more toxic. This increased toxicity over misonidazole remains unexplained.

5.4. Radiosensitization

Figure 59 compares the radiosensitizing property of the four iodinated test compounds along with reference compounds. The data are expressed as sensitizer enhancement ratio (SER) against substrate concentrations. The SER values were calculated using hypoxic EMT-6 cells *in vitro* as described in section 4.1.4.

Figure 59. Comparison of sensitizer enhancement ratio as a function of substrate concentration for sugar-coupled 2-nitroimidazoles and reference compounds.

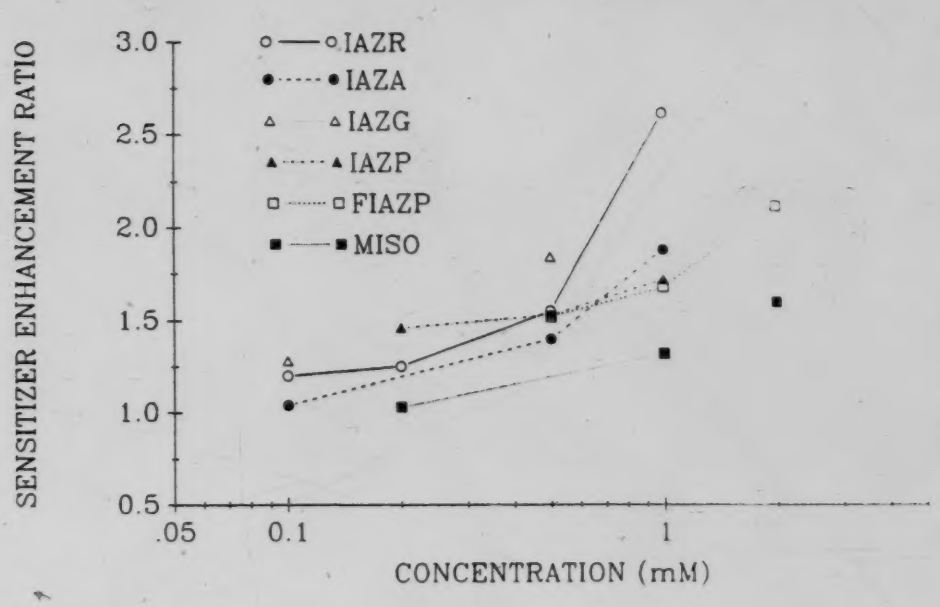

IAZG is the most potent radiosensitizer in the series and is 1.8 times more efficient than IAZA when concentrations of the two were compared to achieve a particular SER. IAZA, IAZP and FIAZP are approximately equipotent radiosensitizer at both lower (0.5 mM) and higher (1.0 mM) concentrations. With increased substrate concentration the increase of SER values for IAZA and IAZG are more prominent than IAZP and FIAZP. Although a relatively sharp rise in SER for FIAZP is observed at 2.0 mM, on a concentration basis to achieve a

particular SER, it is actually 1.5 and 2.6 times less potent than IAZA and IAZG, respectively (Figure 59).

A linear regression analysis was performed to assess the relationship between partition coefficients and SER's of the iodinated and non-iodinated test substrates. The SER's for 90% cell kill at 1.0 mM concentrations were analyzed with the respective partition coefficient values, as shown in Table 14.

Table 14. Partition coefficient and SER of sugar-coupled 2-nitroimidazoles.

Compound	P	SER[a]
AZA	0.52	1.424
AZG	0.07	1.562
AZP	0.18	1.274
FAZP	1.52	1.47
IAZA	4.98	1.88
IAZG	0.57	2.14[b]
IAZP	0.89	1.72
FIAZP	6.26	1.68

[a]Sensitizer enhancement ratio calculated at 90% cell kill of EMT-6 cells in culture, with 1.0 mM test substrates. [b]SER for IAZG at 1.0 mM, was obtained by extrapolation, from the SER vs conc. curve.

The regression analysis yielded correlations of $r^2 = 0.27$ and $r = 0.47$ for iodinated compounds, while the non-iodinated compounds showed a values of $r^2 = 0.35$ and $r = 0.59$.

These suggest that there is a poor correlation between the partition coefficient and the SER's observed in this test system. The non-iodinated compounds are observed to give a better r value than their iodinated counterparts, suggesting again, correlations are stronger at the lower P range.

Table 15. Cytotoxicity and SER of sugar-coupled 2-nitroimidazoles.

Compound	Cytotoxicity[a]	SER[b]
AZA	0.102	1.424
AZG	0.156	1.562
AZP	0.126	1.274
FAZP	0.215	1.47
IAZA	0.606	1.88
IAZG	0.555	2.14[c]
IAZP	0.417	1.72
FIAZP	0.409	1.68

[a]Cytotoxicity expressed as reciprocal of time (hr^{-1}) for 90% cell kill at 1.0 mM. [b]SER for 90% cell kill at 1.0 mM. [c]Extrapolated SER at 1.0 mM IAZG, obtained from SER vs conc. curve.

A linear regression analysis was performed to determine the relationship between SER and cytotoxicity. This analysis was performed with the data shown in Table 15. The regression analysis of the non-iodinated compounds yielded r^2 = 0.18 and r = 0.42, showing poor correlation between cyto-

toxicity and SER. However, the iodinated compounds yielded $r^2 = 0.54$ and $r = 0.73$, indicating that there is some correlation between the SER and cytotoxicity. Similar observations have also been reported for other derivatives of 2-nitroimidazole[12]. However, the factors contributing to the poor correlation between cytotoxicity and SER's obtained with non-iodinated compounds remain undetermined.

The SER values of these iodinated compounds, when compared with the literature values of IAZR and misonidazole under similar test conditions[12], show that on a concentration basis to reach a particular SER, IAZG is at least 1.2 and 4 times more potent a radiosensitizer than IAZR and misonidazole, respectively (Figure 59). IAZA, IAZP and FIAZP, at equimolar concentrations (1.0 mM) are 1.4, 1.5 and 1.6 times less potent than IAZR. However, compared to misonidazole IAZA is 1.4, IAZP is 1.3 and FIAZP is 1.2 times more potent (Figure 59).

5.5. Initial Binding Rate

A comparison of the initial binding rates of radioiodinated IAZA, IAZP and IAZG along with the literature values for IAZR and misonidazole[12], as a function of substrate concentration, is shown in Figure 60. The binding rates were evaluated as the amount (pmol) of the test substrate bound to the acid-insoluble fraction of 10^6 cells (hypoxic EMT-6 cells) per hour. In this study, IAZG demonstrated the

Figure 60. Comparison of initial binding rates of sugar-coupled 2-nitroimidazoles and reference compounds to the acid-insoluble fraction of hypoxic EMT-6 cells plotted as a function of substrate concentration.

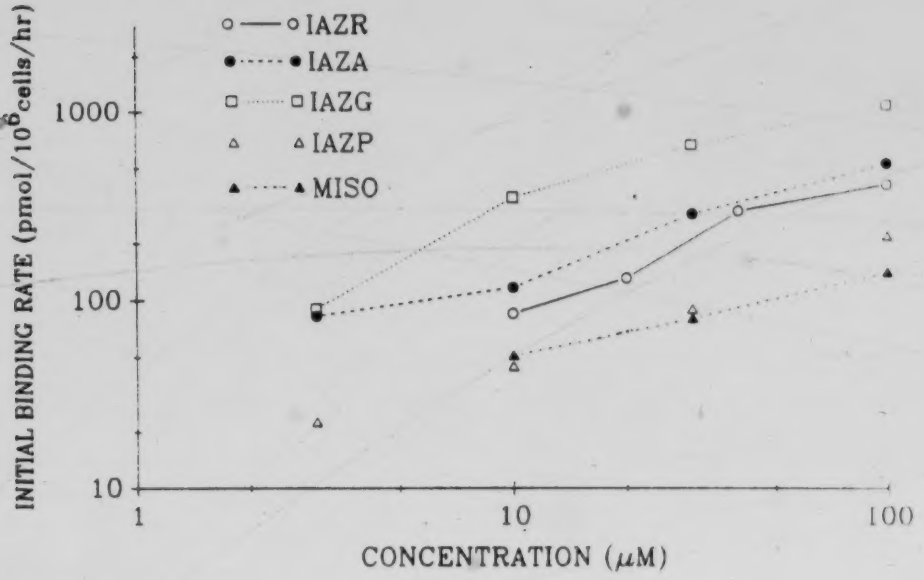

highest binding rate followed by IAZA and then IAZP. The binding rate calculated for IAZG is the highest for any 2-nitroimidazole reported to date. IAZG showed a binding rate 2.8 and 6.8 times higher than that of IAZA and IAZP, respectively, at a concentrations of 100 μM. At lower concentrations (3 μM) both IAZA and IAZG have approximately

similar binding rates. However, with the increase in concentrations, the binding rates for IAZG increase more rapidly than the corresponding IAZA values. IAZP had the lowest binding rate in the series. With increasing concentrations, the binding rate increase for IAZP was similar although lower by an order of magnitude than IAZG (Figure 58).

The dependence of the initial binding rate on partition coefficient and its relationship to cytotoxicity were determined from the data shown in Table 16, using linear regression analysis. The data for cytotoxicity and initial binding rate are at 0.1 mM substrate concentration. The regression analysis relating the binding rate and partition coefficient yielded $r^2 = 0.05$ and $r = 0.23$, showing that there is no correlation between the partition coefficient and in vitro initial binding rate in this test system. However, the regression values for binding rate and cytotoxicity showed $r^2 = 0.6$ and $r = 0.77$, indicating that the cytotoxicity is related to some extent to the binding rate. These data are derived from measurement on only three compounds and should be viewed cautiously.

As compared to misonidazole and IAZR[12], IAZG at equimolar concentration (100 μM) shows 10.5 and 3.6 times higher binding rates, respectively (Figure 60). The binding rate for IAZA over the concentration range between 10 and 100 μM is comparable to that for IAZR and is 2 to 3 times higher

Table 16. Initial binding rate, partition coefficient and cytotoxicity (hr^{-1}) of iodinated sugar-coupled 2-nitroimidazoles.

Compound	Binding rate[a]	P	Cytotoxicity[b]
IAZA	527	4.98	0.129
IAZG	1100	0.57	0.105
IAZP	218	0.89	0.121

[a]Initial binding rate as pmol/10^6 cells/h at 0.1 mM substrate conc. [b]Cytotoxicity as reciprocal of time for 90% cell kill at 0.1 mM substrate conc.

than for misonidazole[12]. IAZP was found to have a binding rate 1.9 times lower than IAZR. However, compared to misonidazole it is at least 1.5 times greater at equimolar concentrations (100 μM).

5.6. Biodistribution

Detailed analyses of biodistribution of the four (radio) iodinated compounds tested are given separately in the previous sections (4.1-4.4). Figure 61 shows the tumor to blood ratio of ^{125}I radioactivity for the four test compounds in the series labelled with ^{125}I, following intravenous (i.v.) injection into Balb/c mice bearing EMT-6 tumors.

All compounds except ^{125}I-IAZG show a gradual increase of tumor to blood ratio of radioactivity up to 8 h after injection. Between 8 and 24 h, both ^{125}I-IAZP and ^{125}I-FIAZP show a further increase in tumor to blood ratio, reaching maximum

Figure 61. Comparison of tumor to blood ratios at various time periods, following i.v. administration of ^{125}I labelled test substrates into Balb/c mice bearing EMT-6 tumors.

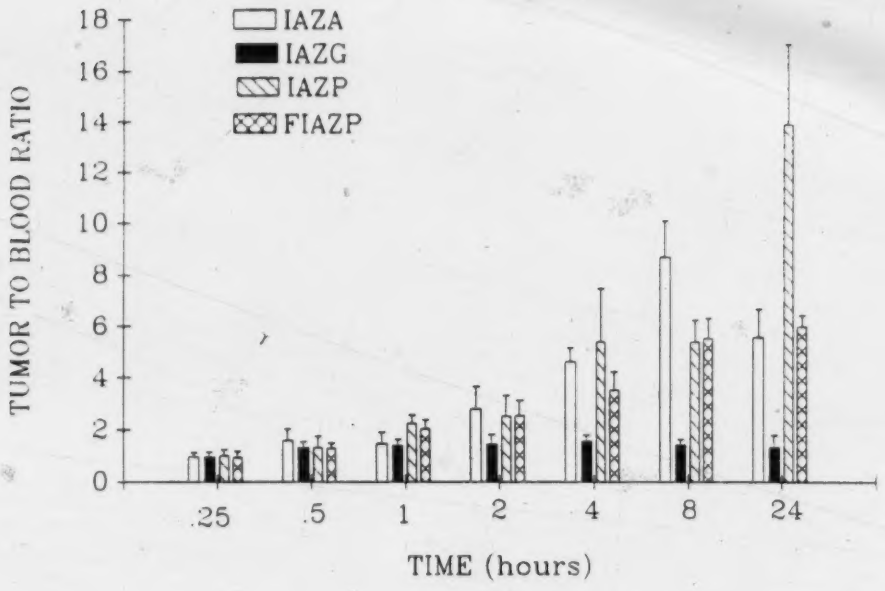

of 13.9 and 6.0, respectively, at 24 h. ^{125}I-IAZA reaches a maximum tumor to blood ratio of 8.7 at 8 h post injection and then drops to 5.8 at 24 h. ^{125}I-IAZG, however, shows approximately constant tumor to blood ratios of 1.5 and 1.3 between 2 and 24 h after administration.

From these data, it appears that IAZP, which shows the highest tumor to blood ratio, would be preferred for non-invasive diagnosis of tissue hypoxia. This compound (IAZP)

also showed greater *in vivo* radiochemical stability (see Table 8). Despite this favourable result, the utility of this compound is restricted at present due to poor radiochemical yield in radioiodination of IAZP. Therefore, the application of IAZP as an *in vivo* marker is dependent upon the development of a radioiodination technique that provides improved radiochemical yield. Apart from IAZP, IAZA was judged to be best compound in the series. The higher tumor to blood ratio compared to IAZG and FIAZP, along with the greater radiolabelling efficiency makes IAZA more promising for non-invasive diagnosis of hypoxic tissue. IAZG, though easy to radiolabel with radioiodine, is not as good as IAZA or IAZP due to the lower tumor to blood ratio observed in the Balb/c - EMT-6 mouse model. FIAZP, despite showing somewhat higher tumor to blood ratio than IAZG, was judged to be least suitable compound in the series for several reasons. In the first instance, no suitable time period was found for imaging tumors, as persistently higher tissue to blood ratios were observed in the biodistribution study (Section 4.4.4). These high tissue levels would interfere in imaging studies. Furthermore, as with IAZP, radioiodination of FIAZP requires improved radiolabelling yields in order that quantities adequate for scintigraphy can be prepared.

6. CONCLUSIONS

The primary objective of research described in this thesis was to evaluate the potential of four, novel, radioiodinated, sugar-coupled 2-nitroimidazoles as non-invasive markers of tumor hypoxia. The *in vitro* and *in vivo* studies reported in the previous chapters have now led to the following conclusions.

1. IAZA and IAZG can be radioiodinated by exchange labelling with high radiochemical yield. Two different methods of radioiodination were investigated. The pivalic acid melt method was preferred due to its shorter reaction time when compared to the solvent exchange method using dimethyl formamide. Radioiodinated IAZP and FIAZP were synthesized by direct radioiodination of their synthetic precursors AZP and FAZP, respectively. Attempts to radioiodinate IAZP and FIAZP by exchange labelling were unsuccessful.
2. In general terms, all of the iodinated and non-iodinated compounds are selectively cytotoxic toward hypoxic EMT-6 cells in culture. In common with a number of other 2-nitroimidazole derivatives, the cytotoxicity increased with the time of incubation and with the substrate concentrations. The iodinated compounds were more lipophilic and more toxic than their non-iodinated

precursors. Among the iodinated compounds, there is no correlation between the cytotoxicity and partition coefficient. IAZA and IAZG are more cytotoxic than the others in the series.

3. Like many 2-nitroimidazole derivatives, all the test compounds have the property of sensitizing hypoxic cells towards the damaging effects of ionizing radiation. The iodinated compounds are more potent radiosensitizers than their non-iodinated counterparts. Radiosensitizing effectiveness depends on the substrate concentrations. The degree of sensitization measured in terms of SER has no correlation with P, but there does appear to be some correlation between SER and cytotoxicity. IAZG is the most potent radiosensitizer in the series. At equimolar concentrations the iodinated analogs studied in this work are uniformly more potent as radiosensitizers than misonidazole.

4. The most unique feature of these compounds (IAZA, IAZG, IAZP) is their hypoxia-selective binding properties. The binding rate increased with the increase of substrate concentrations. At equimolar concentrations the binding rates are 7-30 times higher with hypoxic cells than with aerobic cells. IAZG binding rates are highest in the series and are higher than any 2-nitroimidazole tested to date with EMT-6 cells in culture. The binding rate of these compounds is dependent on the degree of

hypoxia; the rate decreased sharply with an increase in cellular oxygen concentration. This clearly demonstrates the oxygen dependent binding property of the test compounds. There is some relationship between cytotoxicity and binding rate in the in vitro studies, but the binding rate and partition coefficients do not show a direct correlation.

5. In in vivo biodistribution studies with Balb/c mice bearing EMT-6 tumors, IAZP had the highest tumor to blood ratio in the series at 24 hour post injection. This ratio is highest for any 2-nitroimidazole reported to date in studies with this tumor model. IAZA had a relatively high tumor to blood ratio at 8 hour post injection. IAZG had a low but constant ratio up to 24 hours. FIAZP had a higher ratio than IAZG. But at the same time other tissues had a persistently higher ratio than the tumor. In vivo deiodination followed by subsequent accumulation of radioactivity in thyroid was common to all the radioiodinated compounds. However, IAZP and FIAZP were radiochemically much more stable than IAZA and IAZG. All of the four compounds were rapidly eliminated from the body. The renal route is the predominant route for excretion, although liver and subsequent bowel radioactivity noted in the imaging studies suggests that the hepatobiliary route also

contributes. More than 97% of the injected dose was eliminated within 24 hours after injection.

6. Complete delineation of tumor tissue in mice with blocked and unblocked thyroid is possible with IAZA and IAZG labelled with ^{123}I. IAZA scintigrams were in good agreement with the biodistribution data. IAZG scintigrams in mice bearing small tumors were also in good agreement with biodistribution data. However, with large tumors, the level of tumor tissue radioactivity was greater than would be expected from the biodistribution studies.
7. IAZA and IAZP were non-toxic to Balb/c mice at a dosage 100 to 120 times higher than the human dose (mg per kg body weight) anticipated for *in vivo* scintigraphic studies. This suggests that IAZA and IAZP could be employed for *in vivo* scintigraphic studies in human subjects without any toxicity.

These compounds offer the first practical, non-invasive modality for the assessment of tumor hypoxia and they are clearly superior to other compounds investigated for this purpose. Their unique physico-chemical and biological properties along with their hypoxia-selective binding characteristics make these compounds extremely promising for non-invasive diagnosis of tissue hypoxia. These compounds may promise to have a far reaching impact not only for the

detection of tumor hypoxia but also in studies with other compromised tissues such as ischemic myocardium and infarcted brain.

BIBLIOGRAPHY

1. **Dewey, D.L.** "Effect of oxygen and nitric oxide on radiosensitivity of hypoxic cells in tissue culture" Nature 186:780-782, 1960.

2. **Adams, G.E.** "Hypoxic cell sensitizers for radiotherapy" In Cancer, vol.6, Becker, F.F. ed. Plenum Press; New York, London, pp.181-223, 1977.

3. **Brown, J.M.** "Radiosensitizers : Rationale and potential" Cancer Treat. Rep. 65(suppl.2):95-102, 1981.

4. **Emmersion, P.T.** "X-ray damage to DNA and loss of biological function : Effects of sensitizing aspects" In Advances in Radiation Chemistry, vol.3, Burton, M. and Magee, J.L. eds., Wiley; New York, pp.209-282, 1972.

5. **Cooke, B.C., Fielden, E.M., Johnson, M. and Smithen, C.E.** "Polyfunctional radiosensitizers 1. Effects of a nitroxyl biradical on the survival of mammalian cells in vitro" Radiat. Res. 65:152-162, 1976.

6. **Adams, G.E., Ahmed, I., Freiden, E.M., O'Neil, P. and Stratford, I.J.** "The development of some nitroimidazoles as hypoxic cell sensitizers" Cancer Clin. Trials. 3:37-42, 1980.

7. **Shibamoto, Y., Nishimoto, S., Mi, F., Sasi, K., Kagiya, T. and Abe, M.** "Evaluation of various types of new hypoxic cell sensitizers using EMT-6 single cell-spheroid-solid tumor system" Int. J. Radiat. Biol. 52:347-357, 1987.

8. **Chapman, J.D., Baer, K. and Lee, J.** "Characteristics of the metabolism induced binding of misonidazole to hypoxic mammalian cells" Cancer Res. 43:1523-1528, 1983.

9. **Chapman, J.D., Ngan-Lee, J., Stobbe, C.C. and Meeker, B.E.** "Radiation-induced and metabolism-induced reactions of hypoxic sensitizers with cellular molecules" In Advanced Topics on Radiosensitizers of Hypoxic Cells, Breceia, A., Rimondi, C. and Adams, G.E. eds., Plenum Press, New York, pp.91-103, 1983.

10. Chapman, J.D., Franko, A.J. and Sharplin, J. "A marker for hypoxic cells with potential clinical applicability" Br. J. Cancer. 43:546-550, 1981.

11. Wiebe, L.I., Jette, D.C. and Chapman, J.D. "Electron affinic compounds for labelling hypoxic cells : The synthesis and characterization of 1-[2-(2-iodophenoxy)-ethyl]-2-nitroimidazole" Nuklearmedizin 2:63-67, 1984.

12. Jette, D.C., Wiebe, L.I., Flanagan, R.J., Lee, J. and Chapman, J.D. "Iodoazomycin Riboside (1-[5-iodo-5-deoxy-ribofuranosyl]-2-nitroimidazole), a hypoxic cell marker. 1. Synthesis and in vitro characterization" Radiat. Res. 105:169-179, 1986.

13. Wiebe, L.I., Jette, D.C., Chapman, J.D., Flanagan, R.J. and Meeker, B.E. "Iodoazomycin Riboside (1-[5-iodo-5-deoxy-ribofuranosyl]-2-nitroimidazole), a hypoxic cell marker. In vivo evaluation in experimental tumors" Nucl. Med. Clin. Oncology 402-407, 1986.

14. Thomlinson, R.H. and Gray, L.H. "The histologic structure of some human lung cancers and possible implications for radiotherapy". Br. J. Cancer 9:539-549, 1955.

15. Narayan, V.L. and Lee, W.W. "Development of radiosensitizers : A medicinal chemistry perspective" In Advances in Pharmacology and Chemotherapy, Vol.19, Academic Press, pp.155-205, 1982.

16. Brown, J.M. "Evidence for acutely hypoxic cell in mouse tumors and a possible mechanism of reoxygenation" Br. J. Radiol.52:650-656, 1979.

17. Sutherland, R.M. and Franko, A.J. "On the nature of the radiobiologically hypoxic fraction in tumors" Int. J. Radiat. Oncol. Biol. Phys. 6:117-120, 1980.

18. Tannock, I.F. "The relation between cell proliferation and the vascular system in a transplanted mouse mammary tumor" Br. J. Cancer 22:258-273, 1968.

19. Tannock, I.F. "A comparison of cell proliferation parameters in solid and ascites Ehrlich tumors" Cancer Res. 29:1527-1534, 1969.

20. Freyer, J.P. and Sutherland, R.M. "Regulation of growth saturation and development of necrosis in EMT-6/Ro multicellular spheroids by the glucose and oxygen supply" Cancer Res. 46:3504-3512, 1986.

21. **Folkman, J.**"Tumor angiogenesis : A possible control point in tumor growth" Ann. Int. Med. 82:96-100, 1975.

22. **Denekamp, J. and Hobson, B.** "Endothelial-cell proliferation in experimental tumors" Br. J. Cancer. 46:711-720, 1982.

23. **Warren, B.A.** "Tumor blood circulation : Angiogenesis, vascular morphology and blood flow of experimental and human tumors" In The Vascular Morphology of Tumors, Peterson, H.I., ed., CRC Press Inc. Boca Raton, pp.1-47, 1979.

24. **Holthusen, H.** "Bertrage zur biologie der strahlenwirkung" Pfluger's Archiv. fur die Gesante Physiologie 187:1-24, 1921. Cited by **Fowler, J.F.** In "Chemical modifiers of radiosensitivity - Theory and reality : A review" Int. J. Radiat. Oncol. Biol. Phys. 11:665-674, 1985.

25. **Fowler, J.F. and Denekamp, J.** "A review of hypoxic cell radiosensitization in experimental tumor" Pharmacol. Ther. 7:413-444, 1979.

26. **Gray, L.H., Conger, A.D., Ebert, M., Hornsey, S. and Scott, O.A.C.** "Concentration of oxygen dissolved in tissues at time of irradiation as a factor in radiotherapy" Br. J. Radiol. 26:638-648, 1953.

27. **Withers, H.R.** "The four R's of radiotherapy" Adv. Radiat. Biol. 5:241-271, 1975.

28. **Kallman, R.F. and Rockwell, S.** "Effect of radiation on animal tumor" In Cancer, vol. 6, Becker, F.F. ed., Plenum, New York, pp.225-279, 1977.

29. **Van den Break, H.A.** "Hyperbaric oxygen in radiation therapy. An investigation of dose-effect relationship" Amm. J. Roentgen. 102:8-26, 1968

30. **Henk, J.M. and Smith, C.W.** "Radiotherapy and hyperbaric oxygen in head and neck cancer : Interim report of second clinical trial" Lancet. 2:104-105, 1977.

31. **Temper, K.K., Friedman, A.E., Levine, E.M., Lapin, R. and Camarillo, R.N.** "The pre-operative treatment of severely anemic patients with perfluorochemical oxygen-transport fluid, Fluosol-DA" N. Eng. J. Med. 307:277-283, 1982.

32. **Temper, K.K., Lapin, R., Levine, E., Friedman, A. and Shoemaker, W.C.** "Haemodynamic and oxygen transport effect of a perfluorochemical blood substitute, Fluosol-DA (20%)" Crit. Care Med. 8:738-741, 1980.

33. **Rockwell, S.** "Use of perfluorochemical emulsion to improve oxygenation in solid tumor" Int. J. Radiat. Oncol. Biol. Phys. 11:97-103, 1985.

34. **Tercher, B.A. and Rose, C.M.** "Oxygen-carrying perfluorochemical emulsion as an adjuvant to radiation therapy in mice" Cancer Res. 44:4285-4288, 1984.

35. **Hirst, D.G.** "Oxygen delivery to tumors" Int. J. Radiat. Oncol. Biol. Phys. 12:1271-1277, 1986.

36. **Suit, H.D. and Goitein, M.** "Rationale for use of charged-particle and fast-neutron beams in radiation therapy" In Radiation Biology in Cancer Research, Meyn, R.E. and Withers, H.R. eds., Raven Press, New York, pp.547-565, 1980.

37. **Adams, G.E., Asquith, J.C. and Watts, M.E.** "Electron-affinic sensitizers for hypoxic cells irradiated in vitro and in vivo : Current status" In Advances in Chemical Radiosensitization, IAEA STI/PUB/368 Vienna, pp.1-12, 1974.

38. **Bridigs, B.A.** "Sensitization of Escherichia coli to gamma radiation by N-ethylmaleimide" Nature 188:415 (Letter), 1960.

39. **Adams, G.E., Cooke, M.S. and Mitchel, B.D.** "Rapid mixing in radiobiology" Nature 219:1368-1369, 1968.

40. **Parker, L., Skarsgard, L.D. and Emmerson, P.T.** "Sensitization of anoxic mammalian cells by triacetone amine-N-oxyl. Survival and toxicity studies" Radiat. Res. 38:493-500, 1969.

41. **Emmerson, P.T., Fielden, E.M. and Johansen, I.** "A possible steric factor in the sensitization of anoxic bacteria to X-rays by N-oxyl radicals" Int. J. Radiat. Biol. 19:229-236, 1971.

42. **Miller, B.C., Fielden, E.M. and Smithen, C.E.** "Polyfunctional radiosensitizers IV. The effect of contact time and temperature on sensitization of hypoxic chinese hamster cells in vitro by bifunctional nitro oxyl compounds" Br. J. Cancer. 37(suppl.III):73-79, 1978.

43. **Adams, G.E. and Dewey, D.L.** "Hydrated electrons and radiobiological sensitization" Biochem. Biophys. Res. Comm. 12:473-477, 1963.

44. **Adams, G.E. and Cooke, M.S.** "Electron affinic sensitization. I. A structural basis for chemical radiosensitizers in bacteria" Int. J. Radiat. Biol. 15:457-471, 1969.

45. **Asquith, J.C., Adams, G.E. and Wilson, R.L.** "Paranitroacetophenone - an anoxic radiosensitizer for bacterial and mammalian cells" Abstr. IVth Int. Congr. Radiat. Res. #27, pp.11, Evian, France, 1970.

46. **Chapman, J.D., Webb, R.G. and Borsa, J.** "Radiosensitization of mammalian cells by p-nitroacetophenone. I. Characterization in asynchronous and synchronous populations" Int. J. Radiat. Biol. 19:561-573, 1971.

47. **Adams. G.E., Asquith, J.C., Dewey, D.L., Foster, J.L., Michael, B.D. and Wilson, R.L.** "Electron affinic sensitization. II. p-Nitroacetophenone. A radiosensitizer for anoxic bacterial and mammalian cells" Int. J. Radiat. Biol. 19:575-585, 1971.

48. **Chapman, J.D., Raleigh, J.A., Borsa, J., Webb, R.G. and Whitehouse, R.** "Radiosensitization of mammalian cells by p-nitroacetophenone. II. Effectiveness of analogs" Int. J. Radiat. Biol. 21:475-482, 1972.

49. **Berry, J.M. and Asquith, J.C.** "Cell cycle dependent and hypoxic radiosensitizers" In Advances in Chemical Radiosensitization IAEA :STI/PUB/368, Vienna, pp.25-36, 1974.

50. **Adams, G.E.** "Chemical radiosensitization of hypoxic cells" Br. Med. Bull. 29:48-53, 1973.

51. **Reuvers, A.P., Chapman, J.D. and Borsa, J.** "Potential use of nitrofurans in radiotherapy" Nature 237:402-403, 1972.

52. **Chapman, J.D., Reuvers, A.P., Borsa, J., Petkau, A. and McCalla, P.R.** "Nitrofurans as radiosensitizers of hypoxic mammalian cells" Cancer Res. 32:2616-2624, 1972.

53. **Chapman, J.D., Reuvers, A.P. and Borsa, J.** "Effectiveness of nitrofuran derivatives in sensitizing hypoxic mammalian cells to X-rays" Br. J. Radiol. 46:623-630, 1973.

54. **Asquith, J.S., Watts, M.E., Patel, K., Smithen, C.E. and Adams, G.E.** "Electron affinic sensitization. V. Radiosensitization of hypoxic bacteria and mammalian cells in vitro by some nitroimidazoles and nitropyrazoles" Radiat. Res. 60:108-118, 1974.

55. **Raleigh, J.A., Chapman, J.D., Reuvers, A.P., Biaglow, J.E., Durand, R.E. and Rauth, A.M.** "Nitropyrole radiosensitizers : Structure function relationship" Br. J. Cancer. 37(suppl.III):6-10, 1978.

56. **Debus, H.** Ann. 107:199, 1858. Cited by **Hoffman, K.** In The Chemistry of Heterocyclic Compound, Imidazole and its Derivatives, Part-I Weissberger, A. ed., Interscience Inc. New York. pp.127-169, 1953.

57. **Hoffman, K.** "General properties and structure of imidazole" In The Chemistry of Heterocyclic Compound, Imidazole and its Derivatives,Part-I, Weissberger, A. ed., Interscience Inc. New York. pp.127-169, 1953.

58. **Maeda, K., Osato, T. and Umezawa, H.** "A new antibiotic azomycin" J. Antibiotics (Tokyo) Ser.A 6:182-191, 1953.

59. **Beaman, A.G., Tanz, W., Gabriel, T., Keller, O., Toome, V. and Duchinsky, R.** "Studies in the nitroimidazole series, I. Synthesis of azomycin A and related compounds" Antimicrobial agents and chemotherapy 1965:469-477, 1966.

60. **Lancini, G.C. and Lazzari, E.** "The synthesis of azomycin (2-nitroimidazole)" Experimentia 21:83, 1965.

61. **Foster, J.L. and Wilson, R.L.** "Radiosensitization of anoxic cells by metronidazole" Br. J. Radiol. 46:234-235, 1973.

62. **Asquith, J.C., Foster, J.L., Wilson, R.L., Ings, R. and McFadzean, J.A.** "Metronidazole (Flagyl) a radiosensitizer of hypoxic cells" Br. J. Radiol. 47:474-481, 1974.

63. **Rauth, A.M. and Kaufman, K.** "In vivo testing of hypoxic radiosensitizers using KHT murine tumor assayed by the lung colony technique" Br. J. Radiol. 48:209-220, 1975.

64. **Begg, A.C., Sheldon, P.W. and Foster, J.L.** "Demonstration of radiosensitization of hypoxic cells in solid tumors by metronidazole" Br. J. Radiol. 47:399-404, 1974.

65. **Stone, H.B. and Whithers, H.R.** "Tumor and normal tissue response to metronidazole and irradiation in mice" Radiology. 113:441-444, 1974.

66. **Peters, L.J.** "Modification of the radiocurability of a syngeneic murine carcinoma by its site of growth by electron affinic drugs and by ICRF 159" Br. J. Radiol. 49:708-715, 1976.

67. **Sheldon, P.W. and Hill, S.A.** "Hypoxic cell radiosensitizers and local control by X-rays of a transplanted tumor in mice" Br. J. Cancer. 35:795-808, 1977.

68. **Deutsch, G., Foster, J.L., McFadzean, J.A. and Parnell, M.** "Human studies with high dose metronidazole : a non-toxic radiosensitizer of hypoxic cell" Br. J. Cancer. 31:75-80, 1975.

69. **Urtasun, R.C., Band, P., Chapman, J.D., Feldstein, M.L., Mielke, B. and Fryer, C.** "Radiation and high dose metronidazole in supratentorial glioblastomas" N. Eng. J. Med. 294:1364-1367, 1976.

70. **Urtasun, R.C., Chapman, J.D., Band, P., Rabin, H.R., Fryer, C.G. and Sternwind, J.** "Phase I study of high dose metronidazole : A specific in vivo and in vitro radiosensitizer of hypoxic cells" Radiology 117:129-133, 1975.

71. **Denekamp, J. and Harris, S.R.** "Tests of two electron affinic radiosensitizers in vivo using regrowth of an experimental carcinoma" Radiat. Res. 61:191-203, 1975.

72. **Hall, E.J. and Roizen-Towle, L.** "Hypoxic sensitizers : Radiobiological studies at the cellular level" Radiology. 117:453-457, 1975.

73. **Moore, B.A., Palcic, B. and Skarsgard, L.D.** "Radiosensitizing and toxic effects of the 2-nitroimidazole Ro-07-0582 in hypoxic mammalian cells. Radiat. Res. 67:459-473, 1976.

74. **Petersen, E.O.** "Radiosensitizing and toxic effects of the 2-nitroimidazole Ro-07-0582 in different phases of the cell cycle of extremely hypoxic cells in vitro" Radiat. Res. 73:180-191, 1978.

75. **Denekamp, J. and Harris, S.R.** "The response of a transplantable tumor to fractionated irradiation. I. X-rays and the hypoxic cell radiosensitizer Ro-07-0582" Radiat. Res. 66:66-75, 1976.

76. **Fowler, J.F. and Denekamp, J.** "A review of hypoxic cell radiosensitization in experimental tumors" Pharmacol. Ther. 7:413-444, 1979.

77. **Dische, S., Gray, A.J. and Zanelli, G.D.** "Clinical testing of radiosensitizer Ro-07-0582. II. Radiosensitization of normal and hypoxic skin" Clin. Radiol. 27:159-166, 1976.

78. **Gray, A.J., Dische, S., Adams, G.E., Flockhart, I.R. and Foster, J.L.** "Clinical testing of the radiosensitizer Ro-07-0582. I. Dose tolerance, serum and tumor concentration" Clin. Radiol. 27:151-157, 1976.

79. **Thomlinson, R.H., Dische, S., Gray, A.J. and Errington, L.M.** "Clinical testing of the radiosensitizer Ro-07-0582. III. Response to tumors" Clin. Radiol. 27:167-174, 1976.

80. **Urtasun, R.C., Band, P., Chapman, J.D., Rabin, H.R., Wilson, A.F. and Fryer, C.G.** "Clinical phase I study of the hypoxic cell radiosensitizer, Ro-07-0582, a 2-nitroimidazole derivative" Radiobiology 122:801-804, 1977.

81. **Urtasun, R.C., Chapman, J.D., Feldstein, M.L., Band, R.P., Rabin, H.R., Wilson, A.F., Marynowski, B., Starreveld, E. and Shnitka, T.** "Peripheral neuropathy related to misonidazole : Incidence and pathology" Br. J. Cancer. 37 (suppl. III):271-275, 1978.

82 **Saunders, M.I., Dische, S., Anderson, P., Flockhart, I.R.** "The neurotoxicity of misonidazole and its relationship to dose, half life and concentration in the serum" Br. J. Cancer. 37 (suppl. III):268-270, 1978.

83. **Thomas, G., Rauth, A.M., Bush, R., Black, B. and Cummings, B.** "A toxicity study of daily dose misonidazole with pelvic irradiation" Cancer. Clin. Trials. 3:223-230, 1980.

84. **Wasserman, T.H., Stetz, J. and Phillips, T.L.** "Clinical trials of misonidazole in the United States" Cancer. Clin. Trials. 4:7-16, 1981.

85. **Dische, S., Saunders, M.I., Lee, M.E., Adams, G.E. and Flockhart, I.R.** "Clinical testing of the radiosensitizer Ro-07-0582 : Experience with multiple doses" Br. J. Cancer. 35:567-579, 1977.

86. **Brown, J.M.** "The mechanism of cytotoxicity and chemosensitization by misonidazole and other nitroimidazoles" Int. J. Radiat. Oncol. Biol. Phys. 8:675-682, 1982.

87. **Stratford, I.J.** "Mechanism of hypoxic cell radiosensitization and development of new sensitizers" Int. J. Radiat. Oncol. Biol. Phys. 8:391-398, 1982.

88. **Brodie, B.B.** "Physico-chemical factors in drug absorption" In Absorption and distribution of drugs Binns, T.B. ed., Livingstone Ltd., Edinburgh and London, pp.16-48, 1964.

89. **Cohn, V.H.** "Transmembrane movement of drug molecules" In Fundamentals of Drug Metabolism and Disposition La Du, B.N., Mandel, H.G. and Way, E.L. eds.,Williams and Wilkins Co., Weaverly Press Inc. Baltimore, U.S.A., pp.3-18, 1971.

90. **Adams, G.E., Flockhart, I.R., Smithen, C.E., Stratford, I.J., Wardman, P. and Watts, M.E.** "Electron affinic sensitization VII. A correlation between structures, one-electron reduction potentials and efficiencies of nitroimidazoles as hypoxic cell radiosensitizers" Radiat. Res. 67:9-20, 1976.

91. **Agrawal, K.C., Miller, B.C. and Neta, P.** "Radiosensitization of hypoxic mammalian cells by dinitroimidazoles" Radiat. Res. 78:532-541, 1979.

92. **Agrawal, K.C.** "Development of a new radiosensitizer, 2,4, dinitroimidazole-1-ethanol (KA 161)" In Abstracts, 7th Int. Cong. of Pharmacol. pp.253 (Abs.# 643) Pergamon, London/New York, 1978.

93. **Adams, G.E., Clarke, E.D., Flockhart, I.R., Jacobs, R.S., Sehmi, D.S., Stratford, I.J., Wardman, P., Watts, M.E., Parrick, J., Wallace, R.G. and Smithen, C.E.** "Structure-activity relationships in the development of hypoxic cell radiosensitizers. I. Sensitization efficiency" Int. J. Radiat. Biol. 35:133-150, 1979.

94. **Adams, G.E., Clarke, E.D., Gray, P., Jacobs, R.S., Stratford, I.J., Wardman, P., Watts, M.E., Parrick, J., Wallace, R.G. and Smithen, C.E.** "Structure-activity relationships in the development of hypoxic cell radiosensitizers. II. Cytotoxicity and therapeutic ratio" Int. J. Radiat. Biol. 35:151-160, 1979.

95. **Adams, G.E., Fielden, E.M., Hardy, C., Miller, B.C., Stratford, I.J. and Williamson, C.** "Radiosensitization of hypoxic mammalian cells in vitro by some 5-substituted-4-nitroimidazoles" Int. J. Radiat. Biol. 40:153-161, 1981.

96. **Adams, G.E., Stratford, I.J., Wallace, R.G., Wardman, P. and Watts, M.E.** "Toxicity of nitrocompounds toward hypoxic mammalian cells in vitro : Dependence on reduction potential" J. Natl. Cancer. Inst. 64:555-560, 1980.

97. **Brown, D.M., Parker, E. and Brown, J.M.** "Structure-activity relationships of 1-substituted-2-nitroimidazoles : Effect of partition coefficient and side chain hydroxyl groups on radiosensitization in vitro" Radiat. Res. 90:98-108, 1982.

98. **Brown, J.M. and Lee, W.W.** "Pharmacokinetic considerations in radiosensitizer development" In Radiation Sensitizers : Their use in the Clinical Management of Cancer Brady, L.W. ed., Masson Publishing Co. New York, New York, pp.2-13, 1980.

99. **McNally, N.J., Denekamp, J., Sheldon, P.W., Flockhart, I.R. and Stewart, F.A.** "Radiosensitization by misonidazole (Ro-07-0582) : The importance of timing and tumor concentration of sensitizer" Radiat. Res. 73:568-580, 1978.

100. **White, R.A.S., Workman, P. and Brown, J.M.** "Pharmacokinetics and tumor and neural tissue penetrating property of SR-2508 and SR-2555 in the dog - hydrophillic radiosensitizers potentially less toxic than misonidazole" Radiat. Res. 84:542-561, 1980.

101. **Soloway, A.H.** "Correlation of drug penetration of brain and chemical structure" Science 128:1572-1574, 1958.

102. **Soloway, A.H., Whitman, B. and Meser, J.R.** "Penetration of brain and brain tumor by aromatic compounds as a function of molecular substituents" J. Pharmacol. Exp. Ther. 129:310-314, 1960.

103. **Brown, J.M., Yu, N.Y., Brown, M.D. and Lee, W.W.** "SR-2508 : A 2-nitroimidazole amide which should be superior to misonidazole as a radiosensitizer for clinical use" Int. J. Radiat. Oncol. Biol. Phys. 7:695-703, 1981.

104. **Brown, J.M. and Workman, P.** "Partition coefficient as a guide to the development of radiosensitizers which are less toxic than misonidazole" Radiat. Res. 82:171-190, 1980.

105. **White, R.A., Brown, J.M. and Workman, P.** "The pharmacokinetics of misonidazole and other potentially-superior radiosensitizing drugs in the dog" In Radiation Sensitizers : Their use in Clinical Management of Cancer Brady, L.W. ed., Masson Publishing Co. New York, New York. pp.262-266, 1980.

106. **Smithen, C.E., Clarke, E.D., Dale, J.A., Jacobs, R.S., Wardman, P., Watts, M.E. and Woodcock, M.** "Novel (nitro-1-imidazolyl) alkanolamines as potential radiosensitizers with improved therapeutic properties" In Radiation Sensitizers : Their Use in the Clinical Management of Cancer Brady, L.W. ed., Masson Publishing Inc. New York, New York, pp.22-32, 1980.

107. **Williams, M.V., Denekamp, J., Minchinton, A. and Stratford, M.R.L.** "In vivo assessment of basic 2-nitroimidazole radiosensitizers" Br. J. Cancer. 46:127-137, 1982.

108. **Shibamoto, Y., Nishimoto, S., Shimokawa, K., Hisanaga, Y., Zhon, L., Wang, J. Sasai, K., Takashi, M., Abe, M. and Kagiya, T.** "Characteristics of fluorinated nitroazoles as hypoxic cell radiosensitizers" Int. J. Radiat. Oncol. Biol. Phys. 16:1045-1048, 1989.

109. **Hori, H., Murayma, C., Mori, T., Shibamoto, Y., Abe, M., Onoyama, Y. and Inayama, S.** "KIH-802 : 2-nitroimidazole-1-acetohydroxamate as a hypoxic cell radiosensitizer" Int. J. Radiat. Oncol. Biol. Phys. 16:1029-1032, 1989.

110. **Pederson, J.E., Barron, G. and Chapman, J.D.** "Azomycin riboside : A new radiosensitizer" Int. J. Radiat. Oncol. Biol. Phys. 8:415-418, 1982.

111. **Murayama, C., Tanaka, N., Miyamoto, Y., Sakaguchi, M. and Mori, T.** "In vitro and in vivo radiosensitizing effects of 2-nitroimidazole derivative with sugar component" Strahlen Ther-Onkol. 163:385-390, 1987.

112. **Jarvis, S.M., Chapman, J.D., Lee, J.N., Rutledge, K.A., Barr, P.J. and Peterson, A.R.P.** "Azomycin riboside, a sugar homologue of misonidazole with favourable radiosensitizing properties" Cancer Res. 42:4358-4363, 1982.

113. **Sakaguchi, M., Webb, M.W. and Agrawal, K.C.** "Potential radiosensitizing agents. 4. 2-Nitroimidazole nucleosides" J. Med. Chem. 25:1339-1342, 1982.

114. **Sakaguchi, M., Larroquette, C.A. and Agrawal, K.C.** "Potential radiosensitizing agents. 6. 2-Nitroimidazole nucleosides : Arabinofuranosyl and hexapyranosyl analogues" J. Med. Chem. 26:20-24, 1983.

115. **Brown, J.M.** "Key note address : Hypoxic cell radiosensitizers: Where next?" Int. J. Radiat. Oncol. Biol. Phys. 16:987-993, 1989.

116. **Varghese, A.J., Gulyas, S. and Mohindra, J.K.** "Hypoxia-dependent reduction of 1-(2-nitro-1-imidazolyl)-3-methoxy-2-propanol by chinese hamster ovary cells and KHT tumor cells in vitro and in vivo" Cancer Res. 36:3761-3765, 1976.

117. **Wang, C.Y., Behrens, S. Ichikawa, M. and Bryan, G.T.** "Nitroreduction of 5-nitrofuran derivatives by rat liver xanthine oxidase and reduced nicotinamide adenine dinucleotide phosphate-cytochrome c reductase" Biochem. Pharmacol. 23:3395-3404, 1974.

118. **Josephy, P.D., Palcic, B. and Skarsgard, L.D.** "Reduction of misonidazole and its derivatives by xanthine oxidase" Biochem. Pharmacol. 30:849-853, 1981.

119. **Edwards, D.I.** "Reduction of nitroimidazoles in vitro and DNA damage" Biochem. Pharmacol. 35:53-58, 1986.

120. **Rauth, A.M.** "Pharmacology and toxicology of sensitizers: Mechanism studies" Int. J. Radiat. Oncol. Biol. Phys. 10:1293-1300, 1984.

121. **Smith, B.R. and Born, J.L.** "Metabolism and excretion of [^{3}H]-misonidazole by hypoxic rat liver" Int. J. Radiat. Oncol. Biol. Phys. 10:1365-1370, 1984.

122. **Koch, R.L., Rose, C., Rich, T.A. and Goldman, P.** "Comparative misonidazole metabolism in anaerobic bacteria and hypoxic chinese hamster lung fibroblast (V-79-473) cells" Biochem. Pharmacol. 31:411-414, 1982.

123. **Koch, R.L., Beaulieu, B.B. and Goldman, P.** "Role of intestinal flora in the metabolism of misonidazole" Biochem. Pharmacol. 29:3281-3284, 1980.

124. **Franko, A.J.** "Misonidazole and other hypoxic markers : Metabolism and applications" Int. J. Radiat. Oncol. Biol. Phys. 12:1195-1202, 1986.

125. **Mason, R.P. and Holztman, J.L.** "The role of catalytic super oxide formation in the O_2 inhibition of nitroreductase" Biochem. Biophys. Res. Comm. 67:1267-1274, 1975.

126. **Sealy, R.C., Swartz, H.M. and Olive, P.** "Electron spin resonance-spin trapping. Detection of super oxide formation during aerobic microsomal reduction of nitrocompounds" Biochem. Biophys. Res. Comm. 82:680-684, 1978.

127. **Perez-Rayes, E., Kalyanaraman, B. and Mason, R.P.** "The reduction metabolism of metronidazole and ronidazole by aerobic liver microsomes" Mol. Pharmacol. 17:239-244, 1980.

128. **Ings, R.M.J., McFadzean, J.A. and Ormerod, W.E.** "The mode of action of metronidazole in trichomonas vaginalis and other micro organisms" Biochem. Pharmacol. 23:1421-1429, 1974.

129. **Gowrisankar, I.C.R., Phadke, R.P., Oza, S.D. and Talwalker, S.** "Satranidazole : Experimental evaluation of activity against anaerobic bacteria in vitro and in animal models of anaerobic infection" J. Antimicrob. Chemother. 15:463-470, 1985.

130. **Rauth, A.M., McClelland, R.A., Michaels, H.B. and Batistella, R.** "The oxygen dependence of the reduction of nitroimidazoles in a radiolytic model system" Int. J. Radiat. Oncol. Biol. Phys. 10:1323-1326, 1984.

131. **Walton, M.I. and Workman, P.** "Nitroimidazole bioreductive metabolism: Quantitation and characterization of mouse tissue benznidazole nitroreductase in vivo and in vitro " Biochem. Pharmacol. 36:887-896, 1987.

132. **Raleigh, J.A. and Liu, S.F.** "Reductive fragmentation of 2-nitroimidazoles in the presence of nitroreductase - glyoxal formation from misonidazole" Biochem. Pharmacol. 32:1444-1446, 1983.

133. **Raleigh, J.A. and Liu, S.F.** "Reductive fragmentation of 2-nitroimidazoles : Amine and aldehydes" Int. J. Radiat. Oncol. Biol. Phys. 10:1337-1340, 1984.

134. **Knox, R.J., Knight, R.C. and Edwards, D.I.** "Studies on the action of the nitroimidazole drugs. The production of nitroimidazole reduction" Biochem. Pharmacol. 32:2149-2156, 1983.

135. **McClelland, R.A., Fuller, J.R. and Seaman, N.F.** "2-Hydroxyaminoimidazoles - Unstable intermediates in the reduction of 2-nitroimidazoles" Biochem. Pharmacol. 33:303-309, 1984.

136. **Varghese, A.J. and Whitmore, G.F.** "Detection of a reactive metabolite of misonidazole in CHO cells" Radiat. Res. 97:262-271, 1984.

137. **Varghese, A.J. and Whitmore, G.F.** "Detection of a reactive metabolite of misonidazole in human urine" Int. J. Radiat. Oncol. Biol. Phys. 10:1361-1363, 1984.

138. **Panicucci, R., McClelland, R.A. and Rauth, M.** "Stable reduction product of misonidazole" Int. J. Radiat. Oncol. Biol. Phys. 12:1227-1230, 1986.

139. **Goldman, P., Koch, R.L., Yeung, Tin-chuen., Chrystal, E.J.T., Beulieu, B.B., McLafferty, M.A. and Sheldon, G.** "Comparing the reduction of nitroimidazoles in bacteria and mammalian tissues and relating it to biological activity" Biochem. Pharmacol. 35:43-51, 1986.

140. **Smith, B.R., Born, J.L. and Garcia, D.J.** "Influence of hypoxia on the metabolism and excretion of misonidazole by isolated perfused rat liver - A model system" Biochem. Pharmacol. 32:1609-1612, 1983.

141. **Josephy, P.D., Palcic, B. and Skarsgard, L.D.** "In vitro metabolism of misonidazole" Br. J. Cancer. 43:443-450, 1981.

142. **Varghese, A.J.** "Glutathione conjugates of misonidazole" Biochem. Biophys. Res. Comm. 112:1013-1020, 1983.

143. **Varghese, A.J. and Whitmore, G.F.** "Misonidazole-glutathione conjugates in CHO cells" Int. J. Radiat. Oncol. Biol. Phys. 10:1341-1345, 1984.

144. **LaRusso, N.F., Lindmark, D.G. and Miller, M.** "Billiary and renal excretion, hepatic metabolism and hepatic subcellular distribution of metronidazole in rat" Biochem. Pharmacol. 27:2247-2254, 1978.

145. **Shoemaker, D.D., McManus, M.E., Hoerauf, R. and Strong, J.M.** "Studies on the O-demethylation of misonidazole by rat liver microsomes" Cancer. Treat. Rep. 66:1343-1347, 1982.

146. **Chin, J.B. and Rauth, A.M.** "The metabolism and pharmacokinetics of the hypoxic cell radiosensitizer and cytotoxic agent, misonidazole, in C3H mice" Radiat. Res. 86:341-357, 1981.

147. **Flockhart, J.R., Sheldon, P.W., Stratford, I.J. and Watts, M.E.** "A metabolite of the 2-nitroimidazole misonidazole with radiosensitizing properties" Int. J. Radiat. Biol. 34:91-94, 1978.

148. **Marques, R.A., Stratford, B., Flynn, N. and Sadee, W.** "Determination of metronidazole and misonidazole and their metabolites in plasma and urine by high performance liquid chromatography" J. Chromat. 146:163-166, 1978.

149. **Biaglow, J.E.** "Cellular electron transfer and radical mechanisms for drug metabolism" Radiat. Res. 86:212-242, 1981.

150. **Kappus, H.** "Overview of enzyme systems involved in bioreduction of drugs and in redox cycling" Biochem. Pharmacol. 35:1-6, 1986.

151. **Reed, D.J.** "Regulation of reductive processes by glutathione" Biochem. Pharmacol. 35:7-13, 1986.

152. **Jones, D.P., Eklow, L., Thor, H. and Orrenius, S.** "Metabolism of hydrogen peroxide in isolated hepatocytes: Relative contributions of catalase and glutathione peroxidase in decomposition of endogenously generated H_2O_2" Archs. Biochem. Biophys. 210:505-516, 1981.

153. **Sies, H. and Moss, K.M.** "A role of mitochondrial glutathione peroxidase in modulating mitochondrial oxidation in liver" Eur. J. Biochem. 84:377-383, 1978.

154. Biaglow, J.E., Varnes, M.E., Roizen-Towle, L., Clark, E.P., Epp, E.R., Astor, M.B. and Hall, E.J. "Biochemistry of reduction of nitro heterocycles" Biochem. Pharmacol. 35:77-90, 1986.

155. Varnes, M.E. and Biaglow, J.E. "Misonidazole-induced biochemical alterations of mammalian cells : Effects on glycolysis" Int. J. Radiat. Oncol. Biol. Phys. 8:683-686, 1982.

156. Whitmore, G.E. and Varghese, A.J. "The biological properties of reduced nitroheterocycles and possible underlying biochemical mechanisms" Biochem. Pharmacol. 35:97-103, 1986.

157. Biaglow, J.E. "The effect of hypoxic cell radiosensitizing drugs on cellular oxygen utilization" Pharmac. Ther. 10:283-299, 1980.

158. Biaglow, J.E., Jacobson, B., Greenstock, C.L. and Raleigh, J. "Effect of nitrobenzene derivatives on electron transfer in cellular and chemical models" Mol. Pharmacol. 13:269-282, 1977.

159. Heinbrook, D.C. and Sartorelli, A.C. "Biochemistry of misonidazole reduction by NADPH-cytochrome c (P-450) reductase" Mol. Pharmacol. 29:168-172, 1986.

160. Cater, D.B. and Silver, I.A. "Quantitative measurements of oxygen tension in normal tissues and in tumors of patients before and after radiotherapy" Acta. Radiol. 53:233-256, 1960.

161. Cater, D.B., Shoeninger, E.L. and Watkenson, D.A. "Effect of oxygen tension of tumors of breathing oxygen at high pressures" Lancet 2:381-383, 1962.

162. Jamieson, D. and Van Den Brenk, H.A.S. "Comparison of oxygen tensions in normal tissues and Yoshida sarcoma of the rat breathing air or oxygen at 4 atmospheres" Br. J. Cancer. 17:70-79, 1963.

163. Powers, W.E. and Tolmach, L.J. "A multicomponent X-ray survival curve for mouse lymphosarcoma cells irradiated in vivo" Nature 197:710-711, 1963.

164. Hewitt, H.B. and Wilson, C.W. "The effect of tissue oxygen tension on the radiosensitivity of leukaemia cells irradiated in situ in the livers of leukaemic mice" Br. J. Cancer. 13:675-684, 1959.

165. **Van Putten, L.M. and Kallman, R.F.** "Oxygenation status of a transplantable tumor during fractioned radiation therapy" J. Natl. Cancer. Inst. 40:441-451, 1968.

166. **Howes, A.E.** "An estimation of changes in the proportions and absolute numbers of hypoxic cells after irradiation of transplanted C3H mouse mammary tumors" Br. J. Radiol. 42:441-447, 1969.

167. **Thomlinson, R.H. and Craddock, E.A.** "The gross response of an experimental tumor to single doses of X-rays" Br. J. Cancer. 21:108-123, 1967.

168. **Moulder, J.E. and Rockwell, S.** "Hypoxic fractions of solid tumors : Experimental techniques, methods of analysis, and a survey of existing data" Int. J. Radiat. Oncol. Biol. Phys. 10:695-712, 1984.

169. **Grunewald, W.A. and Luebbers, D.W.** "Cryophotometry as a method for analyzing the intracapillary HbO_2 saturation of organs under different O_2 supply conditions" Adv. Exp. Med. Biol. 75:55-64, 1976.

170. **Olive, P.L. and Durand, R.E.** "Fluorescent nitroheterocycles for identifying hypoxic cells" Cancer Res. 43:3276-3280, 1983.

171. **Mueller-Klieser, W., Vaupel, P., Manz, R. and Schmidseder, R.** "Intracapillary oxyhemoglobin saturation of malignant tumors in humans" Int. J. Radiat. Oncol. Biol. Phys. 7:1397-1404, 1981.

172. **Chapman, J.D.** "The detection and measurement of hypoxic cells in solid tumors" Cancer 54:2441-2449, 1984.

173. **Chapman, J.D., Franko, A.J. and Koch, C.J.** "The fraction of hypoxic clonogenic cells in tumor populations" In Biological Bases and Clinical Implications of Tumor Radioresistance Fletcher, G.H., Nervi, E. and Withers, H.R. eds., Masson Pub. Inc., New York, pp.61-73, 1983.

174. **Chapman, J.D., Baer, K. and Lee, J.** "Characteristics of the metabolism-induced binding of misonidazole to hypoxic mammalian cells" Cancer Res. 43:1523-1528, 1983.

175. **Franko, A.J. and Chapman, J.D.** "Binding of ^{14}C-misonidazole to hypoxic cells in V79 spheroids" Br. J. Cancer. 51:229-235, 1985.

176. **Franko, A.J., Chapman, J.D. and Koch, A.J.** "Binding of misonidazole to EMT-6 and V79 spheroids" Int. J. Radiat. Oncol. Biol. Phys. 8:737-739, 1982.

177. **Miller, G.G., Ngan-Lee, J. and Chapman, J.D.** "Intracellular localization of radioactively-labelled misonidazole in EMT-6 tumor cells in vitro" Int. J. Radiat. Oncol. Biol. Phys. 8:741-744, 1982.

178. **Raleigh, J.A., Franko, A.J., Koch, C.J. and Born, J.L.** "Binding of misonidazole to hypoxic cells in monolayer and spheroid culture : Evidence that a side-chain label is bound as effectively as a ring label" Br. J. Cancer. 51:229-235, 1985.

179. **Garrecht, B.M. and Chapman, J.D.** "The labelling of EMT-6 tumors in Balb/c mice with ^{14}C-misonidazole" Br. J. Radiol. 56:745-753, 1983.

180. **Franko, A.J. and Garrecht, B.M.** "Misonidazole retention by normal tissues : A distinction between label on ring and side chain" Int. J. Radiat. Oncol. Biol. Phys. 12:1259-1262, 1986.

181. **Horowitz, M., Blasberg, R., Molnar, P., Strong, J., Kornblith, P., Pleasants, R. and Fenstermacher, J.** "Regional ^{14}C-misonidazole distribution in experimental RT-9 brain" Cancer Res. 43:3800-3807, 1983.

182. **Urtasun, R.C., Koch, C.J., Franko, A.J., Raleigh, J.A. and Chapman, J.D.** "A novel technique for measuring human tissue pO_2 at the cellular level" Br. J. Cancer. 54:453-457, 1986.

183. **Urtasun, R.C., Chapman, J.D., Raleigh, J.A., Franko, A.J. and Koch, C.J.** "Binding of ^{3}H-misonidazole to solid human tumors as a measure of tumor hypoxia" Int. J. Radiat. Oncol. Biol. Phys. 12:1263-1267, 1986.

184. **Rasey, J.S., Hoffman, J.M., Spence, A.M. and Krohn, K.A.** "Hypoxia mediated binding of misonidazole in non-malignant tissue" Int. J. Radiat. Oncol. Biol. Phys. 12:1255-1258, 1986.

185. **Rasey, J.S., Krohn, K.A. and Freauff, S.J.** "Bromomisonidazole: Synthesis and characterization of a new radiosensitizer" Radiat. Res. 91:542-554, 1982.

186. **Jette, D.C., Wiebe, L.I. and Chapman, J.D.** "Synthesis and in vivo studies of the radiosensitizer 4-[^{82}Br]-bromomisonidazole" Int. J. Nucl. Med. Biol. 10:205-210, 1983.

187. **Graunbaum, Z., Freauff, S.J., Krohn, K.A., Wilbur, D.S., Magee, S. and Rasey, J.S.** "Synthesis and characterization of congeners of misonidazole for imaging hypoxia" J. Nucl. Med. 28:68-75, 1987.

188. **Rasey, J.S., Graunbaum, Z., Magee, S., Nelson, N.J., Olive, P.L., Durand, R.E. and Krohn, K.A.** "Characterization of radiolabelled fluoromisonidazole as a probe for hypoxic cells" Radiat. Res. 111:292-304, 1987.

189. **Raleigh, J.A., Franko, A.J., Treiber, E.O., Lunt, J.A. and Allen, P.S.** "Covalent binding of a fluorinated 2-nitroimidazole to EMT-6 tumors in Balb/c mice : Detection by F-19 nuclear magnetic resonance at 2.35 T" Int. J. Radiat. Oncol. Biol. Phys. 12:1243-1245, 1986.

190. **Rasey, J.S., Kon, Wui-Jim., Grierson, J.R., Graunbaum, Z. and Krohn, K.A.** "Radiolabelled fluoromisonidazole as an imaging agent for tumor hypoxia" Int. J. Radiat. Oncol. Biol. Phys. 17:985-991, 1989.

191. **Chapman, J.D., Lee, J. and Meeker, B.E.** "Keynote address : Cellular reduction of nitroimidazole drugs; Potential for selective chemotherapy and diagnosis of hypoxic cells" Int. J. Radiat. Oncol. Biol. Phys. 16:911-917, 1989.

192. **Jerabek, P.A., Patrick, T.B., Kilbourn, M.R., Dischino, D.D. and Welch, M.J.** "Synthesis and biodistribution of ^{18}F-labeled fluoronitroimidazoles : Potential in vivo markers of hypoxic tissue" Appl. Radiat. Isot. 37:599-605, 1986.

193. **Shelton, M.E., Dence, C.S., Hwang, D.R., Welch, M.J. and Bergman, S.R.** "Myocardial kinetics of fluorine-18 misonidazole : A marker of hypoxic myocardium" J. Nucl. Med. 30:351-358, 1989.

194. **Hwang, D.R., Dence, C.S., Bonasera, T.A. and Welch, M.J.** "No-carrier-added synthesis of 3-[^{18}F]-fluoro-1-[2-nitro-1-imidazolyl]-2-propanol. A potential PET agent for detecting hypoxic but viable tissues" Appl. Radiat. Isot. 40:117-126, 1989.

195. **Maxwell, R.J., Workman, P. and Griffiths, J.R.** "Demonstration of tumor-selective retention of fluorinated nitroimidazole probes by ^{19}F magnetic resonance spectroscopy by in vivo" Int. J. Radiat. Oncol. Biol. Phys. 16:925-929, 1989.

196. **Mercer, J.R., Wiebe, L.I. and Chapman, J.D.** "Non-invasive probes of tissue hypoxia : Synthesis, radiolabelling and evaluation of hydroxy acetophenone derivatives of 2-nitroimidazole" Nuc Compact - Eur/Amer. Commun. Nuc. Med. 1991 (in press).

197. **Mannan, R.H., Somayaji, V.V., Lee, J., Mercer, J.R., Chapman, J.D. and Wiebe, L.I.** "Radioiodinated 1-(5-iodo-5-deoxy-ß-D-arbinofuranosyl)-2-nitroimidazole (Iodoazomycin Arabinoside: IAZA), a novel marker of tissue hypoxia" J. Nucl. Med. 1991 (in press).

198. **Ness, R.K. and Fletcher, H.G. Jr.** "The anomeric 2,3,5-tri-O-benzoyl-D-arabinosyl bromides and other D-arabinofuranose derivatives" J. Amer. Chem. Soc. 80:2007-2010, 1958.

199. **Write, R.S. and Khorana, H.G.** "Phosphorylated sugars. V. Syntheis of arabinofuranose and arabinopyranose 1-phosphates" J. Amer. Chem. Soc. 80:1994-1998, 1958.

200. **Mercer, J.R., Mannan, R.H., Somayaji, V.V., Lee, J., Chapman, J.D. and Wiebe, L.I.** "Sugar-coupled 2-nitroimidazoles: Novel in vivo markers for hypoxic tumor tissue" In Advances in Radiopharmacology, proceedings of the Sixth International Symposium on Radiopharmacology, Maddelena, D.J., Snowdon, G.M. and Boniface, G.R. eds., Wollongong University Press, Wollongong, Australlia, pp.104-113, 1990.

201. **Wiebe, L.I.** et al "Unpublished results"

202. **Whistler, R.L. and Wolform, M.L.** Methods in Carbohydrate Chemistry Vol.I, pp.83-88 and Vol.II, pp.211, Academic press, New York, London, 1963.

203. **Chapman, J.D.** et al "Unpublished results"

204. **Sutherland, R.M.** "Selective chemotherapy of non-cycling cells in an in vitro tumor model" Cancer Res. 34:3501-3503, 1974.

205. **Stratford, I.J. and Adams, G.E.** "The toxicity of misonidazole towards hypoxic cells in vitro : A model for mouse and man" Br. J. Radiol. 51:745-746, 1978.

206. **Zeman, E.M., Brown, J.M., Lemmon, M.J., Hirst, V.K. and Lee, W.W.** "SR-4233 : A new bioreductive agent with selective toxicity for hypoxic mammalian cells" Int. J. Radiat. Oncol. Biol. Phys. 12:1239-1242, 1986.

207. **Edwards, D.I., Biol, M.I., Knox, R.J. and Knight, R.C.** "Structure-cytotoxicity relationships of nitroimidazoles in an in vitro system" Int. J. Radiat. Oncol. Biol. Phys. 8:791-793, 1982.

208. **Knight, R.C., Skolimowski, I.M. and Edwards, D.I.** "Interaction of reduced metronidazole with DNA" Biochem. Pharmacol. 27:2089-2093, 1978.

209. **Knight, R.C., Rowley, D.A., Skolimowski, I.M. and Edwards, D.I.** "Mechanism of action of nitroimidazole antimicrobial and hypoxic tumor radiosensitizing drugs: Effects of reduced misonidazole on DNA" Int. J. Radiat. Biol. 36:367-377, 1979.

210. **Rowley, D.A., Knight, R.C., Skolimowski, I.M. and Edwards, D.I.** "The effect of nitroheterocyclic drugs on DNA : An in vitro model of cytotoxicity" Biochem. Pharmacol. 28:3009-3013, 1979.

211. **Palcic, B. and Skarsgard, L.D.** "Cytotoxicity of misonidazole and DNA damage in mammalian cells" Cancer 37 (suppl. III):54-59, 1978.

212. **LaRusso, N.F., Tomasz, M., Miller, M. and Roselyn, I.** "Interaction of metronidazole with nucleic acids in vitro" Mol. Pharmacol. 13:872-882, 1977.

213. **Varghese, A.J. and Whitmore, G.F.** "Binding to cellular macromolecules as a possible mechanism for the cytotoxicity of misonidazole" Cancer Res. 40:2165-2169, 1980.

214. **Olive, P.L.** "Correlation between metabolic reduction rates and electron affinity of nitroheterocycles" Cancer Res. 39:4512-4515, 1979.

215. **Watts, M.E., Dennis, M.F., Jones, N.R. and Stratford, M.R.L.** "A comparison of the intracellular uptake and radiosensitization efficiency in different media of uncharged 2-nitroimidazoles of varying lipophilicity" Int. J. Radiat. Biol. 52:359-370, 1987.

216. **Sieman, D.W.** "Potentiation of chemotherapy by hypoxic cell radiation sensitizers - A review" Int. J. Radiat. Oncol. Biol. Phys. 8:1029-1034, 1982.

217. **Taylor, Y.C. and Rauth, A.M.** "Differences in the toxicity and metabolism of the 2-nitroimidazole misonidazole (Ro-07-0582) in HeLa and chinese hamster ovary cells" Cancer Res. 38:2745-2752, 1978.

218. **Quintiliani, M.** "Radiosensitizers other than nitroimidazoles" In Biological Bases and Clinical Implications of Tumor Radioresistance Fletcher, G.H., Nervi, C. and Withers, H.R. eds., Masson Publishing Inc., New York, pp.83-88, 1983.

219. **Quintiliani, M.** "Molecular mechanism of radiosensitization by iodine containing compound" In Advances in Clinical Radiosensitization Vienna, IAEA, pp.87-103, 1974.

220. **Gross, J.** "Iodine and bromine. Part 1. Iodine metabolism" In Mineral Metabolism an Advanced Treatise, Vol. II. (Part B) Comar, C.L. and Bronner, F. eds., Academic Press, New York, London, pp.221-262, 1962.

221. **Workman, P.** "Pharmacokinetics of hypoxic cell radiosensitizers : A review" Cancer Clin. Trials 3:237-251, 1980.

222. **Anderson, K.E.** "Pharmacokinetics of nitroimidazoles. Spectrum of adverse reaction" Scand. J. Infect. Dis. Suppl.26:60-67, 1981.

223. **Flockhart, I.R., Large, P., Troup, D., Malcolm, S.L. and Marten, T.R.** "Pharmacokinetic and metabolic studies of hypoxic cell radiosensitizer misonidazole" Xenobiotica 8:97-105, 1978.

224. **Ings, R.M.J., Law, G.L. and Parnell, E.W.** "The metabolism of metronidazole (1-2'-hydroxyethyl-2-methyl-5-nitroimidazole)" Biochem. Pharmacol. 15:515-519, 1966.

225. **Parliament, M.B., Chapman, J.D., Urtasun, R.C., McEwan, A.J., Golberg, L., Mercer, J.R., Mannan, R.H. and Wiebe, L.I.** "Non-invasive assessment of human tumor hypoxia with ^{123}I-Iodoazomycin Arabinoside: Preliminary report of a clinical study" Br. J. Cancer 1991 (submitted).

226. **Moulder, J.E. and Rockwell, S.C.** "Survey of published data on the hypoxic fractions of solid rodent tumors" Radiat. Res. 83:376, 1980.

227. **McMahon, R.E.** "Microsomal dealkylation of drugs substrate specificity and mechanism" J. Pharm. Sci. 55:457-466, 1966.

228. **Illing, H.P.A.** "Lipophilicity of acceptor substrate as a factor in "Late Foetal" rat liver microsomal UDP-glucuronosyl transferase activity" Biochem. Pharmacol. 29:999-1006, 1980.

229. **Xu, L.** "Membrane transport and partition of novel pyrimidine nucleosides" M.Sc. Thesis, University of Alberta, Edmonton, Canada, 1988.

230. **Xu, L., Gati, W.P., Knaus, E.E. and Wiebe, L.I.** "Structure-activity-relationships (SAR) in pyrimidine nucleoside transport" In Advances in Radiopharmacology, proceedings of the Sixth International Symposium on Radiopharmacology, Maddelena, D.J., Snowdon, G.M. and Boniface, G.R. eds., Wollongong University Press, Wollongong, Australlia, pp.283-298, 1990.

231. **Fujita, T., Iwasa, J. and Hanch, C.** "A new substituent constant, π, derived from partition coefficients" J. Amer. Chem. Soc. 86:5175-5180, 1964.

232. **Miller, J.P., Kingwana, J.L., Streeter, D.G., Robins, R.K., Simon, L.N. and Roboz, J.** "The relationship between metabolism of ribavirin and its proposed mechanism of action" Ann. N.Y. Acad. Sci. 284:211-229, 1977.

APPENDICES

Appendix 1. Characteristics of the survival curve for cytotoxicity study.

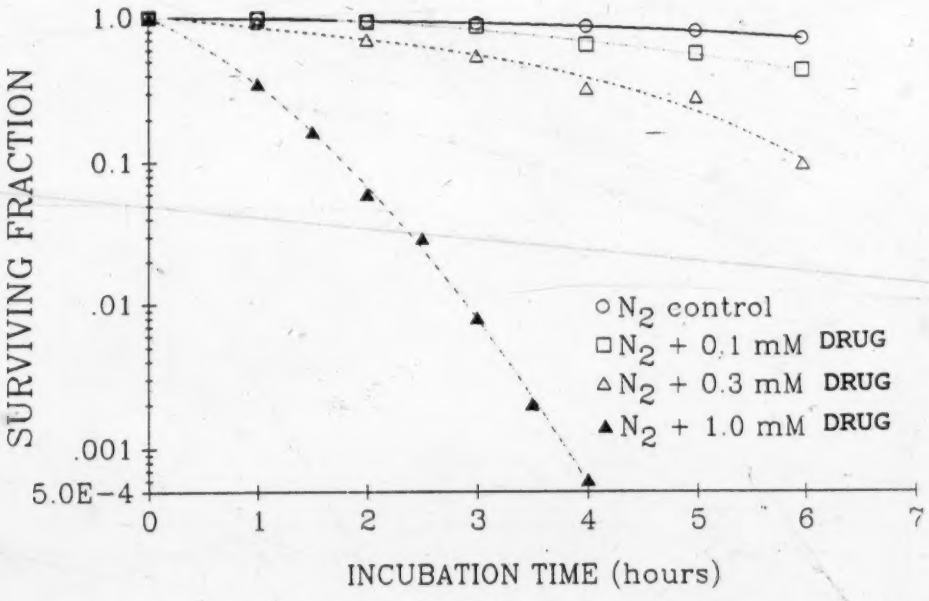

The typical survival curve shown above was constructed in the following manner. Hypoxic EMT-6 cells were incubated with various concentrations of test drug, at several time periods. The cell survival fraction was calculated by measuring the plating efficiencies of these cells. This can be demonstrated by the following example. Suppose a fixed number (200) of treated cells and control cells were plated out and incubated for 6 to 8 days under conditions to give maximum efficiency of colony formation. Let us assume at the end of incubation, the treated and control cells produced 5 and 70 colonies, respectively.

The plating efficiency of treated cells = 5/200 = 0.025
and the plating efficiency of control cells = 70/200 = 0.350

The surviving fraction of treated cells can be calculated by the ratio of plating efficiency (0.025/0.350), which is 0.071. The values of surviving fractions thus obtained are

then plotted on log scale against the time on linear scale to construct the survival curve shown above.

The basic features of the survival curves produced in this manner are:

a) As the concentration of the test drug increased the time required to kill a certain percentage of cells decreased.

b) Drug-free cells show a slow decrease in survival fraction with time. Over the incubation period for up to 6 hour the cell kill percentage is negligible compared to that of drug treated cells. This curve therefore indicates the cell death is only due to the cytotoxic nature of the drug itself.

Appendix 2. Calculation of binding rate.

The binding rate of the test substrates to the EMT-6 cells was calculated by the following procedure. The binding rates are expressed as pmol/10^6 cells/h.

a) The radioactivity of an aliquot of the acid-insoluble fraction was counted in cpm.
b) The cpm of the aliquot was converted to the cpm/10^6 cells.This cpm was then converted to dpm (dpm = cpm/counting efficiency)
c) Dpm was then converted to µCi (µCi = dpm/2.22x10^6)
d) µCi was converted to mg by using the specific activity of the drug. eg. mg = µCi/20 µCi/mg
e) Conversion of mg to mol; Mol = weight in g/mol. wt.
f) Conversion of mol to pmol; 1 pmol = 10^{-12} mol.
g) The pmol/10^6 cells thus obtained was then converted to per hour rate.

The whole process of calculation can be given in the following example.

suppose a drug having mol. wt. of 355, labelled with ^{125}I had a specific activity of 20 µCi/mg. After 60 minutes of incubation with EMT-6 cells the radioactivity bound to an aliquot (5x10^5 cells) of the acid-insoluble fraction was 530 cpm. The counting efficiency was found to be 72%.

The binding rate of this drug would be:

1) 530 cpm/.5 = 1060 cpm/10^6 cells; 1060 cpm/0.72 = 1472.22 dpm/10^6 cells.
2) 1472.22 dpm/2.22 x 10^6 = 6.63 x 10^{-4} µCi
3) 6.63 x 10^{-4} µCi/20 µCi/mg = 3.31 x 10^{-5} mg
4) 3.31 x 10^{-5} mg x 10^{-3}/355 g/mol = 9.32 x 10^{-11} mol/10^6 cells, or 93.2 pmol/10^6 cells.
5) The binding rate therefore would be 93.2 pmol/10^6 cells/h.
6) Six different incubation time periods in 30 min. intervals (30-180 min.) were chosen to calculate the binding rate. The rates were converted to per hour unit for all the 6 time periods. The mean ± S.D. of these 6 time periods values were used to construct binding rate at a given substrate concentration.

Appendix 3. Characteristics of radiation-survival curve.

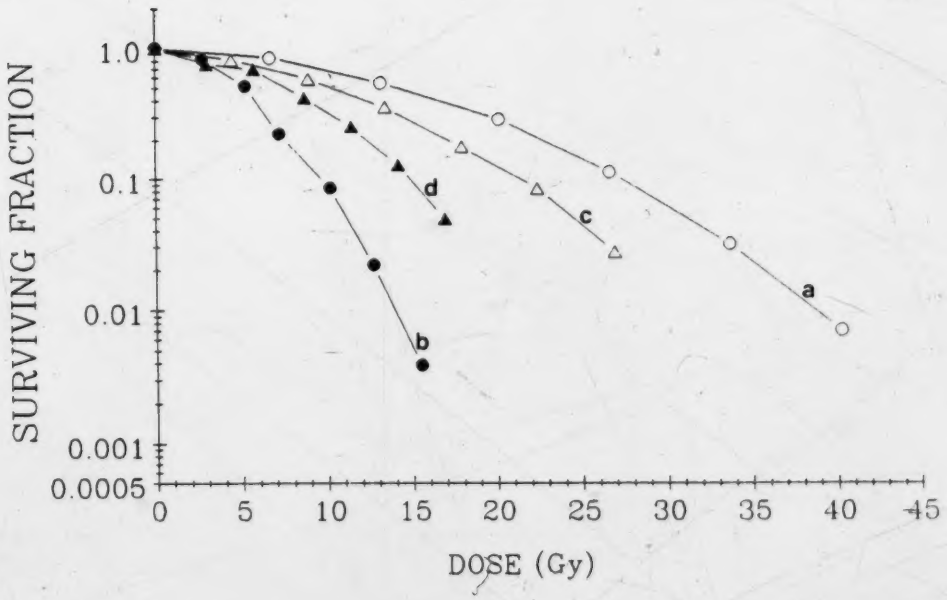

The basic technique for the construction of this curve is similar to that described in Appendix 1 for determination of the cytotoxic curve. In this case the treated cells were exposed to the drug just prior to irradiation. The control cells (hypoxic or aerobic) did not receive any drug or radiation. The surviving fractions obtained after calculating the plating efficiency were plotted against the radiation dose.

The characteristic features of the radiation survival curves shown above are as follows:

1) Curve 'a' represents hypoxic cells irradiated without any drug. The slope of this curve is greater than the others. This suggests the cells are radioresistant at low dose and therefore a high dose is needed to reduce the cell population to a particular surviving fraction (10%).
2) Curve 'b' represents fully oxygenated cells irradiated

without drug. The slope of this curve is reduced relative to curve 'a'. This indicates the cells are sensitive to radiation in the presence of oxygen and low dose would be required to reduce the cell population to 10% survival.

3) Curve 'c' represents hypoxic cells irradiated in presence of 0.1 mM drug. The curve shows a slope higher than curve 'b' but definitely lower than curve 'a'. This indicates that the drug is acting as a radiosensitizer. The 10% survival is achieved with less radiation dose than that required for curve 'a'.

4) Curve 'd' represents hypoxic cells irradiated in presence of 0.5 mM drug. The slope of the curve is obviously less than the curves 'a' and 'c' but is slightly higher than the curve 'b'. Therefore, as the concentration of the drug is increased the slope of the survival curve decreases and approaches the curve 'b'. Thus to reduce the cell population to the 10% survival level a much lower radiation dose would be required than that of curves 'a' and 'c'. This also indicates that the radiosensitizing property of the drug is concentration dependent.

From these features it can be concluded that oxygen enhances the radiation cell damage, hypoxia causes radioresistance and added drug enhances the cell kill under hypoxia. Increased drug concentration present at the time of irradiation increases the radiosensitivity of the cells.

Appendix 4. Radiation dose estimates for the adult for ^{123}I-IAZA.

The dosimetry given in the Table below was calculated for IAZA labelled with ^{123}I. Several factors were considered for this calculation.

1. The total dose was determined for an average adult of 70 kg body weight. The estimate of radiation dose in each organ was calculated on the basis of biodistribution of ^{125}I-IAZA in Balb/c mice bearing subcutaneous EMT-6 tumors.
2. Residence time of radioactivity in each organ was determined by exponential analysis of the percent injected dose per organ versus time curve.
3. The radiation dose from the stomach contents were not considered. In the animal biodistribution studies the determination of percent injected dose per organ for the stomach was made for organ tissue only with contents removed.
4. The radiation doses from the intestine or intestinal contents were not considered. In the biodistribution studies only a section of the intestine was used with the contents removed.
5. The thyroid was not blocked.
6. This calculation of radiation dose estimates was done by using the MIRD method and computer programs (MIRDOSE, Oak Ridge Laboratories, Illinois, U.S.A. and an in-house program from Edmonton Radiopharmaceutical Centre, Alberta, Canada).

Target organ	Total dose (mGy/GBq)
Thyroid	92.8
Heart	2.7
Lung	2.2
Liver	5.5
Kidney	6.1
Spleen	3.5
Testes	2.1
Ovaries	2.7
Stomach	3.6
Total body	1.9